**ARNON AFONSO DE SOUZA CARDOSO**

# SULFUR-RELATED ALLEVIATION MECHANISMS OF SELENIUM TOXICITY IN PLANTS

**LAVRAS – MG**
**2022**

**ARNON AFONSO DE SOUZA CARDOSO**

# SULFUR-RELATED ALLEVIATION MECHANISMS OF SELENIUM TOXICITY IN PLANTS

Thesis presented to the Federal University of Lavras, as part of the requirements of the Postgraduate Program in Soil Science, area of concentration in Soil Fertility and Plant Nutrition, to obtain the title of Doctor.

Dr. Maria Ligia de Souza Silva
Advisor

Dr. Luiz Roberto Guimarães Guilherme
Co-advisor

Dr. Li Li
Co-advisor

Dr. Jiping Liu
Co-advisor

**LAVRAS – MG**
**2022**

**Ficha catalográfica elaborada pelo Sistema de Geração de Ficha Catalográfica da Biblioteca Universitária da UFLA, com dados informados pelo(a) próprio(a) autor(a).**

Cardoso, Arnon Afonso de Souza.
Sulfur-related alleviation mechanisms of selenium toxicity in plants / Arnon Afonso de Souza Cardoso. - 2022.
76 p. : il.

Orientadora: Maria Ligia de Souza Silva.
Coorientadores: Luiz Roberto Guimarães Guilherme, Li Li, Jiping Liu.
Tese (Doutorado) - Universidade Federal de Lavras, 2022.
Bibliografia.

1. Plant Physiology. 2. Plant Nutrition. 3. Plant Stress. I. Silva, Maria Ligia de Souza. II. Guilherme, Luiz Roberto Guimarães. III. Li, Li. IV. Liu, Jiping. V. Título.

**ARNON AFONSO DE SOUZA CARDOSO**

# SULFUR-RELATED ALLEVIATION MECHANISMS OF SELENIUM TOXICITY IN PLANTS

Thesis presented to the Federal University of Lavras, as part of the requirements of the Postgraduate Program in Soil Science, area of concentration in Soil Fertility and Plant Nutrition, to obtain the title of Doctor.

Approved on May 19, 2022.

Dr. Maria Ligia de Souza Silva – Federal University of Lavras (UFLA)
Dr. Guilherme Lopes – Federal University of Lavras (UFLA)
Dr. André Rodrigues dos Reis – São Paulo State University (UNESP)
Dr. Herminia Emilia Prieto Martinez – Federal University of Viçosa (UFV)
Dr. José Lavres Junior – University of São Paulo (USP)

Dr. Maria Ligia de Souza Silva
Advisor

Dr. Luiz Roberto Guimarães Guilherme
Co-advisor

Dr. Li Li
Co-advisor

Dr. Jiping Liu
Co-advisor

**LAVRAS – MG**
**2022**

**Acknowledgments**

The author thanks the Federal University of Lavras (UFLA), the School of Agricultural Sciences of Lavras (ESAL), the Soil Science Department (DCS, ESAL, UFLA), and the Postgraduate Program in Soil Science (PPGCS, ESAL, UFLA) for the support and opportunity. He also is grateful to the Robert W. Holley Center for Agriculture and Health/United States Department of Agriculture (USDA-ARS) and Cornell University for the visiting student period. The author also thanks his advisors Dr. Maria Ligia de Souza Silva, Dr. Luiz Roberto Guimarães Guilherme, Dr. Li Li, and Dr. Jiping Liu for the support and guidance. He also thanks the Brazilian National Research Council (CNPq) for financial support for the research project [423037/2016-1] and Ph.D. scholarship concession [155319/2017-5], and the Coordination for the Improvement of Higher Education Personnel (CAPES - PRINT) for financial support and scholarship for the visiting student period [88887.465626/2019-00]. The author thanks Dr. Aline Marques Mesquita and the DCS staff, Dr. Paulo Eduardo Ribeiro Marchiori and the Plant Physiology Sector staff (Biology Department – DBI, UFLA), and Dr. Flávia Barbosa Silva Botelho (Agriculture Department – DAG, UFLA) for support in the project execution. The author is also grateful to Dr. Franklin Eduardo Melo Santiago, Dr. Lorena Carmen Hernandez Nataren, M.Sc. Aline do Amaral Leite, M.Sc. Marcio Felipe Pinheiro Neri Nunes, Eng. Fabricio Teixeira de Lima Gomes, Eng. João Renato Rodrigues Antonio and all his colleagues from PPGCS and DCS, for support and friendship.

*O presente trabalho foi realizado com apoio da Coordenação de Aperfeiçoamento de Pessoal de Nível Superior – Brasil (CAPES) – Código de Financiamento 001*. *O presente trabalho foi realizado com apoio do Conselho Nacional de Desenvolvimento Científico e Tecnológico (CNPq).*

**TABLE OF CONTENTS**

## General abstract

Selenium and sulfur present a strict relationship in plants and soils, affecting their uptake and accumulation. Thus, addressing this interaction is important to understand selenium nutrition and toxicity in plants, which could influence crop nutrition and production. Here, we aimed to evaluate the impact of selenate exposure on rice plants grown under different sulfate supplies at tillering and grain ripening phases. We studied the effects of varying selenate and sulfate doses on rice plants grown hydroponically or in soils with varying contents of clay. We also performed selenate sorption assays to evaluate the influence of clay content and sulfur doses on selenate adsorption and desorption in soils. Sulfate supply alleviated selenate toxicity in both short-term and long-term experiments. Selenate treatment up-regulated the expression of sulfate transporters, leading to increased sulfur contents in rice seedlings, which enhanced the antioxidant system and alleviated selenate toxicity. However, this enhanced mechanism is absent in seedlings grown under a low sulfur supply. Moreover, soil clay contents strongly influenced selenate availability. A high clay content promoted a higher selenate adsorption capacity, resulting in lower selenium contents in shoots and grains and the absence of toxicity symptoms. In contrast, a low clay content increased the availability of selenate added, which can favor the biofortification of crops. However, high selenate doses caused growth and yield impairment in rice cultivated in low-clay-content soil, with higher selenium concentrations in shoots and grains, potentially increasing the risk of selenate toxicity for humans and animals. In addition, we studied the influence of selenium treatment on sulfur and selenium metabolisms and plant growth of *Arabidopsis* and broccoli with different concentrations of glutathione, a key molecule of sulfur metabolism and plant detoxification. The selenate treatment decreased the glutathione contents in plant tissues. The *pad2-1* plants (a glutathione-deficient *Arabidopsis* mutant) exhibited lower selenate tolerance and higher sulfate transporters (*AtSULTR1;1* and *AtSULTR1;2*) gene expression on roots compared to *Arabidopsis* wild-type (WT), even exhibiting similar selenium and sulfur concentrations on shoots and roots. However, the reduced glutathione (GSH) supply alleviated the selenate toxicity and partially inhibited the sulfate transporters expression, indicating that both selenate effects are directly linked to glutathione metabolism. Conversely, the selenite did not present clear relation with glutathione or *BoSULTR1;1* and *BoSULTR1;2* in broccoli plants, while selenate decreased the glutathione contents and inhibited the growth of broccoli with lower glutathione concentrations severely.


**Keywords:** Antioxidant enzymes. *Arabidopsis thaliana*. *Brassica oleracea*. Broccoli. Glutathione. *Oryza sativa*. Oxidative stress. *pad2-1*. Rice. Selenate. Selenite. Selenium. Sulfate. Sulfate transporters. Sulfur.

**General introduction**

Selenium (Se) is a micronutrient for humans and animals, playing essential roles in the immune and antioxidant system, protecting against various diseases such as hypothyroidism, heart disease, and many types of cancer. The primary means of supplying selenium to humans is by ingesting plant foods rich in this micronutrient. Despite its importance for human health, selenium deficiency is frequent, especially in underdeveloped countries or where the availability of the element in the soil is low.

Selenium is not a nutrient for plants; however, it can be absorbed, increasing the resistance of plants to different types of stress, being considered a beneficial element. However, the high availability of selenium can cause severe phytotoxicity, mainly due to oxidative stress caused by reactive oxygen species. The ability of plants to absorb selenium makes it possible to biofortify foods by providing this element in the soil or by foliar application. Thus, the biofortification of foods with selenium is a strategy to improve their nutritional quality and prevent deficiency. However, selenium uptake and accumulation also increase the risk of toxicity to plants and animals.

Selenium is uptake by plants in selenate and selenite forms. However, it has been observed that selenate is the preferentially absorbed form in several species, probably due to its higher solubility. Selenate is probably uptake by sulfate transporters on roots and assimilated by sulfur metabolic pathways. Thus, selenium and sulfur metabolisms and concentrations are closely related in plants, affecting the uptake and accumulation of these elements. In addition, some studies indicate that sulfate influences selenium sorption in soils and affects its availability for plants, indicating that selenium and sulfur present a relation in soils.

Thus, studies about selenium and sulfur supplies are important to understand the uptake and accumulation of these elements in plants, aiming to improve the biofortification or toxicity resistance. Therefore, the present research project aims to evaluate the effects of selenium treatment in plants with different sulfur and sulfur-compounds contents.

# CHAPTER I

## Sulfate availability and soil selenate adsorption alleviate selenium toxicity in rice plants

### Highlights

1. Sulfate protects rice seedlings from selenate toxicity by competitive uptake inhibition
2. Selenate induces sulfate transporter activity and sulfur accumulation in rice plants
3. Selenate and sulfate interaction shifts from competition in roots to synergism in shoots
4. Selenate-induced sulfur accumulation enhances the antioxidant system, alleviating selenate toxicity
5. Oxisols with high clay content retain selenate in the soil, reducing selenate availability to plants
6. Higher selenate adsorption by Oxisols decreases its availability, uptake, and transport to rice grains


### Abstract

Selenate and sulfate present a strict relationship in plants and soils, affecting their uptake and accumulations. Thus, addressing selenite-sulfate interaction is important to understand selenium nutrition and toxicity in plants, which could influence crop nutrition and production. Here, we aimed to evaluate the impact of selenate exposure on rice plants grown under different sulfate supplies at tillering and grain ripening phases. We studied the effects of varying selenate and sulfate doses on rice plants grown hydroponically or in soils with varying contents of clay. We also performed selenate sorption assays to evaluate the influence of clay content and sulfur doses on selenate adsorption and desorption in soils. Sulfate supply alleviated selenate toxicity in both short-term and long-term experiments. Selenate treatment up-regulated the expression of sulfate transporters, leading to increased sulfur contents in rice seedlings, which enhanced the antioxidant system and alleviated selenate toxicity. However, this enhanced mechanism is absent in seedlings grown under a low sulfur supply. Moreover, soil clay contents strongly influenced selenate availability. A high clay content promoted a higher selenate adsorption capacity, resulting in lower selenium contents in shoots and grains and the absence of toxicity symptoms. In contrast, a low clay content increased the availability of selenate added, which can favor the biofortification of crops. However, high selenate doses caused growth and yield impairment in rice cultivated in the low-clay-content soil, with higher selenium concentrations in shoots and grains, potentially increasing the risk of selenate toxicity for humans and animals.

**Keywords:** *Oryza sativa*, selenium, sulfate transporters, antioxidant enzymes, glutathione, oxidative stress.

**Graphical abstract**

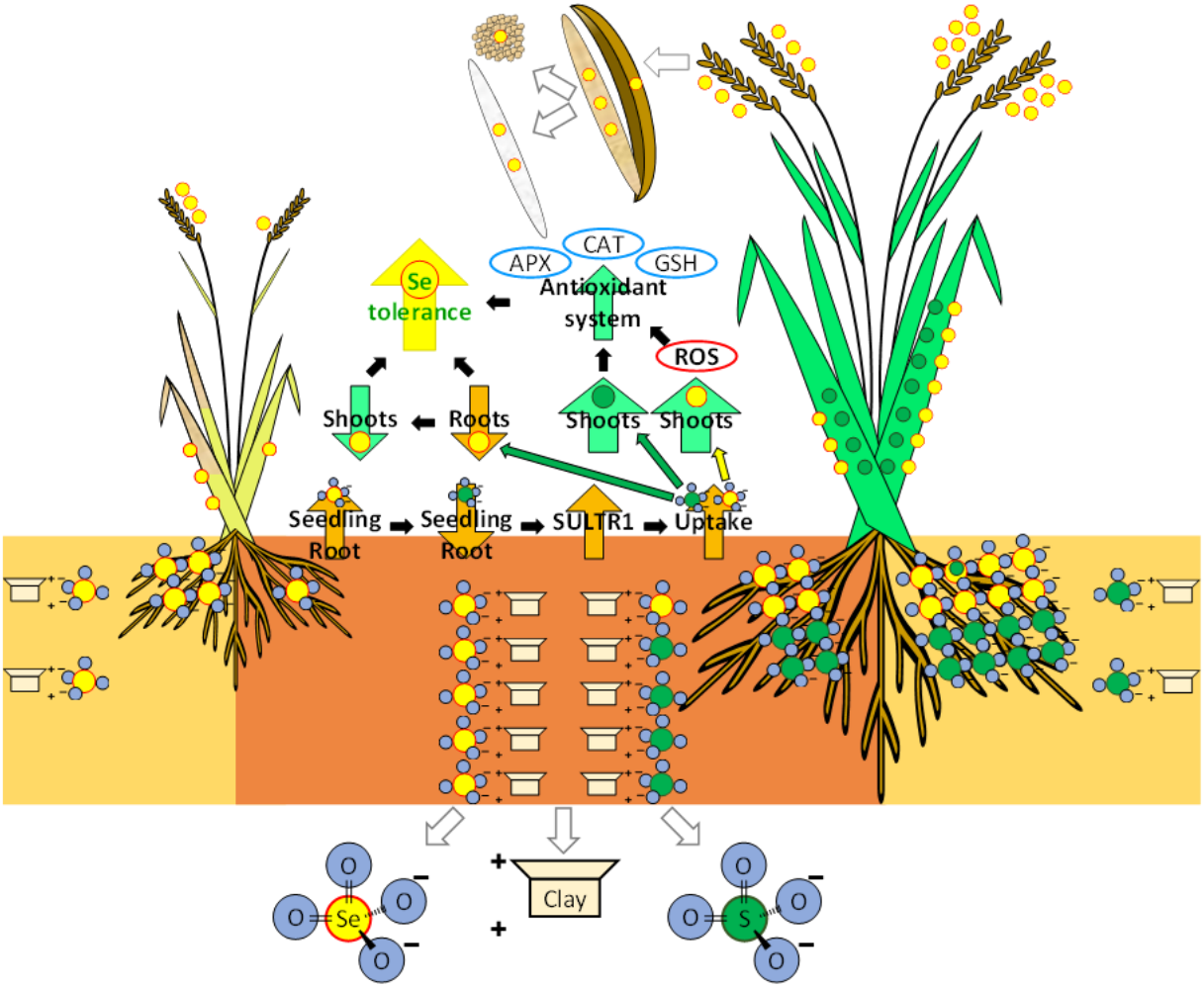


## 1. Introduction

Selenium (Se) is an essential micronutrient for humans and other animals due to its structural function in selenoproteins necessary for the immune and anticarcinogenic systems (Wiesner-Reinhold et al., 2017; Winkel et al., 2012). Thus, Se must be present adequately in diets for the proper functioning of human beings (FAO and WHO, 2004). However, it is estimated that Se deficiency affects about 800 million people worldwide (Malagoli et al., 2015), which increases the risk of several diseases, such as hypothyroidism, cardiovascular disease, and several types of cancer (Alfthan et al., 2015; Wiesner-Reinhold et al., 2017).

Se is not an essential element for plants but a beneficial element for plant growth and crop production (Jing et al., 2017; Kaur et al., 2017). Se uptake capacity varies among plants, with Se concentrations correlated with the bioavailability in the soil for most species

(Puccinelli et al., 2017). In addition, Se availability is also affected by soil types. For instance, soils with higher clay contents with positive charge predominance have a more robust binding capacity for Se anions and thus lower Se availability (Santos et al., 2021), resulting in a low Se concentration in crops and foods.

Although plants absorb both selenite ($SeO_3^{2-}$) and selenate ($SeO_4^{2-}$), selenate is the ionic form preferentially taken up by many species (Peng et al., 2017). In addition, higher sulfate ($SO_4^{2-}$) uptake capacity is associated with higher selenate uptake (Wiesner-Reinhold et al., 2017), suggesting that sulfate transporters co-transport selenate and sulfate in plants (Toler et al., 2007; Zhang et al., 2003). Thus, adequate selenate and sulfate supply for crops is necessary, considering sulfur is a macronutrient for plants, and sufficient sulfur supplies are required for adequate crop production.

Although Se is considered a beneficial element, high Se concentrations can cause severe toxicity in plants and animals (Garousi et al., 2016; Sharma et al., 2017). High Se concentrations in the cells induce the production of reactive oxygen species (ROS), such as peroxide and superoxide (Schiavon et al., 2012), which causes lipid peroxidation in cell membranes and oxidative stress, a primary degenerative process responsible for phytotoxicity (Łabanowska et al., 2012; Tian et al., 2017). Since S can favor the antioxidant system (Dixit et al., 2016; Terzi and Yıldız, 2015), S supply can mitigate selenium toxicity and enhance plants' tolerance. This effect is especially vital to the Se non-accumulator crops like rice (*Oryza sativa* L.), which have high nutritional importance but present low Se uptake and low Se concentrations in plant tissues (Gupta and Gupta, 2017).

Interestingly, a low dosage of Se supply can stimulate sulfur uptake, probably by inducing the expression of sulfate transporters (Boldrin et al., 2016; Tian et al., 2017), which in turn enhances the antioxidant enzyme activities and the overall antioxidant system of the plant (Akbulut e Çakir 2010; Schiavon et al. 2012). Conversely, sulfate can increase soil selenium desorption, increasing its availability and toxicity risk (Santos et al., 2021). Thus, we aimed to evaluate the effects of selenate and sulfate doses on rice plants at the tillering stage in nutrient solutions and grain ripening stage in soils with different Se sorptions. Our results could provide insights into the selenate metabolism in rice plants, the risk of selenium toxicity for humans and animals, and alleviation mechanisms linked to sulfur metabolism.

## 2. Material and methods

### 2.1. Hydroponic rice cultivation (short-term experiment)

#### *2.1.1. Experimental design*

The hydroponic experiments included four treatments with three replicates using a complete randomized design. Each replicate consisted of 16 young rice plants. The treatments were four combinations between selenate and sulfate doses on the nutrient solution: T1 = 0 µM Se + 0.1 mM S; T2 = 0 µM Se + 0.5 mM S; T3 = 20 µM Se + 0.1 mM S; and T4 = 20 µM Se + 0.5 mM S. The selenate and sulfate sources were sodium selenate ($Na_2SeO_4$) and magnesium sulfate ($MgSO_4$), respectively. The Mg concentration was balanced using $MgCl_2$ solution (Table S1).

#### *2.1.2. Experimental conditions*

Rice seeds (*Oryza sativa* L. cv. BRS sertaneja) were germinated in the commercial peat moss compost (PRO-MIX® BK25V). Two-week-old seedlings were rinsed with distilled water and transferred to plastic trays containing 7-L Hoagland nutrient solutions (100% ionic strength, pH 6.5) with sulfur concentrations adjusted to the treatment conditions (Table S1). After one week, selenate with indicated concentrations was added to freshly changed nutrient solutions. The plants were harvested one week after the selenate treatment (28 days after sowing). First, the relative chlorophyll index was measured in new leaves using a hand-held chlorophyll meter (SPAD-502 model, Minolta®, Japan). Then, the plants were rinsed with distilled water and separated into shoots and roots. Plant materials for biochemical analyses were immediately frozen with liquid nitrogen and stored (-80 ºC). For selenium and sulfur determinations, plant materials were washed with a $CaCl_2$ solution (2 mM) for 2 minutes, rinsed with distilled water, dried for 72 h (65 ºC) in an oven with air circulation, and weighed using a digital scale.

### 2.2. Soil characterization

#### *2.2.1. Particle-size distribution analysis and texture classification*

Soil samples were collected in two Oxisols (0-20 cm depth) under natural vegetation. The soils were classified as Rhodic Haplustox and Xanthic Haplustox (USDA, 1999). The soil samples were homogenized and sieved (4 mm). Sub-samples of each soil were collected for particle size and chemical analysis. The particle-size distribution analysis was carried out according to USDA (2014). The sand content (> 0.02 mm) was determined by sieving, and the clay content (< 0.002 mm) was determined by the pipette method. The silt content (0.002 -

0.02 mm) was calculated as the difference between the sample weight and clay and sand contents. The particle size results of Rhodic Haplustox samples were 620 g $kg^{-1}$ clay, 310 g $kg^{-1}$ sand, and 70 g $kg^{-1}$ silt; and of Xanthic Haplustox samples were 240 g $kg^{-1}$ clay, 710 g $kg^{-1}$ sand, and 50 g $kg^{-1}$ silt. Soil textures were calculated using Soil Texture Calculator software (USDA, 2022). Rhodic Haplustox was classified as clay texture soil (CT soil), and Xanthic Haplustox as sandy clay loam texture soil (SCLT soil).

*2.2.2. Soil selenium and sulfur concentrations*

For Se-concentration determination, soil samples (0.5 g) were treated in 8 ml hydrochloric acid (37%) and 2 ml nitric acid (65%) (McGrath and Cunliffe, 1985). The extracts were then subject to 60 (180 min), 105 (60 min), and 140 ºC (30 min) treatments. After cooling, the extracts were filtered and transferred to volumetric flasks. The volume was adjusted to 25 ml with deionized water, and the extracts were analyzed by graphite furnace atomic absorption spectrometry (GFAAS). The pseudo-total Se concentrations were 0.6 and 0.3 mg Se $kg^{-1}$ CT and SCLT soils, respectively. The sulfur concentrations were determined by the turbidimetric method (Ajwa and Tabatabai, 1993), and the results were 2.5 and 4.6 mg $dm^{-3}$ S in CT and SCLT soils, respectively.

*2.2.3. Soil acidity correction and fertilization*

Soil sub-samples were collected for acidity and fertility analyses (Table S2). The samples were transferred to cylindric plastic pots (5 $dm^3$ capacity). Both soil samples received 0.6 g $dm^{-3}$ of limestone powder (45% CaO + 11% MgO) to raise the base saturation to 70%. After limestone homogenization, the soil samples were incubated for 20 days. Then, essential fertilization was applied in solution form, which consisted of (mg $dm^{-3}$): 200 N ($NH_4H_2PO_4$), 450 P ($NH_4H_2PO_4$), 300 K ($K_2SO_4$ adjusted to S doses and KCl), 0.8 B ($H_3BO_3$), 1.3 Cu ($CuCl_2$ $2H_2O$), 3.6 Mn ($MnCl_2$ $4H_2O$), 0.15 Mo ($H_2MoO_4$), and 4.0 Zn [$(ZnNO_3)_2$]. Then, the soil samples were incubated for ten days. At incubation periods, the soil moisture was maintained at 70% of field capacity.

2.3. Selenium sorption experiments

*2.3.1 Experimental design*

After the second incubation period, sorption assays were performed to evaluate the soil textures and sulfate-dosage effects on selenate adsorption and desorption in the samples. A completely randomized experimental design was used, with six treatments and four

replications. Each replication consisted of one soil sample. The treatments were combinations of different soil textures and sulfate doses (mg $dm^{-3}$ S): T1 = CT soil without sulfur addition; T2 = SCLT soil without sulfur addition; T3 = CT soil + 45 S; T4 = SCLT soil + 45 S; T5 = CT soil + 90 S; T6 = SCLT soil + 90 S. The sulfur was added at basic fertilization, using potassium sulfate ($K_2SO_4$) in solution form. The K was balanced among the sulfur doses using KCl solution (1 M). Ten days after sulfur treatment, soil samples (50 g) were collected for sorption assays.

*2.3.2. Adsorption and desorption assays*

Soil samples were dried at room temperature and ground. Then, the soil samples (3.0 g) were added to tubes with 30 ml of Se equilibrium solution (30 mM NaCl + 0.4 mg $L^{-1}$ Se, as $Na_2SeO_4$). The Se concentration in the assay condition corresponds to 4.0 mg $kg^{-1}$ Se in the soil. The tubes were shaken for 72 hours (12 h shaking 12 h rest in a horizontal shaker at 120 rpm and room temperature). The tubes were centrifuged (3500 rpm for 20 min), and the supernatants were collected for adsorption determination. The tubes received 30 ml of NaCl solution (30 mM) and were shaken and centrifuged again. The supernatants were collected for desorption determination. The Se concentrations in the supernatants were determined by the GFAAS, and Se adsorption and desorption were calculated according to Lessa et al. (2016).

2.4. Rice cultivation in the soil (long-term experiments)

*2.4.1. Experimental design*

Experiments were performed to study the influence of selenate and sulfate doses on the rice plants grown in the CT and SCLT soils under greenhouse conditions. A randomized block experimental design was used with fifteen treatments and four replications. Each replicate consisted of a pot with five plants. The treatments consisted of combinations between five selenate doses (0.0, 0.5, 1.0, 2.0, and 4.0 mg $dm^{-3}$ Se; corresponding to around 0.0, 6.3, 12.5, 25, and 50 µmol $dm^{-3}$ Se, respectively) and three sulfate doses in the soil (0, 45, and 90 mg $dm^{-3}$ S, corresponding to around 0.0, 1.4, and 2.8 mmol $dm^{-3}$ S, respectively). The selenate and sulfate sources were sodium selenate ($Na_2SeO_4$) and potassium sulfate ($K_2SO_4$), respectively, applied in solution form. The sulfur doses were applied at basic fertilization, and the selenium doses were applied seven days after transplanting rice seedlings. The K was balanced among the sulfur doses using KCl solution.

*2.4.2. Experimental conditions*

Rice seeds (*Oryza sativa* L. cv. BRS pepita) were germinated in trays filled with sterilized sand. The two-week-old seedlings were transplanted to the pots containing soil samples. Successive thinning was performed until five plants remained per pot. Nitrogen and potassium topdressing fertilization was performed at 30, 60, and 90 days after the transplant, supplying 100 mg $dm^{-3}$ K ($KNO_3$) and 100 mg $dm^{-3}$ N ($KNO_3$ and $NH_4NO_3$). The plants were harvested at the end of the grain ripening phase (120 days after the transplant). Before the harvest, two recently expanded leaves were collected per pot, frozen in liquid nitrogen, and stored (-80 ºC) for biochemical analyses. The relative chlorophyll index was measured as previously mentioned. The plants were divided into shoots and panicles and dried for 72 h (65 ºC) in an oven with air circulation. The number of panicles was determined, and panicles were threshed manually. The paddy rice-grain and shoot dry matters were determined using a digital scale.

*2.4.3 Rice grain processing*

The paddy rice was processed as described by Eyarkai Nambi et al. (2017). It was dehusked using a rubber roll sheller, and the brown rice was collected. Then, half of each brown rice sample was milled using a vertical milling machine to obtain the white rice.

2.5. Plant analysis

*2.5.1. Selenium and sulfur determinations*

Dried plant materials were ground for selenium and sulfur determinations. The plant materials included shoots and roots from the short-term experiment and shoots, brown rice, white rice, and rice husks from the long-term experiment. The ground samples (0.500 g) were digested in acid solution (6 ml $HNO_3$ + 2 ml $HClO_4$) in a digester block following the heating sequence: 50, 100, and 150 ºC for 60 min each, and 200 ºC until the extracts were translucent (around 30 min). Then, the extracts were transferred to volumetric flasks (10 ml), and the sample volume was adjusted with deionized water. The Se concentrations in shoots and roots were determined by inductively coupled plasma optical emission spectroscopy (ICP-OES) and in white rice, brown rice, and rice husks by GFAAS. The S concentrations were determined by ICP-OES.

*2.5.2. Gene expression analysis*

Root samples from the short-term experiment were used to evaluate the expression of genes involved in selenate and sulfate uptake. Total RNAs were extracted from fresh samples (100 mg) using Trizol reagent (Life Technologies™). The cDNAs were synthesized using the Superscript III Reverse Transcriptase kit (Invitrogen™). Real-time quantitative-polymerase chain reaction (RT-qPCR) was realized using SYBR Green Universal Master Mix (Applied Biosystems™) and a CFX384TM real-time PCR system (Bio-Rad®). The primer sequences are presented in Table S3.

*2.5.3. Stress indicators ($H_2O_2$ and MDA concentrations)*

Fresh plant materials (200 mg) (shoots and roots from the short-term experiment and shoots from the long-term experiment) were macerated in liquid nitrogen with 30 mg of polyvinylpyrrolidone (PVPP), homogenized in 1.5 ml trichloroacetic acid solution (1.0 g $L^{-1}$), and centrifuged at 12,000 *g* and 4º C for 15 min. For hydrogen peroxide ($H_2O_2$) determination, 45 µl of supernatant was added to 45 µl potassium phosphate buffer (10 mM, pH 7.0) and 90 µl potassium iodide solution (1.0 M). The mixture was analyzed in a spectrophotometer at 390 nm, and the $H_2O_2$ concentration was obtained using a standard curve (Velikova et al., 2000). For malondialdehyde (MDA) determination, 125 µl of supernatant was added to 250 µl thiobarbituric acid (5 g $L^{-1}$) and trichloroacetic acid solution (100 g $L^{-1}$). The mixture was maintained in a water bath at 95 ºC for 30 min and cooled in an ice bath. It was then analyzed in a spectrophotometer at 535 and 600 nm, and MDA concentrations were obtained using the coefficient of molar extinction of 156 $mM^{-1}$ $cm^{-1}$.

*2.5.4. Antioxidant enzymes (catalase and ascorbate peroxidase activities)*

Samples (200 mg) of fresh material (shoots from short-term and long-term experiments) were macerated in liquid nitrogen with 30 mg PVPP and homogenized in tubes with 1.5 ml potassium phosphate buffer (100 mM $KH_2PO_4$, 0.1 mM EDTA, and 10 mM ascorbic acid, pH 7.8). The tubes were centrifuged at 13,000 *g* and 4 ºC for 10 min. The supernatant (protein extract) was collected. Protein extract samples (6.0 µl) were added to 294 µl Bradford reagent for soluble protein determination (Bradford, 1976). The mixture was shaken in a vortex and analyzed in a spectrophotometer at 595 nm. The soluble protein concentrations were obtained using a standard curve.

Catalase (CAT, EC 1.11.1.6) activity was determined in a 180 µl reaction mixture containing 9 µl protein extract, potassium phosphate buffer (100 mM $KH_2PO_4$, pH 7.0), and

hydrogen peroxide (12.5 mM). The reaction mixture was analyzed in a spectrophotometer at 240 nm for 3 min (15-sec intervals), and the activity was obtained using the molar coefficient extinction of 36 $mM^{-1}$ $cm^{-1}$ (Havir and McHale, 1987). The ascorbate peroxidase (APX, EC 1.11.1.11) activity was determined in a 180 µl reaction mixture consisting of 9 µl protein extract and potassium phosphate buffer (100 mM $KH_2PO_4$, pH 7.0), ascorbic acid (0.5 mM), and hydrogen peroxide (0.1 mM). The reaction mixture was analyzed in a spectrophotometer at 240 nm for 3 min (15-sec intervals), and the activity was determined using the molar coefficient extinction of 2.8 $mM^{-1}$ $cm^{-1}$ (Nakano and Asada, 1981).

*2.5.5. Reduced glutathione (GSH) concentrations*

Samples (100 mg) of fresh plant material (shoots and roots from the short-term experiment) were macerated in liquid nitrogen and homogenized in 1.0 ml sulfosalicylic acid solution (6 g $L^{-1}$). The samples were centrifuged at 8000 *g* and 4 ºC for 10 min. The reaction mixture consisted of 120 µl of glutathione reductase (3.3 units $ml^{-1}$), 1.68 mM DTNB, 60 µl of NADPH solution (0.8 mM), and 20 µl of supernatant (Rahman et al., 2007). The reaction mixture was analyzed in a spectrophotometer at 412 nm for 2 min (30-sec intervals). GSH concentrations were calculated using a standard curve.

2.6. Statistical analysis

The data were analyzed using SAS University Edition® software (Statistical Analysis System, Cary, North Carolina). Data normality was checked before analyses. Then, the data were submitted for analysis of variance. When the treatment effects were significant, the treatments were compared by the Scott-Knott test ($p < 0.05$) using the SISVAR® software (Ferreira, 2019).

## 3. Results

3.1. Sulfate protects rice seedlings from selenate toxicity by competitive uptake inhibition

Selenium (Se) toxicity was acute in plants with low sulfur (S) supply (0.1 mM) in the nutrient solution. A higher S supply (0.5 mM) had no impact on plant growth under selenate treatment (20 µM Se). However, plants with a low S supply under Se treatment showed strong chlorosis on leaves (Figure 1a) with a low relative chlorophyll index (Figure S1). In addition, these plants showed 43 and 53% reductions in shoots and root biomasses, respectively (Figures 1a and 1b), compared to the control treatment (0.5 mM S without Se). Conversely,

Se treatment did not affect plants grown with 0.5 mM S in the nutrient solution (Figures 1a, 1b, and 1c), indicating that a higher S supply alleviates Se toxicity in rice plants.

The protective action of S might be related to an inhibition effect on Se uptake. Under 20 μM Se treatment, the plants had 24 and 65% fewer Se concentrations in the shoot and root, respectively, under the high (0.5 mM) S treatment than under the low (0.1 mM) S supply condition (Figures 1d and 1e). The inhibitory effect of S on Se accumulation was stronger in the roots since the higher S supply significantly decreased the Se accumulation in the root tissues, despite the increasing root biomass production (Figure S2d). The antagonism between S and Se absorptions was evidenced by the ~20% reduction in S concentrations in the roots under the Se treatment, compared to the non-treated control, regardless of the status of the sulfur supply (Figure 1g). Conversely, Se treatment sharply induced the S content in shoots of rice plants grown under 0.5 mM S in the nutrient solution (Figure 1f). These plants presented S concentrations 2.2-folds higher compared to all other treatments (Figure 1f).

3.2. Selenate induces the expression of sulfur transporter genes in rice roots

The Se treatment influenced the expression of both *OsSULTR1;1* and *OsSULTR1;2* in rice roots. However, the 20 μM Se treatment induced a 27-fold increase in *OsSULTR1;1* expression in the root under the low-S (0.1 mM) but not the high-S (0.5 mM) condition (Figure 2a). In contrast, the Se treatment comparably up-regulated *OsSULTR1;2* gene expression by 2-folds in the roots regardless of the S supply conditions (Figure 2b).

3.3. Sulfur enhances the antioxidant system of rice plants

Under selenate exposure, the plants grown with 0.5 mM S exhibited 6.7 and 2.5-folds higher CAT and APX activities than plants grown with 0.1 mM S in the nutrient solution (Figures 3a and 3b). Similarly, Se treatment led to a 34% increase in GSH concentrations in the shoots of the rice plants treated with a high (0.5 mM) but not a low (0.1 mM) S concentration (Figure 3c). Conversely, a 2.8-fold higher GSH concentration was observed in the roots treated with Se under the low S (0.1 mM) condition (Figure 1d).

Higher concentrations of the oxidative stress indicators $H_2O_2$ and MDA were observed in plants grown under the low S (0.1 mM) – Se (0 μM) and the high S (0.5 mM) + Se (20 μM) conditions (Figure 3e-h). For example, 64% and 26% higher $H_2O_2$ concentrations were produced in the shoots and roots of the rice plants grown in the low-S + none-Se medium and the high-S + Se medium compared with the other treatment, respectively (Figures 3e and 3f).

Similarly, the plants with higher $H_2O_2$ concentrations also showed ~40% greater MDA concentrations in the shoots and roots under the same conditions mentioned above (Figure 3g, h). These results indicated that the higher S supply enhanced the antioxidant mechanisms in rice plants grown with the Se treatment.

3.4. Selenium sorption reactions are related to soil clay content

Soil types influenced Se adsorption and desorption in the soils. In general, under our experimental conditions, the Se adsorptions were significantly higher in the clay texture (CT) soil than in the sandy clay loam texture (SCLT) soil (Figure 4a). The difference was more pronounced in the absence of S addition, where the Se adsorption was 2.8-folds higher in the CT soil than in the SCLT soil (Figure 4a). This difference in Se adsorption reflected the difference in clay contents in that the CT soil has a 2.6-folds higher clay content (620 g $kg^{-1}$) than the SCLT soil (240 g $kg^{-1}$).

Furthermore, S supplies did not affect Se adsorption in the CT soil, whereas the Se adsorption increased with the enhanced S supplies in the SCLT soil (Figure 4a). For instance, in the absence of S addition, the CT soil adsorbed 67% (2.70 mg $kg^{-1}$), and the SCLT soil 24% (0.96 mg $kg^{-1}$) of the Se added to the soils (4.0 mg $kg^{-1}$). On the other hand, although the S addition (45 and 90 mg $dm^{-3}$ S) did not affect the Se adsorption in the CT soil, the S supplies increased Se adsorption by 84% in the SCLT soil.

Unlike the Se adsorption, the S doses affected Se desorption in both soil types studied (Figure 4b). In addition, the Se desorptions were higher in the CT soil than in SCLT soil under our experimental conditions (Figure 4b). For example, the Se desorption was 12-folds higher in the CT soil than in the SCLT soil under the non-S condition (Figure 4b). Furthermore, the Se desorbed in this condition (without S addition) corresponds to 14 (CT soil) and 4% (SCLT soil) of the selenium adsorbed in the previous assay, indicating that most selenium adsorbed remained bonded to the soil (86% in CT soil and 96% in SCLT soil). The S addition had distinct effects on Se desorption for different texture soils. For instance, the S supplies decreased and increased the Se desorption by 37% and 159% in the CT and SCLT soils, respectively, in an S-dose-dependent manner (Figure 4b).

3.5. Selenate toxicity is stronger in rice grown in soil with lower selenium adsorption

In the high-Se-adsorption CT soil, the added Se doses had no significant impacts on rice growth, i.e., the shoot biomass (Figure 5a), and grain yields, i.e., the dry grain matters (Figure 5b), regardless of the S supply status. In contrast, in the lower selenium adsorption

capacity SCLT soil, higher doses of Se (>2.0 mg $dm^{-3}$) caused significant decreases in growth (Figure 5b) and grain yields (Figure 5d) when S addition was absent. For instance, plants grown in the SCLT soil without S addition showed a 43% reduction in shoot production at the highest Se dose (4.0 mg $dm^{-3}$) compared with the non-Se condition (Figure 5b). In addition, higher Se doses (2.0 and 4.0 mg $dm^{-3}$) also caused a 42% decrease in grain production under the non-S supply condition (Figure 5d). We also observed a reduction of 22% in the grain production of plants grown with S addition (45 and 90 mg $dm^{-3}$) at the highest Se dose (4.0 mg $dm^{-3}$). These results evidence that sulfur also alleviates the selenate toxicity in rice plants at the grain ripening stage. Furthermore, plants with S addition showed better growth and production in both soils than without S supply (Figures 5 and S3).

The Se concentrations in rice shoots increased with increasing selenate doses in both soils (Figures 6a and 6b). However, the plants grown in the CT soil exhibited increased Se concentrations in shoots just at selenate doses above 1.0 mg $dm^{-3}$ under sulfur addition, indicating the sulfur enhanced the selenate availability and uptake in this soil. Conversely, the plants in the SCLT soil presented selenium increases at selenate doses above 0.5 mg $dm^{-3}$ regardless of the sulfur supply status, except for the 4 mg $dm^{-3}$ Se dose. Thus, the Se concentration in plants was higher in the SCLT soil than in the CT soil under the same conditions, suggesting a higher Se availability in the SCLT soil. The Se concentrations in plants grown under the highest selenium dose with sulfur addition were 157 and 79 mg $kg^{-1}$ in the SCLT and CT soils, respectively.

We observed higher S concentrations in the shoots of the plants grown under the S-addition condition (Figure 6). Furthermore, we also observed that a higher sulfur dose (90 mg $dm^{-3}$ S) promoted a slight increase in the S concentration compared to the addition of 45 mg $dm^{-3}$ S in both soils. The Se doses did not affect the S concentrations in the shoots of the rice plants grown in the CT soil (Figure 6c). However, the Se doses enhanced the S uptake and accumulation in the shoots of the rice plants grown in the SCLT soil (Figures 6d and S4d). The highest Se dose increased by 55% the S concentration in plants cultivated with 90 mg $dm^{-3}$ S than plants grown without Se at the same S supply.

Similarly, the increased selenate doses increased Se contents in rice grain and husk in both soils (Figures 7 and S5). However, Se concentrations were enhanced by the S doses in the CT soil but dramatically decreased in the SCLT soil. In the CT soil, the highest Se dose promoted ~2.5-fold and 6.5-fold higher Se concentrations in the rice grain (brown and white rice) and husk, respectively, compared to those under the non-S supply condition (Figure 7a, c, and e). Conversely, the same S doses reduced the Se concentrations by 40 and 56% in the

white rice and the brown rice husk, respectively, of the plants grown in the SCLT soil at the highest Se dose, compared to the absence of S (Figure 7b, d, and f).

## 4. Discussion

We observed that sulfate supply enhanced rice tolerance to selenate in both short- and long-term experiments. In the short-term experiment, the selenate treatment promoted higher selenium contents in the plants grown with 0.1 mM S, causing severe toxicity symptoms (Figures 1 and S2). These results suggest that rice seedlings grown under the S-limited condition can absorb greater selenate amounts, inducing toxicity and growth impairment. At the same time, higher sulfate availability reduced selenate uptake, relieving Se toxicity by decreasing Se concentrations in plants, particularly in the roots. Thus, a competition between selenate and sulfate uptake was evidenced in rice seedlings, contributing to the S protective effect against Se toxicity.

This competition probably is due to the shared S and Se uptake transporters in the roots (Boldrin et al., 2016; Tian et al., 2017). Conversely, the Se and S contents in plants from long-term experiments indicate a synergism between the two components, suggesting that tolerance mechanisms are related to the growth stage. These divergent results can be related to rice seedlings' higher nutrient uptake capacity (Fageria, 2004; Hashim et al., 2015), allowing enough sulfate uptake to inhibit selenate absorption, and can explain the higher selenium and sulfur contents on rice seedlings, despite the shorter time.

Moreover, the synergism between selenate and sulfate in the long-term experiments can be related to the influence of selenate upon the sulfur transporters observed in the short-time experiment. The selenate treatment induced the expression of genes that encode the transporters responsible for sulfate uptake on rice roots, with specific effects according to the gene studied. Selenate increased the *SULTR1;2* expression by around 2-folds regardless of sulfur supply (Figure 2b) while increasing the *SULTR1;1* expression by 27-folds at low sulfur supply (Figure 2a). Despite the reports of *SULTR1;1* upregulation by selenate (Boldrin et al., 2018; El Mehdawi et al., 2018; Tian et al., 2017), its induction mechanisms remain unknown. However, the *SULTR1;2* response is probably related to the sulfur concentration reduction in root tissue by selenate treatment (Figure 1g) since its expression responds to low sulfate concentrations in roots (Zheng et al., 2014). Thus, *SULTR1;2* upregulation consists of a sulfur-deficiency-alleviation mechanism, inducing the expression of the transporter gene to increase sulfate uptake (Zhang et al., 2014), which can be responsible for the sulfur content

increase in the shoots of the rice plants grown with 0.5 mM S under a Se-treated condition (Figures 1f and S2c).

Similarly, the selenate-upregulated *SULTR1;2* expression was associated with higher S contents in plants grown in the SCLT soil upon selenate exposure (Figures 6d and S4d). This result suggests that a higher S-transporter activity can enhance the sulfur accumulation from tillering to the grain ripening phase of the rice plants. In contrast, low S availability probably could nullify this effect since the plants grown in the short-time experiment with 0.1 mM S under Se treatment did not exhibit an increase in sulfur content in the shoots (Figures 1f and S2c), even though a higher *SULTR1;2* expression was present (Figure 2b). However, a higher SULTR1;2 activity also can increase the selenium accumulation, considering the affinity of SULTR1;2 for selenate uptake (Shibagaki et al., 2002), which can contribute to the synergism between sulfate and selenate uptake in the long-term experiments (Figures 6b, 6d, S4b, and S4d). Thus, the relationship between selenate and sulfate uptake on rice plants seems to vary according to the plant's developmental stage, presenting inhibitory competition in the tillering phase but synergism at the late stage of the ripening phase.

Despite the inhibitory competition between S and Se uptake, rice seedlings cultivated with higher sulfate availability under selenate exposure exhibited expressive selenium concentrations, mainly in the shoots (Figure 1). However, despite their high selenium contents, these plants did not present visual toxicity symptoms and growth impairment. These results suggest that a higher sulfur supply can alleviate selenate toxicity through other protective mechanisms, which act after selenate uptake and transport to the shoots, in addition to selenate uptake inhibition. This protective action probably is related to the S-enhanced antioxidant system against the Se-caused oxidative stress. This hypothesis is supported by increased $H_2O_2$ concentrations in shoots of rice plants exposed to selenate under a high sulfur supply compared to the control treatment (Figure 3e). The oxidative stress could be caused by higher MDA concentrations in these plants, considering MDA is a product of cell membrane degradation by ROS (Morales and Munné-Bosch, 2019).

However, the plants exposed to selenate under high sulfur supply also presented higher CAT and APX activities and higher GSH contents, which probably counteracted the ROS deleterious effects since CAT and APX activities are crucial for $H_2O_2$ degradation (Zámocký et al., 2014). Similarly, GSH is a vital molecule for ROS detoxification, acting as a substrate for antioxidant enzymes (e.g., GSH peroxidases and GSH sulfotransferases) and a precursor for phytochelatins (Anjum et al., 2011). Interestingly, the plants cultivated with low sulfur supply and selenate exposure did not enhance the antioxidant system. Thus, these

results indicate that sulfur is necessary for the antioxidant system in response to selenate toxicity, as indicated by the higher sulfur content in the shoots of the plants (Figure 1f). This positive effect probably is related to the sulfur role in the constitution of cysteine and methionine, amino acids required for protein and enzyme synthesis (Günal et al., 2019).

Similarly, cysteine is required for GSH formation (Ravilious and Jez, 2012). Thus, sulfur uptake and accumulation promoted by selenate are essential to the antioxidant system in rice plants. However, this mechanism is ineffective under a low sulfur supply. Furthermore, divergent results were observed in plants' enzymatic activities and stress indicators during the long-term experiments (Figure S6), probably caused by the metabolism reduction at the ripening phase (Liu et al., 2017).

The selenate sorption dynamics were related to the clay content, with higher selenium adsorption in the soil containing higher clay contents. This hypothesis is supported by the percentual values of the clay content and selenate adsorption, with CT soil presenting 62% clay and 67% Se adsorbed, while SCLT presented 24% clay and 24% Se adsorbed. This reaction is probably caused by the binding between the positive charges in the clay minerals and the selenate negative charges (Araujo et al., 2020; Lessa et al., 2016), which can be more pronounced in tropical soils, like the Oxisols studied, considering their positive charge predominance (Jiang et al., 2011). Therefore, the higher selenate adsorption and corresponding lower Se availability resulted in lower selenate uptake in plants cultivated in the CT soil, leading to no plant toxicity symptoms.

Conversely, the plants cultivated in the SCLT soil presented higher selenium contents and growth and yield impairment. Sulfate increased the selenate adsorption in the SCLT soil and decreased the desorption in CT soil, suggesting that S decreased selenate availability. However, these effects are temporary since the plants cultivated with sulfur supply presented higher selenium contents in both soils. Thus, sulfate promoted higher selenate contents probably by increases in root growth and by the competition with selenate for the positive charges in the soil, releasing the selenate adsorbed (Araujo et al., 2020; Santos et al., 2021).

Taken together, soils with low clay contents present lower selenate adsorption capacity, increasing selenate availability and accumulation in shoots, husks, brown rice, and white rice. Thus, the lower selenate adsorption on soils increases the selenate toxicity risk for rice plants and, consequently, for humans and animals consuming rice grains with high selenium contents. Interestingly, we did not detect selenium on rice grains of plants grown without selenate addition on both soils, despite the selenium availability indicated by the small concentrations in their shoots and in the soils under natural conditions. These results

suggest that the selenium supply is required to enrich the rice grains due to its small availability in the soils. At last, future studies aiming to evaluate the selenium biofortification in rice grains can adopt selenate doses around 0.14 and 0.02 mg $dm^{-3}$ Se for CT and SCLT similar soils, respectively. These selenate doses would promote selenium concentrations around 50 μg Se (selenium amount required per person per day approximately, according to Winkel et al., 2012) per 100 g of dry rice grains, according to regression equations of selenium concentrations (Table S4).

## 5. Conclusions

Selenate treatment decreases the sulfur concentrations in the roots of rice seedlings, inducing the sulfate transporter activity and sulfur accumulation from tillering to ripening stages. A high sulfur content enhances the antioxidant mechanisms, counteracting selenate toxicity. However, this alleviation mechanism is ineffective in rice plants grown under sulfur deficiency. In the long term, selenate treatment probably enhanced both selenium and sulfur accumulations in rice plants through sulfate transporters induction. Furthermore, the selenate uptake can also be regulated by the clay content in the soils, with higher clay contents decreasing its availability through the higher adsorption capacity. Conversely, soils with lower clay contents possess higher selenate availability, promoting higher selenium contents in rice shoots and grains and possibly increasing the toxicity risk to plants and animals.

## REFERENCES

Ajwa, H.A., Tabatabai, M.A., 1993. Comparison of some methods for determination of sulfate in soils. Commun. Soil Sci. Plant Anal. 24, 1817–1832. https://doi.org/10.1080/00103629309368920

Akbulut, M., Çakir, S., 2010. The effects of Se phytotoxicity on the antioxidant systems of leaf tissues in barley (*Hordeum vulgare* L.) seedlings. Plant Physiol. Biochem. 48, 160–166. https://doi.org/10.1016/j.plaphy.2009.11.001

Alfthan, G., Eurola, M., Ekholm, P., Venäläinen, E.R., Root, T., Korkalainen, K., Hartikainen, H., Salminen, P., Hietaniemi, V., Aspila, P., Aro, A., 2015. Effects of nationwide addition of selenium to fertilizers on foods, and animal and human health in Finland: From deficiency to optimal selenium status of the population. J. Trace Elem. Med. Biol. 31, 142–147. https://doi.org/10.1016/j.jtemb.2014.04.009

Anjum, N.A., Ahmad, I., Mohmood, I., Pacheco, M., Duarte, A.C., Pereira, E., Umar, S., Ahmad, A., Khan, N.A., Iqbal, M., Prasad, M.N.V., 2011. Modulation of glutathione and its related enzymes in plants' responses to toxic metals and metalloids - A review. Environ. Exp. Bot. 75, 307–324. https://doi.org/10.1016/j.envexpbot.2011.07.002

Araujo, A.M., Lessa, J.H. de L., Chanavat, L.G., Curi, N., Guilherme, L.R.G., Lopes, G., 2020. How sulfate content and soil depth affect the adsorption/desorption of selenate and selenite in tropical soils? Rev. Bras. Cienc. do Solo 44, e0200087. https://doi.org/10.36783/18069657RBCS20200087

Boldrin, P.F., de Figueiredo, M.A., Yang, Y., Luo, H., Giri, S., Hart, J.J., Faquin, V., Guilherme, L.R.G., Thannhauser, T.W., Li, L., 2016. Selenium promotes sulfur accumulation and plant growth in wheat (*Triticum aestivum*). Physiol. Plant. 158, 80–91. https://doi.org/10.1111/ppl.12465

Boldrin, P.F., Faquin, V., Da Consolação Sampaio Clemente, A., De Andrade, T., Guilherme, L.R.G., 2018. Genotypic variation and biofortification with selenium in brazilian wheat cultivars. J. Environ. Qual. 47, 1371–1379. https://doi.org/10.2134/jeq2018.01.0045

Bradford, M.M., 1976. A rapid and sensitive method for the quantitation of microgram quantities of protein utilizing the principle of protein-dye binding. Anal. Biochem. 72, 248–254. https://doi.org/10.1016/0003-2697(76)90527-3

Dixit, G., Singh, A.P., Kumar, A., Mishra, S., Dwivedi, S., Kumar, S., Trivedi, P.K., Pandey, V., Tripathi, R.D., 2016. Reduced arsenic accumulation in rice (*Oryza sativa* L.) shoot involves sulfur mediated improved thiol metabolism, antioxidant system and altered arsenic transporters. Plant Physiol. Biochem. 99, 86–96. https://doi.org/10.1016/j.plaphy.2015.11.005

El Mehdawi, A.F., Jiang, Y., Guignardi, Z.S., Esmat, A., Pilon, M., Pilon-Smits, E.A.H., Schiavon, M., 2018. Influence of sulfate supply on selenium uptake dynamics and expression of sulfate/selenate transporters in selenium hyperaccumulator and nonhyperaccumulator Brassicaceae. New Phytol. 217, 194–205. https://doi.org/10.1111/nph.14838

Eyarkai Nambi, V., Manickavasagan, A., Shahir, S., 2017. Rice milling technology to produce brown rice, in: Manickavasagan, A., Santhakumar, C., Venkatachalapathy, N. (Eds.), Brown Rice. Springer International Publishing, Cham, pp. 3–21. https://doi.org/10.1007/978-

3-319-59011-0_1

Fageria, N.K., 2004. Dry matter yield and nutrient uptake by lowland rice at different growth stages. J. Plant Nutr. 27, 947–958. https://doi.org/10.1081/PLN-120037529

FAO, Food and Agriculture Organization of the United Nations, WHO, World Health Organization, 2004. Vitamin and mineral requirements in human nutrition, 2nd ed, World Health Organization and Food and Agriculture Organization of the United Nations. World Health Organization, Geneva. https://doi.org/9241546123

Ferreira, D.F., 2019. Sisvar: a computer analysis system to fixed effects split plot type designs. Rev. Bras. Biometria 37, 529. https://doi.org/10.28951/rbb.v37i4.450

Garousi, F., Veres, S., Kovács, B., 2016. Comparison of selenium toxicity in sunflower and maize seedlings grown in hydroponic cultures. Bull. Environ. Contam. Toxicol. 97, 709–713. https://doi.org/10.1007/s00128-016-1912-6

Günal, S., Hardman, R., Kopriva, S., Mueller, J.W., 2019. Sulfation pathways from red to green. J. Biol. Chem. 294, 12293–12312. https://doi.org/10.1074/jbc.REV119.007422

Gupta, M., Gupta, S., 2017. An overview of selenium uptake, metabolism, and toxicity in plants. Front. Plant Sci. 7, 1–14. https://doi.org/10.3389/fpls.2016.02074

Hashim, M.M. az, Yusop, M.K., Othman, R., Wahid, S.A., 2015. Characterization of nitrogen uptake pattern in malaysian rice MR219 at different growth stages using 15N isotope. Rice Sci. 22, 250–254. https://doi.org/10.1016/j.rsci.2015.09.005

Havir, E.A., McHale, N.A., 1987. Biochemical and developmental characterization of multiple forms of catalase in tobacco leaves. Plant Physiol. 84, 450–455. https://doi.org/10.1104/pp.84.2.450

Jiang, J., Xu, R. Zhao, A. 2011. Surface chemical properties and pedogenesis of tropical soils derived from basalts with different ages in Hainan, China. Catena 87, 334–340. https://doi.org/10.1016/j.catena.2011.06.016

Jing, D.W., Du, Z.Y., Ma, H.L., Ma, B.Y., Liu, F.C., Song, Y.G., Xu, Y.F., Li, L., 2017. Selenium enrichment, fruit quality and yield of winter jujube as affected by addition of sodium selenite. Sci. Hortic. 225, 1–5. https://doi.org/10.1016/j.scienta.2017.06.036

Kaur, S., Singh, D., Singh, K., 2017. Effect of selenium application on arsenic uptake in rice (*Oryza sativa* L.). Environ. Monit. Assess. 189. https://doi.org/10.1007/s10661-017-6138-5

Łabanowska, M., Filek, M., Kościelniak, J., Kurdziel, M., Kuliś, E., Hartikainen, H., 2012. The effects of short-term selenium stress on Polish and Finnish wheat seedlings-EPR, enzymatic and fluorescence studies. J. Plant Physiol. 169, 275–284. https://doi.org/10.1016/j.jplph.2011.10.012

Lessa, J.H.L., Araujo, A.M., Silva, G.N.T., Guilherme, L.R.G., Lopes, G., 2016. Adsorption-desorption reactions of selenium (VI) in tropical cultivated and uncultivated soils under Cerrado biome. Chemosphere 164, 271–277. https://doi.org/10.1016/j.chemosphere.2016.08.106

Liu, H., Zhang, C., Wang, J., Zhou, C., Feng, H., Mahajan, M.D., Han, X., 2017. Influence and interaction of iron and cadmium on photosynthesis and antioxidative enzymes in two rice cultivars. Chemosphere 171, 240–247. https://doi.org/10.1016/j.chemosphere.2016.12.081

Malagoli, M., Schiavon, M., Dall'Acqua, S., Pilon-Smits, E.A.H., 2015. Effects of selenium biofortification on crop nutritional quality. Front. Plant Sci. 6, 1–5. https://doi.org/10.3389/fpls.2015.00280

McGrath, S.P., Cunliffe, C.H., 1985. A simplified method for the extraction of the metals Fe, Zn, Cu, Ni, Cd, Pb, Cr, Co and Mn from soils and sewage sludges. J. Sci. Food Agric. 36, 794–798. https://doi.org/10.1002/jsfa.2740360906

Morales, M., Munné-Bosch, S., 2019. Malondialdehyde: Facts and Artifacts. Plant Physiol. 180, 1246–1250. https://doi.org/10.1104/pp.19.00405

Nakano, Y., Asada, K., 1981. Hydrogen peroxide is scavenged by ascorbate-specific peroxidase in spinach chloroplasts. Plant Cell Physiol. 22, 867–880. https://doi.org/10.1093/oxfordjournals.pcp.a076232

Peng, Q., Wang, M., Cui, Z., Huang, J., Chen, C., Guo, L., Liang, D., 2017. Assessment of bioavailability of selenium in different plant-soil systems by diffusive gradients in thin-films (DGT). Environ. Pollut. 225, 637–643. https://doi.org/10.1016/j.envpol.2017.03.036

Puccinelli, M., Malorgio, F., Rosellini, I., Pezzarossa, B., 2017. Uptake and partitioning of selenium in basil (*Ocimum basilicum* L.) plants grown in hydroponics. Sci. Hortic. 225, 271–276. https://doi.org/10.1016/j.scienta.2017.07.014

Rahman, I., Kode, A., Biswas, S.K., 2007. Assay for quantitative determination of glutathione and glutathione disulfide levels using enzymatic recycling method. Nat. Protoc. 1, 3159–3165. https://doi.org/10.1038/nprot.2006.378

Ravilious, G.E., Jez, J.M., 2012. Structural biology of plant sulfur metabolism: From assimilation to biosynthesis. Nat. Prod. Rep. 29, 1138–1152. https://doi.org/10.1039/c2np20009k

Santos, M.J.V. dos, De Lima Lessa, J.H., De Assis, M.B., Raymundo, J.F., Ribeiro, B.T., Guilherme, L.R.G., Lopes, G., 2021. Selenium desorption in tropical soils by sulfate and phosphate, and selenium biofortification of Mombaça grass under increasing rates of phosphate fertilisation. Crop Pasture Sci. 56–66. https://doi.org/10.1071/CP21059

Schiavon, M., Moro, I., Pilon-Smits, E.A.H., Matozzo, V., Malagoli, M., Dalla Vecchia, F., 2012. Accumulation of selenium in Ulva sp. and effects on morphology, ultrastructure and antioxidant enzymes and metabolites. Aquat. Toxicol. 122–123, 222–231. https://doi.org/10.1016/j.aquatox.2012.06.014

Sharma, V.K., McDonald, T.J., Sohn, M., Anquandah, G.A.K., Pettine, M., Zboril, R., 2017. Assessment of toxicity of selenium and cadmium selenium quantum dots: A review. Chemosphere 188, 403–413. https://doi.org/10.1016/j.chemosphere.2017.08.130

Shibagaki, N., Rose, A., McDermott, J.P., Fujiwara, T., Hayashi, H., Yoneyama, T., Davies, J.P., 2002. Selenate-resistant mutants of Arabidopsis thaliana identify *Sultr1;2*, a sulfate transporter required for efficient transport of sulfate into roots. Plant J. 29, 475–486.

https://doi.org/10.1046/j.0960-7412.2001.01232.x

Terzi, H., Yıldız, M., 2015. Interactive effects of sulfur and chromium on antioxidative defense systems and BnMP1 gene expression in canola (*Brassica napus* L.) cultivars differing in Cr(VI) tolerance. Ecotoxicology 24, 1171–1182. https://doi.org/10.1007/s10646-015-1468-y

Tian, M., Hui, M., Thannhauser, T.W., Pan, S., Li, L., 2017. Selenium-induced toxicity is counteracted by sulfur in broccoli (*Brassica oleracea* L. var. *italica*). Front. Plant Sci. 8, 1–13. https://doi.org/10.3389/fpls.2017.01425

Toler, H.D., Charron, C.S., Kopsell, D.A., Sams, C.E., Randle, W.M., 2007. Selenium and sulfur increase sulfur uptake and regulate glucosinolate metabolism in *Brassica oleracea*. Acta Hortic. 744, 311–316. https://doi.org/10.17660/ActaHortic.2007.744.32

USDA, United States Department of Agriculture, 1999. Soil taxonomy: A basic system of soil classification for making and interpreting soil surveys. U.S. Dep. Agric. Handb. 436.

USDA, United States Department of Agriculture, 2014. Kellogg soil survey laboratory methods manual. URL https://www.nrcs.usda.gov/wps/portal/nrcs/detail/soils

USDA, United States Department of Agriculture, 2022. Soil texture calculator. URL https://www.nrcs.usda.gov/wps/portal/nrcs

Velikova, V., Yordanov, I., Edreva, A., 2000. Oxidative stress and some antioxidant systems in acid rain-treated bean plants. Plant Sci. 151, 59–66. https://doi.org/10.1016/S0168-9452(99)00197

Wiesner-Reinhold, M., Schreiner, M., Baldermann, S., Schwarz, D., Hanschen, F.S., Kipp, A.P., Rowan, D.D., Bentley-Hewitt, K.L., McKenzie, M.J., 2017. Mechanisms of selenium enrichment and measurement in brassicaceous vegetables, and their application to human health. Front. Plant Sci. 8. https://doi.org/10.3389/fpls.2017.01365

Winkel, L.H.E., Johnson, C.A., Lenz, M., Grundl, T., Leupin, O.X., Amini, M., Charlet, L., 2012. Environmental selenium research: From microscopic processes to global understanding. Environ. Sci. Technol. 46, 571–579. https://doi.org/10.1021/es203434d

Zámocký, M., Gasselhuber, B., Furtmüller, P.G., Obinger, C., 2014. Turning points in the evolution of peroxidase–catalase superfamily: molecular phylogeny of hybrid heme peroxidases. Cell. Mol. Life Sci. 71, 4681–4696. https://doi.org/10.1007/s00018-014-1643-y

Zhang, B., Pasini, R., Dan, H., Joshi, N., Zhao, Y., Leustek, T., Zheng, Z.L., 2014. Aberrant gene expression in the Arabidopsis *SULTR1;2* mutants suggests a possible regulatory role for this sulfate transporter in response to sulfur nutrient status. Plant J. 77, 185–197. https://doi.org/10.1111/tpj.12376

Zhang, Y., Pan, G., Chen, J., Hu, Q., 2003. Uptake and transport of selenite and selenate by soybean seedlings of two genotypes. Plant Soil 253, 437–443. https://doi.org/10.1023/A:1024874529957

Zheng, Z.L., Zhang, B., Leustek, T., 2014. Transceptors at the boundary of nutrient transporters and receptors: A new role for *Arabidopsis* SULTR1;2 in sulfur sensing. Front. Plant Sci. 5, 1–5. https://doi.org/10.3389/fpls.2014.00710

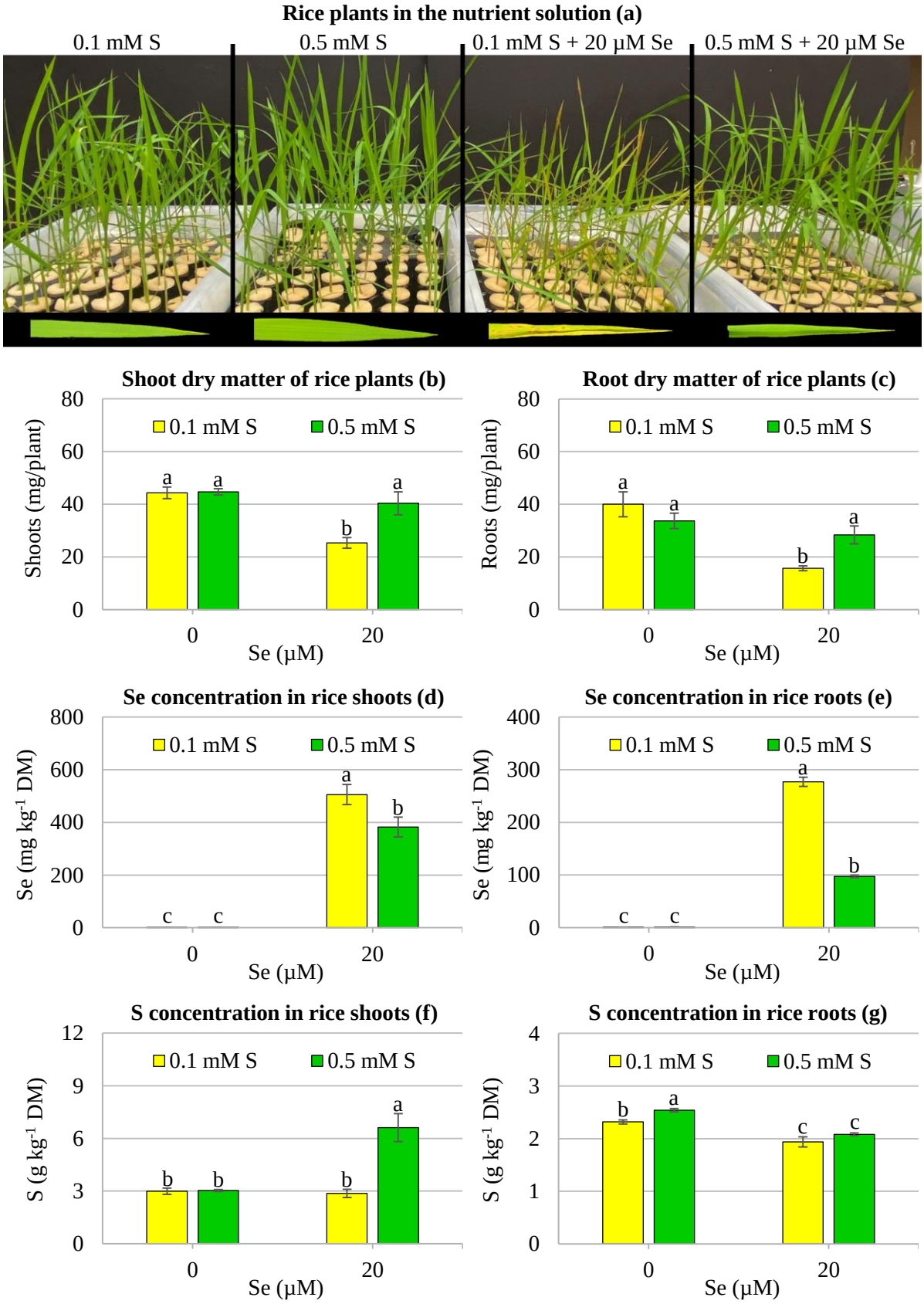


Figure 1. Short-term experiment with rice plants grown in the nutrient solution containing different S and Se doses. Plants at harvest time (a). Shoots (b) and roots production (c). Se concentrations in shoots (d) and roots (e). S concentrations in shoots (f) and roots (g). Columns with different letters differ by the Scott-Knott test (n = 12, $p < 0.05$).

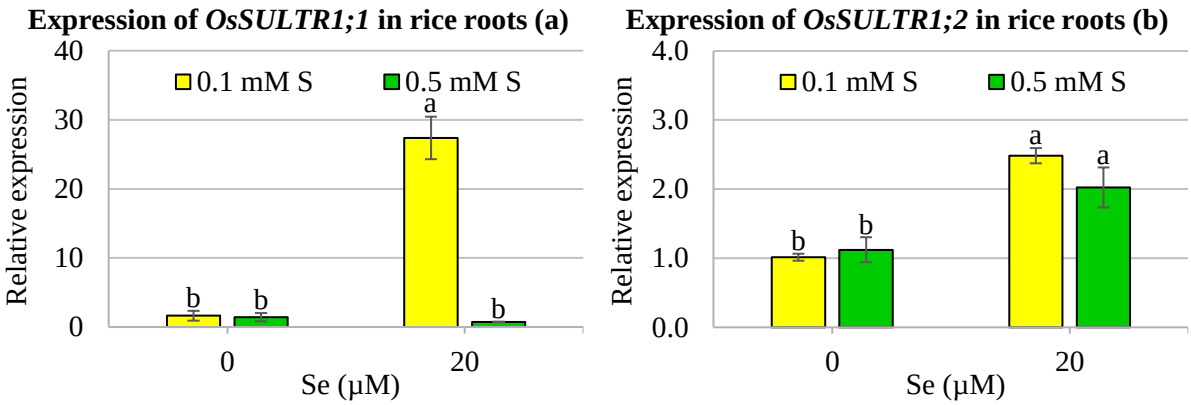


Figure 2. Relative expression of *OsSULTR1;1* (a) and *OsSULTR1;2* (b) in roots of rice plants grown in the nutrient solution under S and Se doses (short-term experiment). Columns with different letters differ by the Scott-Knott test (n = 12, $p < 0.05$).

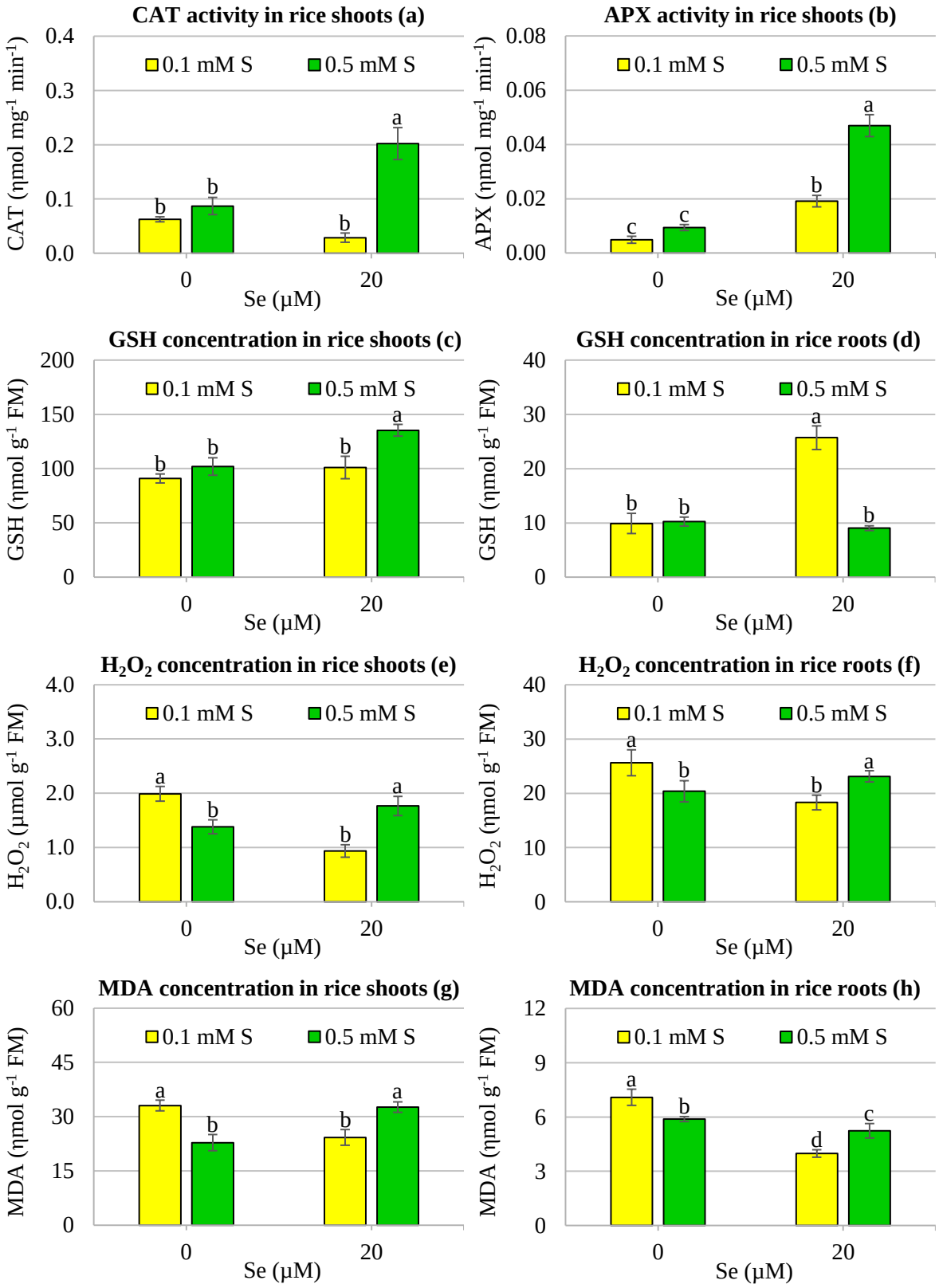


Figure 3. Antioxidant mechanisms and stress indicators in rice plants grown in the nutrient solution under S and Se doses (short-term experiment). Catalase (CAT, a) and ascorbate peroxidase (APX, b) shoot activities. Reduced glutathione (GSH) concentrations in shoots (c) and roots (d). Hydrogen peroxide ($H_2O_2$) concentrations in shoots (e) and roots (f). Malondialdehyde (MDA) concentrations in shoots (g) and roots (h). Columns with different letters differ by the Scott-Knott test (n = 12, $p < 0.05$).

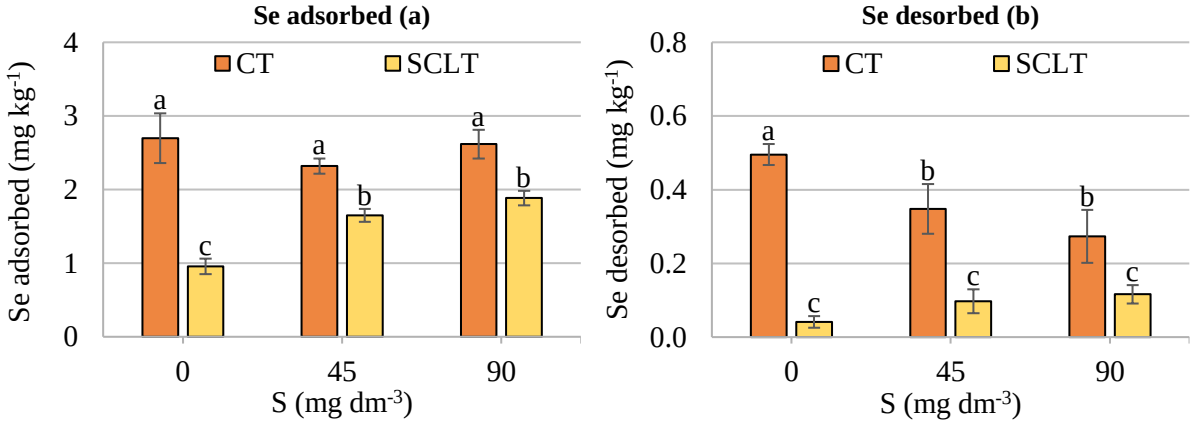


Figure 4. Selenium sorption in soils with different textures under S doses. Concentrations of Se adsorbed after 72 h of exposure to 4.0 mg $kg^{-1}$ Se (a). Concentrations of Se desorbed after 72 h extraction in the samples of adsorption assay (b). CT: clay texture. SCLT: sandy clay loam texture. Columns with different letters differ by the Scott-Knott test (n = 24, $p < 0.05$).

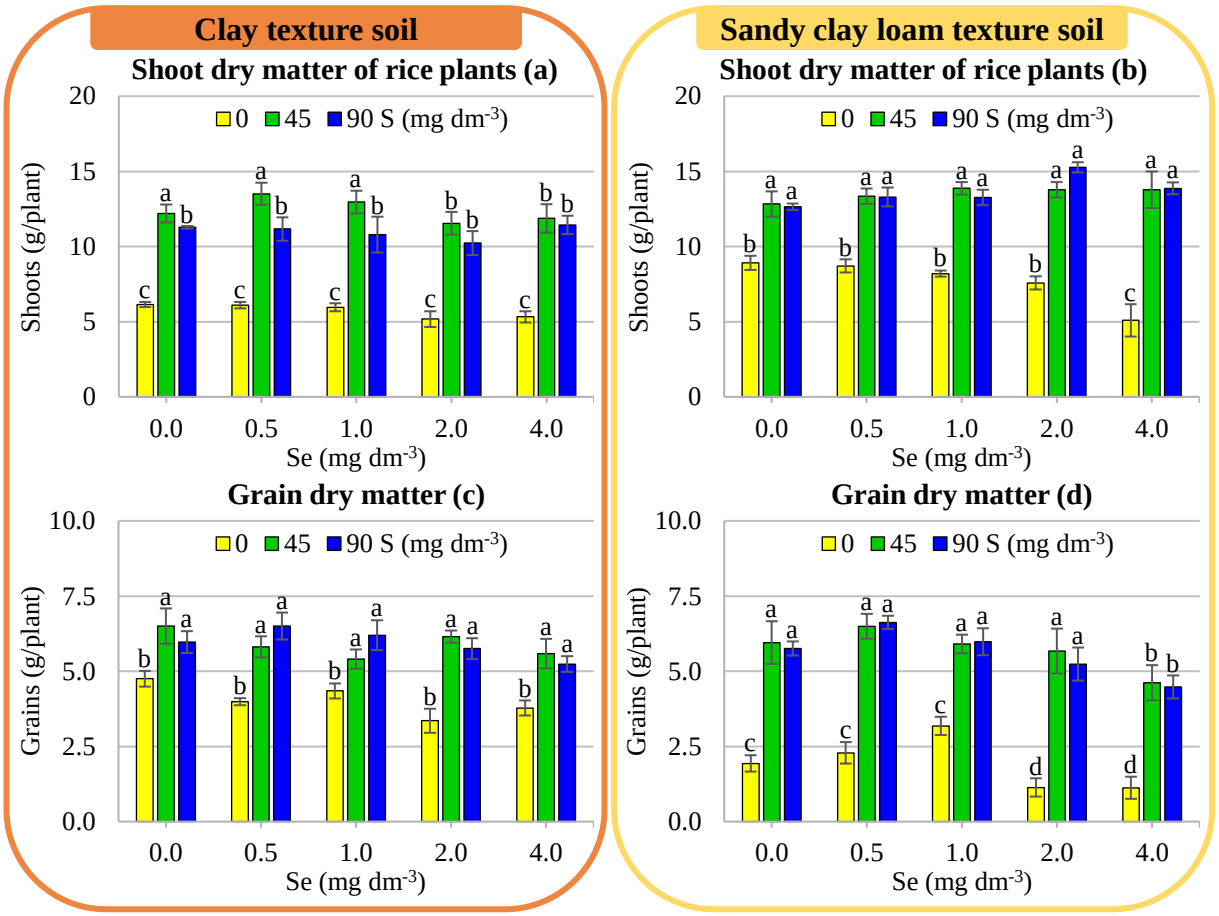


Figure 5. Growth and yield of rice plants cultivated in soils with different textures under S and Se doses (long-term experiment). Shoots (a and b) and grains (c and d) production. Columns with different letters in each soil differ by the Scott-Knott test (n = 60, $p < 0.05$).

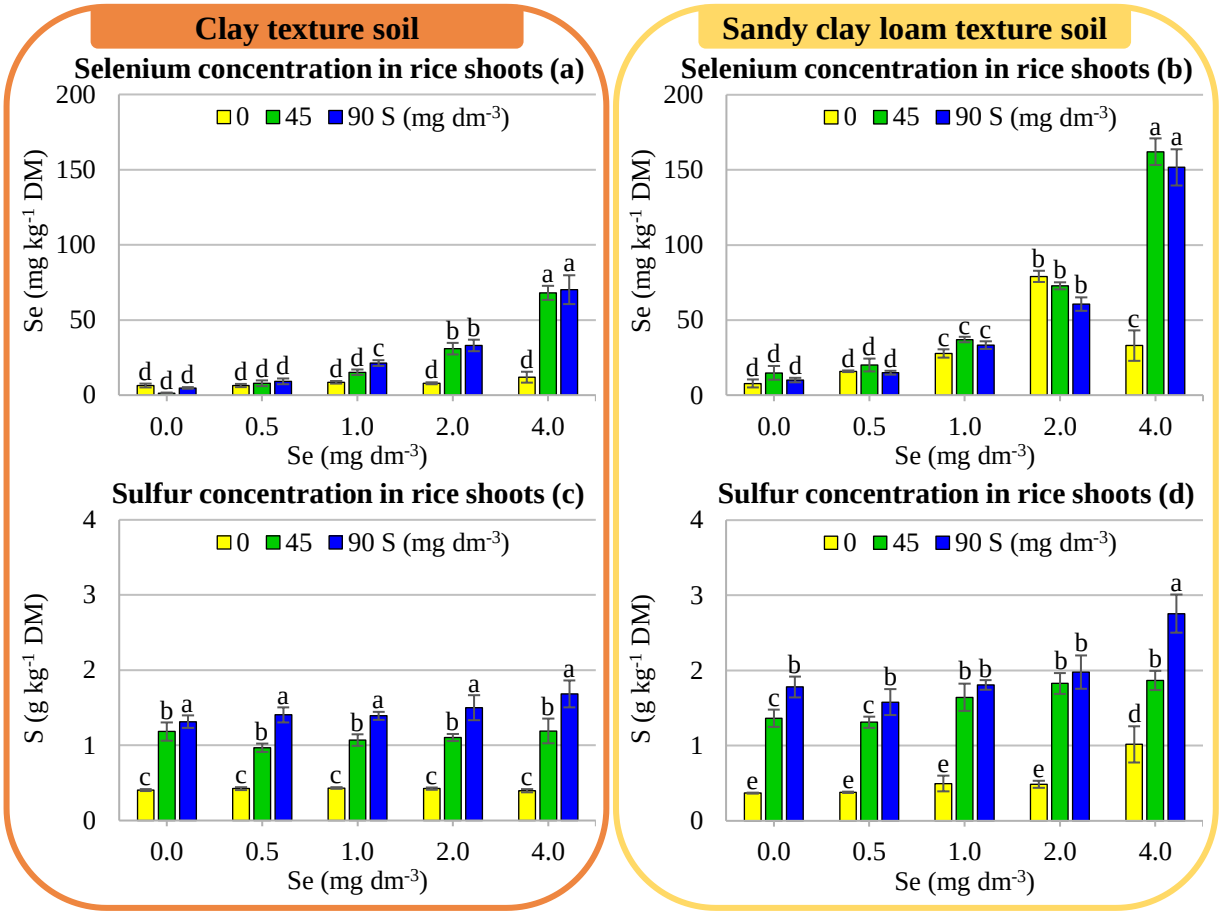


Figure 6. Selenium (a and b) and sulfur (c and d) concentrations in shoots of rice plants cultivated in soils with different textures under Se and S doses (long-term experiment). Columns with different letters in each soil differ by the Scott-Knott test (n = 60, $p < 0.05$).

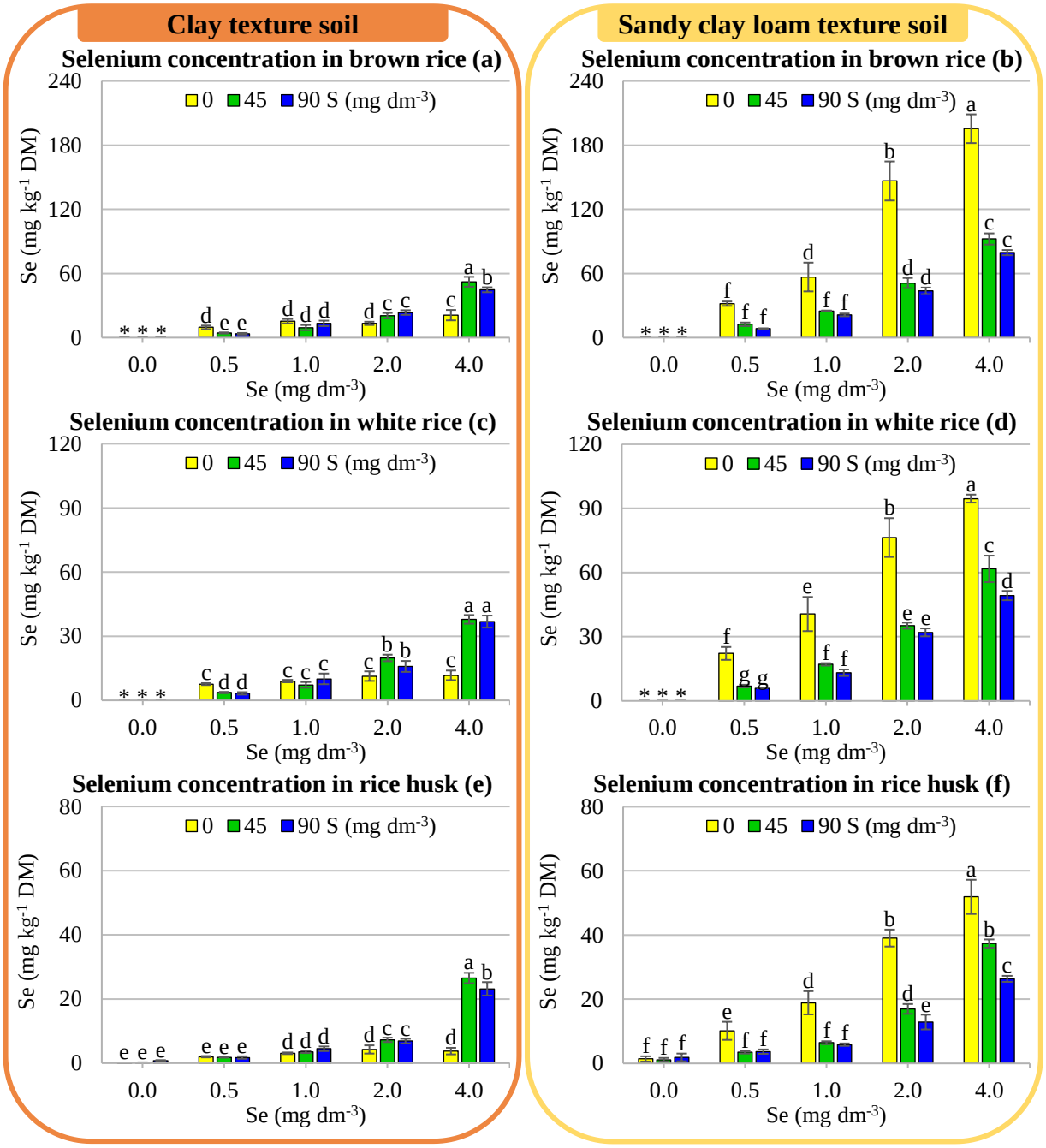


Figure 7. Selenium concentrations in rice grains cultivated in soils with different textures under Se and S doses (long-term experiment). Selenium concentrations in brown rice (a and b), white rice (c and d), and husk (e and f). Columns with different letters in each soil differ by the Scott-Knott test (n = 60, $p < 0.05$). *Below detection limit.

## Supplemental

Table S1. Nutrient solution compositions (ml $L^{-1}$).

| Treatment | $Na_2SeO_4$ (20 mM) | $MgSO_4$ (1 M) | $MgCl_2$ (1 M) | $KNO_3$ (1 M) | $Ca(NO_3)_2$ (1 M) | $KH_2PO_4$ (1 M) | Micronutrient solution | Fe-EDTA |
|---|---|---|---|---|---|---|---|---|
| 0 µM Se + 0.1 mM S (T1) | - | 0.1 | 1.9 | 5 | 5 | 1 | 1 | 1 |
| 0 µM Se + 0.5 mM S (T2) | - | 0.5 | 1.5 | 5 | 5 | 1 | 1 | 1 |
| 20 µM Se + 0.1 mM S (T3) | 1 | 0.1 | 1.9 | 5 | 5 | 1 | 1 | 1 |
| 20 µM Se + 0.5 mM S (T4) | 1 | 0.5 | 1.5 | 5 | 5 | 1 | 1 | 1 |

Micronutrient solution: $H_3BO_3$ (46 mM), $CuCl_2$ (0.3 mM), $MnCl_2 \cdot 4H_2O$ (9.1 mM), $H_2MoO_4$ (0.1 mM), and $ZnCl_2$ (0.7 mM). Fe-EDTA: $FeCl_2 \cdot 6H_2O$ (100 mM) + EDTA (89 mM) dissolved in NaOH (89 mM).

Table S2. Soil chemical properties.

| | pH | SOC | Se | S | P | K | Ca | Mg |
|---|---|---|---|---|---|---|---|---|
| | | -- g $kg^{-1}$ -- | ---------- mg $kg^{-1}$ ---------- | | | | --- $cmol_c$ $kg^{-1}$ --- | |
| CT soil | 5.5 | 3.8 | 0.6 | 2.5 | 0.6 | 16 | 0.3 | 0.1 |
| SCLT soil | 6.5 | 5.2 | 0.3 | 4.6 | 0.1 | 33 | 0.1 | 0.1 |
| | **Al** | **H + Al** | **V** | **B** | **Cu** | **Fe** | **Mn** | **Zn** |
| | --- $cmol_c$ $kg^{-1}$ --- | | -- % -- | ---------- mg $kg^{-1}$ ---------- | | | | |
| CT soil | 0.04 | 1.8 | 19 | 0.01 | 0.9 | 30 | 5.4 | 0.6 |
| SCLT soil | 0.30 | 1.8 | 15 | 0.03 | 0.1 | 28 | 1.3 | 0.1 |

pH in water (soil-to-solution ratio 1:2.5). SOC: soil organic carbon. Se: pseudo-total content. Al and H + Al by titration method with 0.025 M NaOH. V: base saturation [(Ca + Mg + K) / Ca + Mg + K + 'H + Al')]·100.

Table S3. Primers used in the study.

| Gene ID | Description | Sequence |
|---|---|---|
| *OsSULTR1;1* (Os03g09970) | *O. sativa* sulfate transporter 1;1 | F: GGCGGCCATCATCATCATC<br>R: CCTTCTTTGACATCGGCTGG |
| *OsSULTR1;2* (Os03g09980) | *O. sativa* sulfate transporter 1;2 | F: GAAGAAGAACCTCCTGGCG<br>R: TCGAACACCGGGAAGACGT |
| *OsACT* (Os03g50885) | O. sativa actin | F: CTTCATAGGAATGGAAGCTGCGGGTA<br>R: CGACCACCTTGATCTTCATGCTGCTA |

F: forward primer. R: reverse primer.

Table S4. Regression equations for selenium concentrations in rice tissues (mg $kg^{-1}$ Se in dry matter) as a function of soil selenate doses (x = mg $dm^{-3}$ Se) under S doses.

| | | CT soil | | SCLT soil | |
|---|---|---|---|---|---|
| Tissue | S (mg $dm^{-3}$) | Equation | $R^2$ | Equation | $R^2$ |
| SDM | 0 | $Se = 1.34^{**}x + 6.20$ | 0.88 | $Se = -12^{**}x^2 + 57.6^{**}x - 2.62$ | 0.80 |
| brown rice | 0 | $Se = 2.74^{**}x + 9.71$ | 0.79 | $Se = 47.37^{**}x + 18.81$ | 0.92 |
| white rice | 0 | $Se = 1.11^{**}x + 7.80$ | 0.78 | $Se = 20.09^{**}x + 20.75$ | 0.89 |
| husk rice | 0 | $Se = -0.61^{**}x^2 + 3.3^{**}x + 0.27$ | 0.99 | $Se = 12.76^{**}x + 5.13$ | 0.94 |
| SDM | 45 | $Se = 16.80^{**}x - 0.47$ | 0.99 | $Se = 38.06^{**}x + 4.31$ | 0.98 |
| brown rice | 45 | $Se = 13.81^{**}x - 4.31$ | 0.99 | $Se = 22.77^{**}x + 2.50$ | 0.99 |
| white rice | 45 | $Se = 9.98^{**}x - 1.55$ | 0.99 | $Se = 15.47^{**}x + 1.20$ | 0.99 |
| husk rice | 45 | $Se = 6.61^{**}x - 2.05$ | 0.94 | $Se = 9.35^{**}x - 0.96$ | 0.99 |
| SDM | 90 | $Se = 16.48^{**}x + 3.00$ | 0.99 | $Se = 36.26^{**}x - 0.20$ | 0.98 |
| brown rice | 90 | $Se = 11.36^{**}x - 0.01$ | 0.99 | $Se = 20.17^{**}x + 0.37$ | 0.99 |
| white rice | 90 | $Se = 9.18^{**}x - 0.57$ | 0.99 | $Se = 12.65^{**}x + 1.07$ | 0.97 |
| husk rice | 90 | $Se = 5.62^{**}x - 1.02$ | 0.95 | $Se = 6.30^{**}x + 0.65$ | 0.99 |

SDM: shoot dry matter. ** $p > 0.01$.

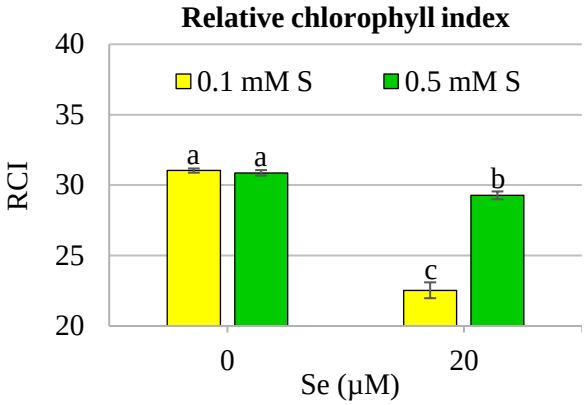


Figure S1. Relative chlorophyll index (RCI) in leaves of rice plants grown in nutrient solutions under S and Se doses (short-term experiment). Columns with different letters differ by the Scott-Knott test (n = 12, $p < 0.05$).

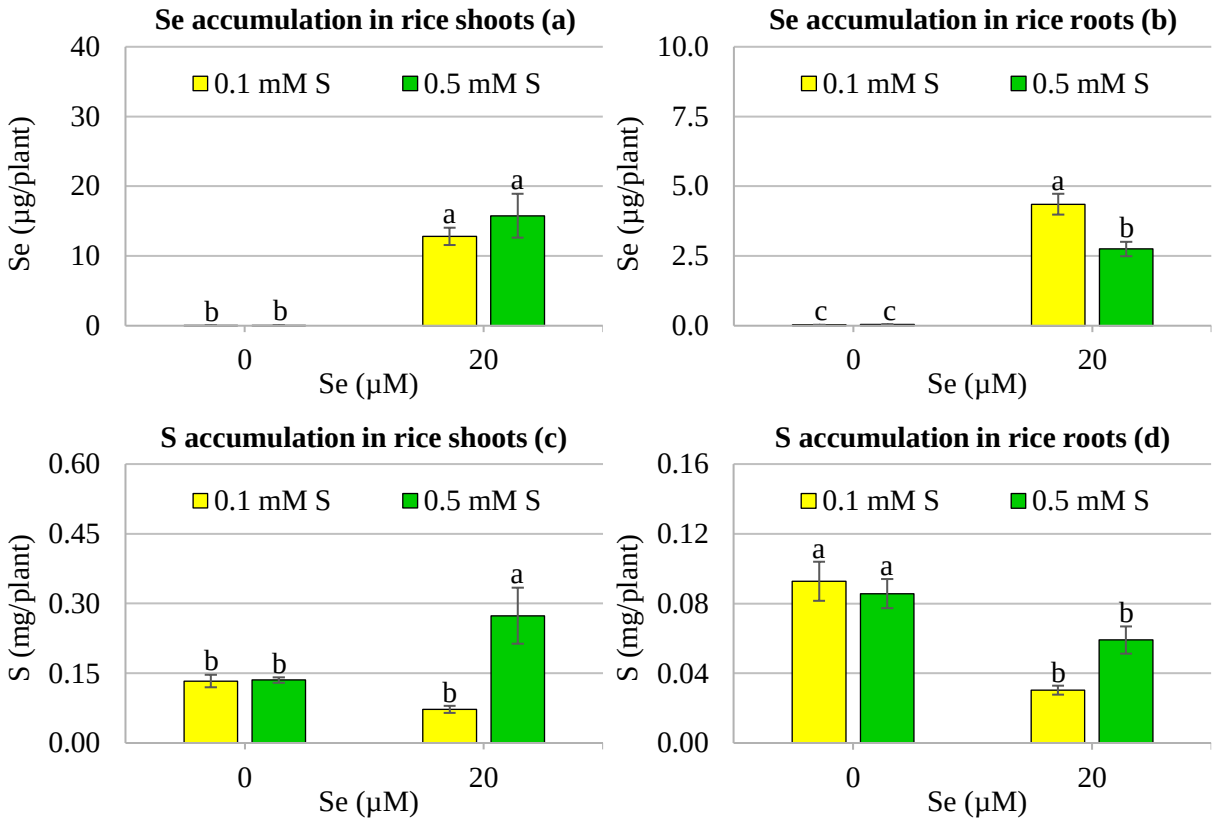


Figure S2. Selenium and sulfur accumulations in rice plants grown in the nutrient solution under S and Se doses (short-term experiment). Selenium accumulations on shoots (a) and roots (b). Sulfur accumulations in shoots (c) and roots (d). Columns with different letters differ by the Scott-Knott test (n = 12, $p < 0.05$).

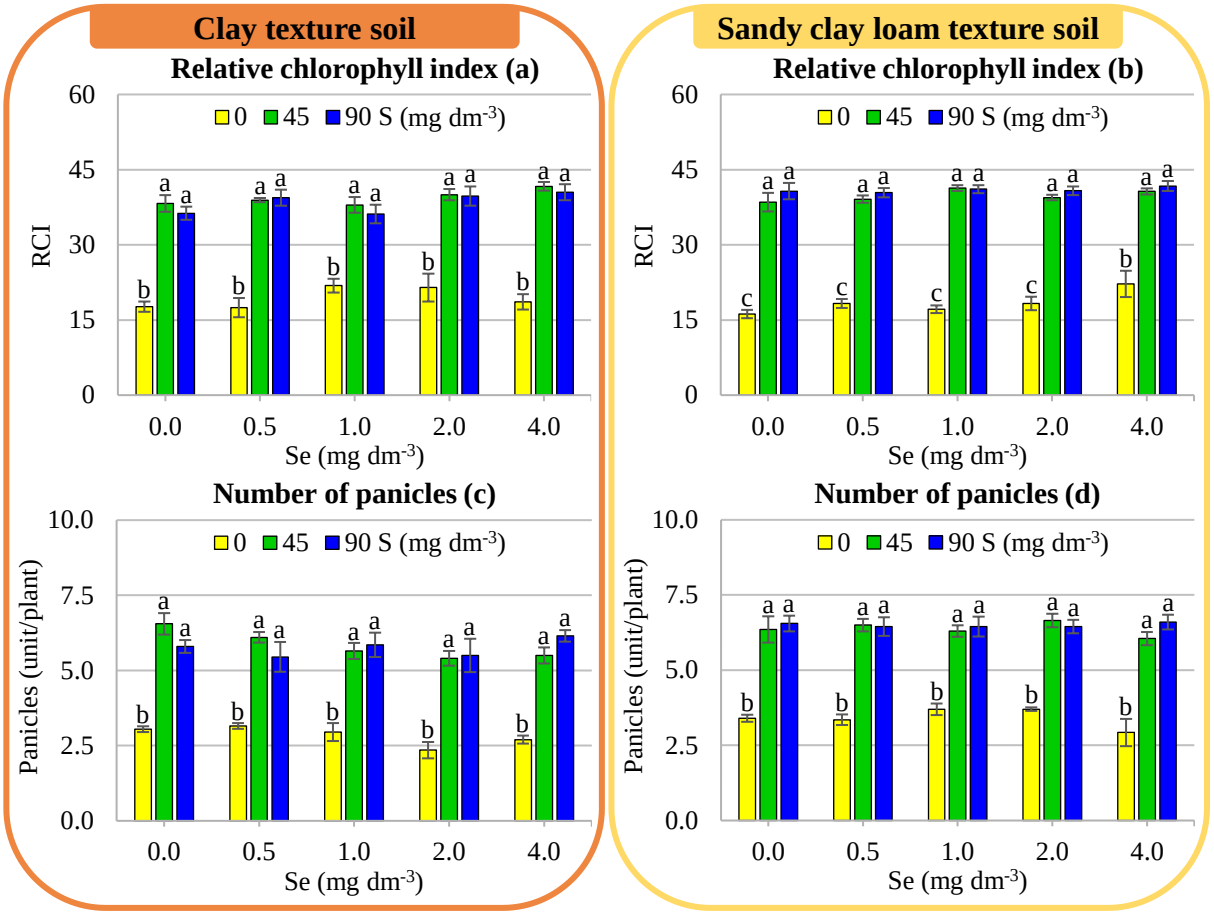


Figure S3. Relative chlorophyll index (RCI, a and b) and the number of panicles (c and d) in rice plants cultivated in soils with different textures under S and Se doses (long-term experiment). Columns with different letters in each soil differ by the Scott-Knott test (n = 60, $p < 0.05$).

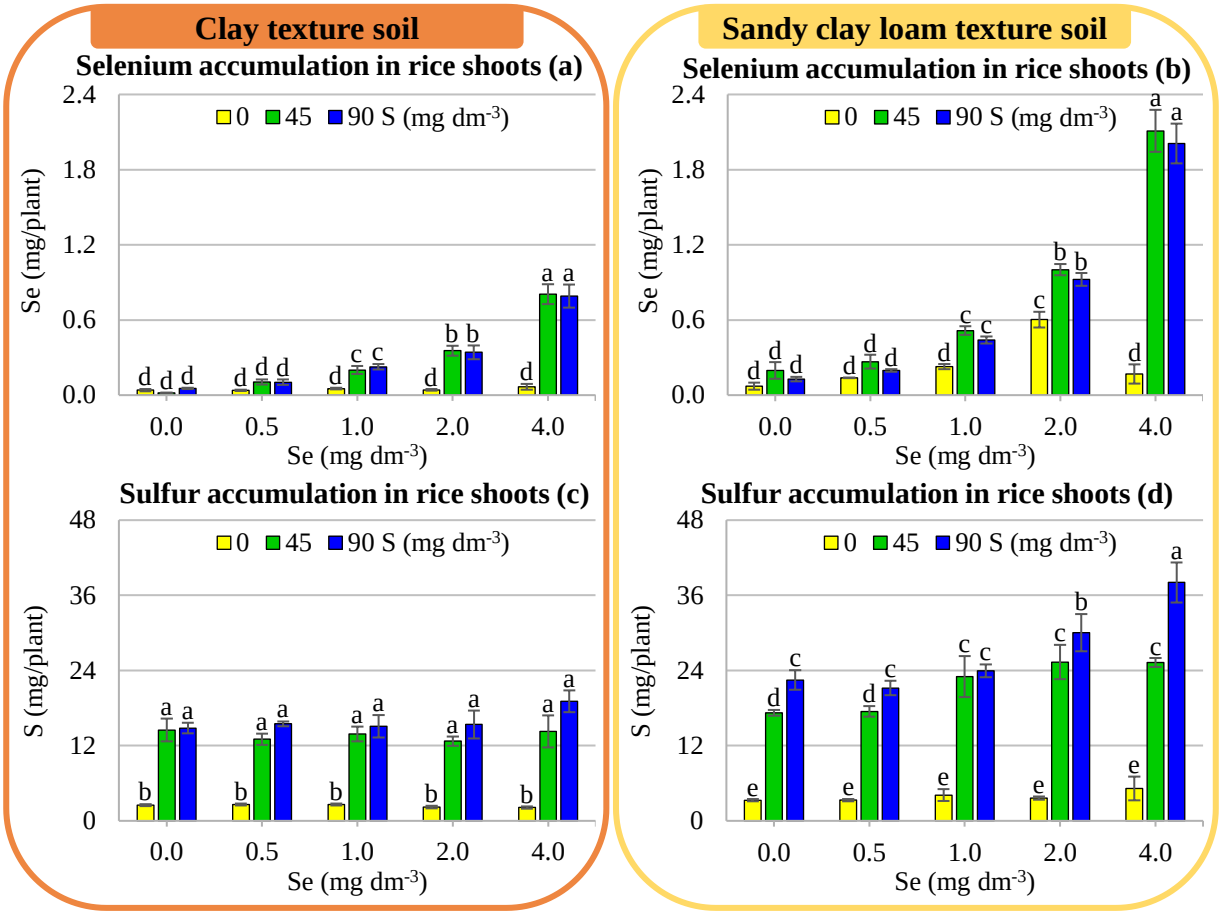


Figure S4. Selenium (a and b) and sulfur (c and d) accumulations in shoots of rice plants cultivated in soils with different textures under S and Se doses (long-term experiment). Columns with different letters in each soil differ by the Scott-Knott test (n = 60, $p < 0.05$).

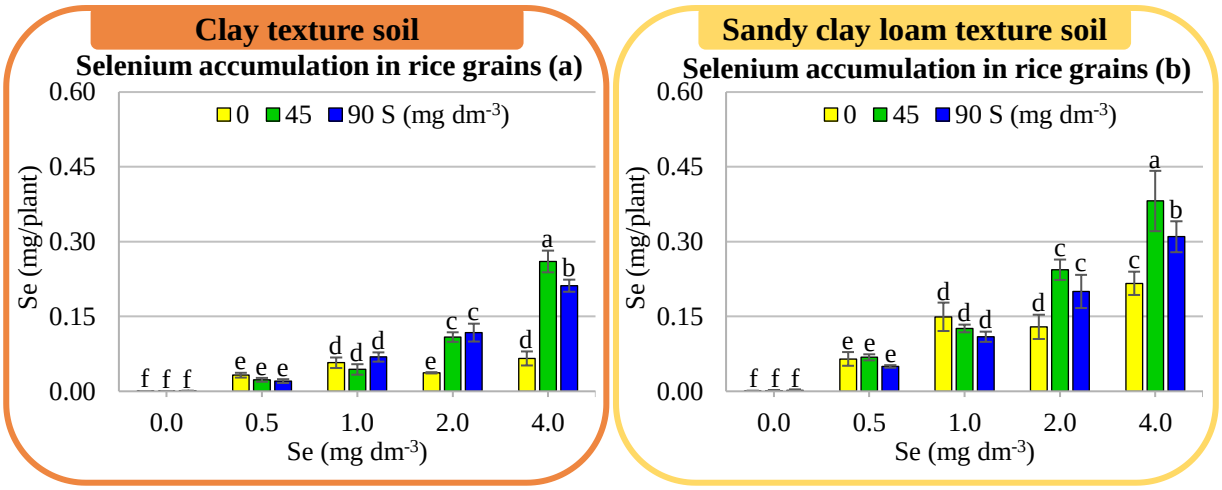


Figure S5. Selenium accumulations (a and b) in paddy rice grains (brown rice and husk) of rice plants cultivated in soils with different textures under S and Se doses (long-term experiment). Columns with different letters in each soil differ by the Scott-Knott test (n = 60, $p < 0.05$).

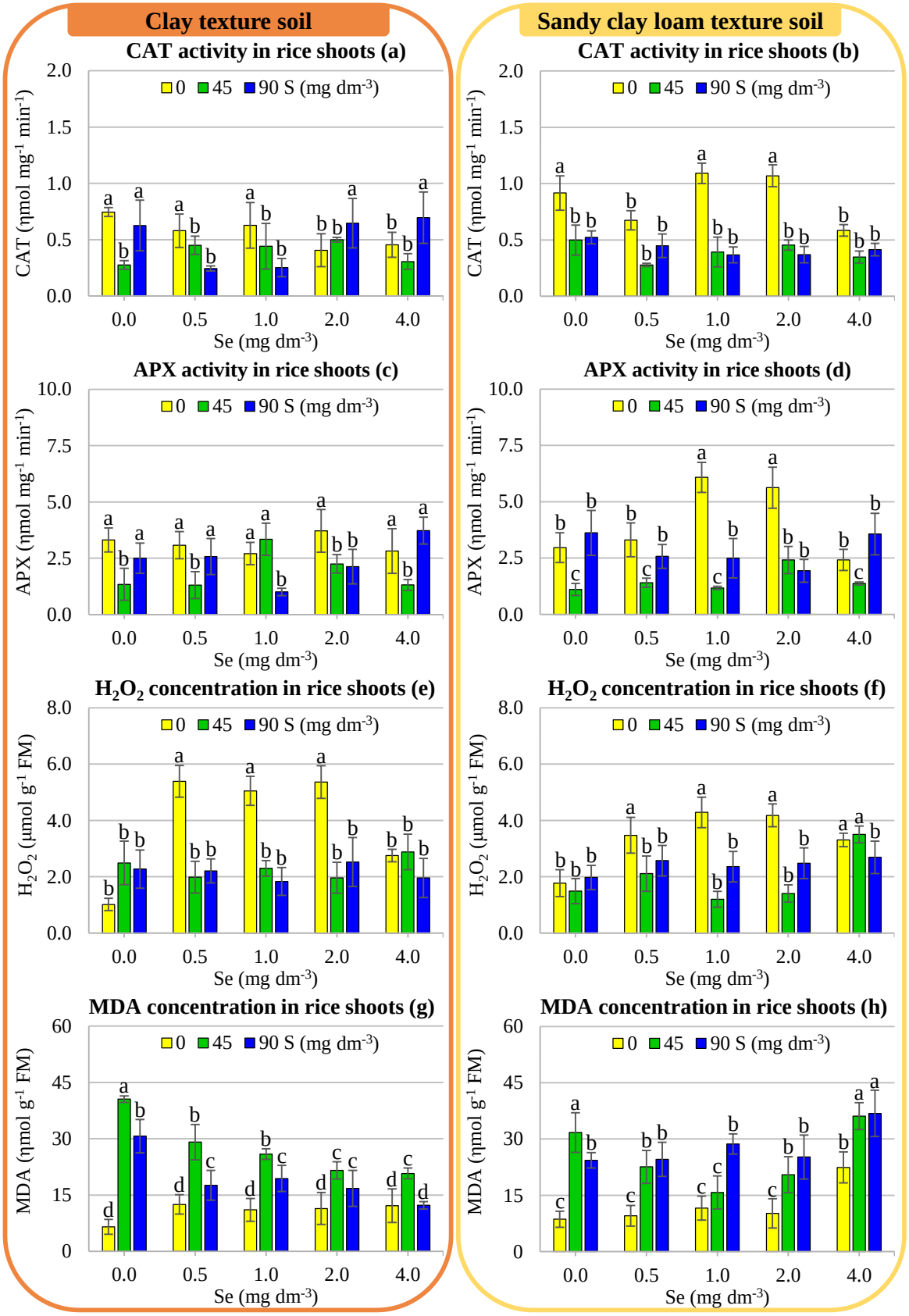


Figure S6. Antioxidant mechanisms and stress indicators in rice plants cultivated in soils with different textures under S and Se doses (long-term experiment). Catalase (CAT, a and b) and ascorbate peroxidase (APX, c and d) activities. Hydrogen peroxide ($H_2O_2$, e and f) and malondialdehyde (MDA, g and h) concentrations. Columns with different letters in each soil differ by the Scott-Knott test (n = 60, $p < 0.05$).

# CHAPTER II

## Selenate toxicity and sulfate uptake upregulation are related to glutathione metabolism in plants

### Highlights

1. The selenate's induction on *SULTR1;1* expression is higher on plants with low glutathione contents
2. The external GSH supply can partially inhibit the selenate's induction on *SULTR1;1* expression
3. Glutathione is crucial for selenate tolerance in plants
4. GSH is primarily used for selenate non-enzymatic assimilation
5. The sulfate uptake upregulation is a defense mechanism against selenate toxicity but is ineffective if sulfate can not be converted to glutathione
6. Selenite effect on glutathione metabolism and sulfate uptake is significantly lower than selenate
7. Selenite toxicity is less marked than selenate in broccoli due to its low transport to the shoots


### Abstract

Selenium (Se) and sulfur (S) compounds present a strict relationship in plant metabolism. Selenate ($SeO_4^{2-}$) can compete with sulfate ($SO_4^{2-}$) for uptake transporters on roots. However, the synergism between selenate and sulfate also has been reported, which is not observed for selenite ($SeO_3^{2-}$). Furthermore, the selenate and selenite toxicity mechanisms seem to be different in plants, which can be linked to their specific influence on sulfur metabolism. Thus, we studied the influence of selenium treatment on sulfur and selenium metabolisms and plant growth of *Arabidopsis* and broccoli with different concentrations of glutathione, a key molecule of sulfur metabolism and plant detoxification. The selenate treatment decreased the glutathione contents in plant tissues. The *pad2-1* plants (a glutathione-deficient *Arabidopsis* mutant) exhibited lower selenate tolerance and higher sulfate transporters (*AtSULTR1;1* and *AtSULTR1;2*) gene expression on roots compared to *Arabidopsis* wild-type (WT), even exhibiting similar selenium and sulfur concentrations on shoots and roots. However, the reduced glutathione (GSH) supply alleviated the selenate toxicity and partially inhibited the sulfate transporters expression, indicating that both selenate effects are directly linked to glutathione metabolism. Conversely, the selenite did not present

clear relation with glutathione or *BoSULTR1;1* and *BoSULTR1;2* in broccoli plants, while selenate decreased the glutathione contents and inhibited the growth of broccoli with lower glutathione concentrations severely.

**Keywords:** *Arabidopsis thaliana*, *Brassica oleracea*, broccoli, *pad2-1*, selenite, selenium, sulfate transporters, sulfur.

**Graphical abstract**

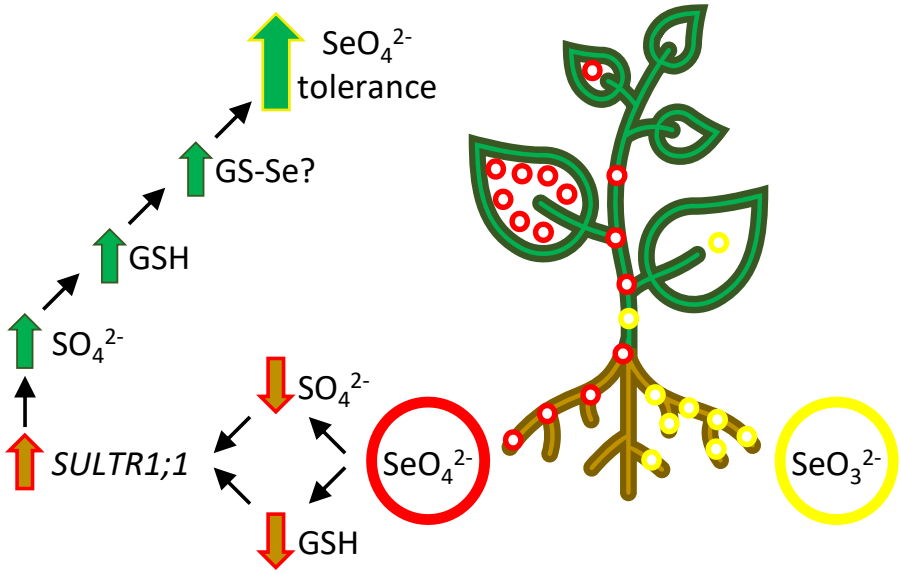


## 1. Introduction

Selenium (Se) is a nutrient for humans and animals, and adequate concentrations are required to prevent disorders in immunologic and anticarcinogenic systems (Alfthan et al., 2015). Selenium is not considered a plant nutrient; however, it can favor plant growth and yield in some conditions and is considered a beneficial element (Kaur et al., 2017). Conversely, high selenium concentrations cause severe phytotoxicity (Tian et al., 2017). The plants can absorb both the selenite ($SeO_3^{2-}$) and selenate ($SeO_4^{2-}$) ionic forms. The selenate uptake is carried by sulfate transporters in the root membrane, while the phosphate transporters absorb selenite (Zhang et al., 2003; Zhang et al., 2014). However, sulfur (S) metabolic pathways probably assimilate both selenite and selenate since they are analogs for sulfite ($SO_3^{2-}$) and sulfate ($SO_4^{2-}$), respectively. Thus, plants with a higher sulfur assimilation capacity can also demonstrate higher selenium assimilation (Wiesner-Reinhold et al., 2017).

Sulfur is a nutrient for all organisms, playing several roles in humans, animals, and plants, mainly related to its structural role in cysteine and methionine amino acids and other

compounds (Günal et al., 2019). Sulfate is the sulfur form mainly absorbed by plants, and its availability influences plant growth and development, strictly affecting crop yields (Capaldi et al., 2015). Considering selenate and sulfate are absorbed by the same transporters on roots, there is a possibility of competitive inhibition in their uptakes (Toler et al., 2007). However, selenite does not inhibit sulfate uptake (Tian et al., 2017), suggesting that selenate and selenite have different effects on sulfur metabolism. Furthermore, the toxicity caused by selenate and selenite can be hugely distinct according to the sulfur supply (Tian et al., 2017). Thus, studies about sulfur and selenium metabolisms are crucial for comprehending selenium biofortification and phytotoxicity mechanisms.

Despite the inhibition between sulfate and selenate absorptions, some studies have demonstrated that selenate can increase sulfur accumulation in some plant species (Ramos et al., 2011; Takahashi et al., 2000; White et al., 2004). This effect may be correlated with an increase in the high-affinity sulfur transporter SULTR1;1 activity in the root membrane, while high-affinity sulfur transporter SULTR1;2 is less affected by selenate (Boldrin et al., 2016). Interestingly, selenite does not affect the *SULTR1;1* gene expression, indicating this effect is specific for selenate (Tian et al., 2017). The increase in SULTR1;1 activity is a mechanism to improve sulfur uptake under deficiency conditions (Takahashi et al., 2000; Yoshimoto et al., 2002). Thus, selenate exposure appears to mimic the sulfur deficiency in plants (Schiavon et al., 2012). However, the mechanisms responsible for the sulfur transporters inducing promoted by selenate are still unknown.

The sulfate uptake and assimilation are down-regulated by some sulfur compounds, like glutathione and sulfate (Maruyama-Nakashita et al., 2004; Takahashi et al., 2011). Previous studies have demonstrated that selenate can inhibit sulfate uptake and decrease the glutathione content in plants. Takahashi *et al.* (2000) observed an increase in abundance of *SULTR1;1* mRNA and reduced glutathione (GSH) decrease in roots of *Arabidopsis* plants after selenate treatment. Similarly, Van Hoewyk *et al.* (2008) and Grant *et al.* (2011) related selenate decreased the GHS in *Arabidopsis*, suggesting that selenate toxicity can be correlated with GSH biosynthesis disruption. Since GSH can inhibit the sulfate transporters' activities and selenate can disrupt the GSH metabolism, maybe selenate induces the sulfur uptake through GSH metabolism disruption. Furthermore, selenium forms toxicities can also be related to glutathione metabolism since selenite and selenate effects on sulfur metabolism seem different. Thus, we studied the influence of inorganic selenium forms on sulfur and selenium metabolisms and the growth of *Arabidopsis* and broccoli with different glutathione contents.

## 2. Material and methods

### 2.1. *Arabidopsis* seedlings in MS medium

#### *2.1.1. Experimental design*

The treatments consisted of combinations of two *Arabidopsis thaliana* genotypes and nine ½ MS medium compositions (Table S1). The genotypes studied were *A. thaliana* Col-0 wild-type (WT) and glutathione-deficient mutant *pad2-1* (CS3804, At4g23100). The MS medium compositions consisted of three selenate doses (0, 5, and 15 µM $Na_2SeO_4$), combined or not with reduced glutathione (50 µM GSH) and buthionine sulfoximine (50 µM BSO), an inhibitor of GSH synthesis (Koprivova and Kopriva, 2014). The *pad2-1* plants were not grown under BSO treatment. Thus, we performed 15 treatments in a completely randomized design with three replications. The control treatment consisted of WT plants grown without selenate, GSH, or BSO treatments. For root growth measurement, each replication consisted of one square Petri dish (100 x 100 x 15 mm) filled with 60 ml MS medium and 40 *Arabidopsis* seeds. For biochemical analyses, each replication consisted of two round Petri dishes (150 x 15 mm) filled with 120 ml MS medium and 20 mg *Arabidopsis* seeds (around 1000 seeds).

#### *2.1.2. Growth conditions*

The *Arabidopsis* seeds were sterilized with ethanol (75%) and washed with autoclaved deionized water. Then, the seeds were resuspended in 0.15% agar autoclaved. The basic ½ MS medium was prepared with 2.15 g $L^{-1}$ Murashige and Skoog salt (RPI®, M10200), 10 g $L^{-1}$ sucrose, 8 g $L^{-1}$ agar, and selenate treatments. The acidity was adjusted to pH 5.8 using KOH solution (0.1 M). Then, the MS medium was autoclaved and cooled in a water bath at 42 ºC for 40 minutes. The GSH and BSO solutions were filtered (0.22 µm mesh) and added to the MS medium after cooling. The MS medium was added to the Petri dishes and cooled at room temperature for 60 minutes. Then, the seeds were spread in the solid MS medium and transferred to a growth chamber in the vertical position (16 h light / 8 h dark, 25 ºC). The plants were harvested seven days after the sowing. The root length was measured using the ImageJ® software, and the plant material was washed with deionized water, frozen in liquid nitrogen, and stored (-80 ºC) for biochemical analyses.

2.2. *Arabidopsis* plants in nutrient solution

*2.2.1. Experimental design*

The treatments consisted of combinations of two *A. thaliana* genotypes (WT and *pad2-1*) with three selenate doses (0, 5, and 15 µM $Na_2SeO_4$) in the nutrient solution (Table S2). Thus, six treatments were performed in a completely randomized design with three replications. Each replication consisted of one pot with 50 plants. The control treatment consisted of WT plants grown without selenate treatment.

*2.2.2. Growth conditions*

The seeds were sterilized and resuspended as described. Then, the seeds were spread on aluminum square meshes (5 x 5 cm, 2 mm mesh) attached to polystyrene support on the bottom lateral sides and covered with autoclaved agar (0.8%). The meshes were placed into Magenta boxes (300 ml) covered with aluminum foil and filled with Hoagland solution (50% ionic strength, pH 6.5). The plants were cultivated in a growth chamber (16 h light / 8 h dark, 25 ºC). We performed thinning until remain 50 seedlings per pot. After one week, the nutrient solution was changed to Hoagland solution (100% ionic strength, pH 6.5) with selenate treatments, which was changed every three days. The plants were harvested one week after selenate treatment (14 days after sowing). The plant material was rinsed with $CaCl_2$ solution (2 mM) and deionized water. Then, it was divided into shoots and roots and dried in an air-circulation oven (65 ºC for 72 h). The shoots and root productions were measured using a digital scale, and plant material was destined for selenium and sulfur determinations.

2.3. *Arabidopsis* plants in peat moss compost

*2.3.1. Experimental design*

The treatments consisted of six combinations between two *A. thaliana* genotypes (WT and *pad2-1*) and three selenate doses (0, 5, and 15 µM $Na_2SeO_4$) in the compost, using a completely randomized design with three replications. Each replication consisted of one pot with two plants. The control treatment consisted of WT plants grown without selenate treatment.

*2.3.2. Growth conditions*

The seeds were sterilized and resuspended as described. Then, the seeds were spread in round Petri dishes (150 x 15 mm) filled with 120 ml ½ MS medium and transferred to a growth chamber (16 h light / 8 h dark, 25 ºC) in the horizontal position. After one week, four

seedlings were transplanted to the pots (300 ml) filled with peat moss compost (PRO-MIX® BK25V). Thinning was realized until two seedlings remained. One week after the transplanting, the selenate treatments were applied in solution form. The plants were daily watered using deionized water. The plants were harvested one week after selenate treatment (21 days after sowing), and shoots were rinsed with $CaCl_2$ solution (2 mM) and deionized water. The shoots were dried, the production was measured as described, and the plant material was destined for selenium and sulfur determinations.

## 2.4. Broccoli plants in nutrient solution

### *2.4.1. Experimental design*

The treatments consisted of two sulfur doses (0.5 and 2.0 mM $MgSO_4$) combined or not with two selenium doses (50 and 80 µM Se) applied in two ionic forms (selenite – $Na_2SeO_3$ and selenate – $Na_2SeO_4$) in the nutrient solution (Table S3). Thus, ten treatments were carried out in a completely randomized design, with three replications and one pot with four broccoli plants per replication. The control treatment consisted of the 2.0 mM S dose without selenium addition.

### *2.4.2. Growth conditions*

The broccoli seeds (*Brassica oleracea* var. *italica*, cv. Marathon) were sterilized with sodium hypochlorite (1%) and washed with deionized water. The seeds were sowed in plastic trays (30 x 30 x 10 cm) filled with peat moss compost (PRO-MIX® BK25V) and transferred to a greenhouse (14 h light / 10 h dark, 22 - 28 ºC). One week after sowing, the seedlings were transplanted to plastic trays (7 L) filled with Hoagland solution (50% ionic strength, pH 6.5) with sulfur adjusted to 0.5 mM S under artificial aeration. After one week, the seedlings were selected according to size uniformity and transplanted to pots (2.2 L) filled with Hoagland solution (100% ionic strength, pH 6.5) and sulfur and selenium doses under artificial aeration. The nutrient solution was changed every three days, and plants were harvested two weeks after the treatments (28 days after sowing). The plant material was washed with $CaCl_2$ solution (2 mM) and deionized water. New leaves and root tips were immediately frozen in liquid nitrogen and stored (-80 ºC) for biochemical analyses. The plant material was dried, and shoots and root productions were measured as described. Then, the plant material was destined for selenium and sulfur determinations.

## 2.5. Plant analyses

### *2.5.1. Gene expression*

Genes related to sulfate and selenate uptake and assimilation were analyzed in *Arabidopsis* and broccoli tissues. RNA samples were extracted from plant material using Trizol reagent (Life Technologies™), and cDNA samples were synthesized using Superscript III Reverse Transcriptase kit according to manufacturer instructions (Invitrogen™). The reverse transcription-polymerase chain reactions (qRT-PCR) were performed using SYBR Green Universal Master Mix (Applied Biosystems™) and a real-time PCR system (Bio-Rad®, CFX384TM). The primer sequences used are presented in Table S4.

### *2.5.2. Glutathione concentrations*

The reduced (GSH) and oxidized (GSSG) glutathione concentrations in plant tissues were measured according to Rahman *et al.* (2007). Fresh samples (50 mg) were ground in liquid nitrogen, homogenized in 0.5 ml sulfosalicylic acid solution (6 g $L^{-1}$), and transferred to 1.5 ml tubes. The samples were centrifuged (8000 *g* and 4 ºC for 10 min), and the supernatant was collected. The aliquot used for GSSG determination was treated with 2-vinylpyridine to derivatize GSH. The GSH and GSSG concentrations were determined in a 200 µl reaction mixture consisting of supernatant (20 µl), glutathione reductase (5 units $ml^{-1}$), DTNB (0.5 mM), and NADPH (0.25 mM). The mixtures were analyzed in a spectrophotometer at 412 nm for 2 minutes (30-sec intervals), and GSH and GSSG concentrations were calculated using standard curves.

### *2.5.3. Selenium and sulfur concentrations*

The dried plant materials were ground, and samples (0.200 g) were digested using 8 ml of acid solution ($HNO_3$ + $HClO_4$, 3:1 ratio) under heating (50, 100, and 150 ºC for 60 min each and 200 ºC for 30 min). The samples were diluted with deionized water and analyzed by inductively coupled plasma optical emission spectroscopy (ICP-OES). The sulfur and selenium concentrations were calculated using standard curves.

### *2.5.4. Glutathione reductase and peroxidase activities*

Fresh samples (200 mg) were ground in liquid nitrogen with PVPP (30 mg), homogenized in 1.5 ml phosphate buffer (100 mM $KH_2PO_4$, 0.1 mM EDTA, and 10 mM ascorbic acid, pH 7.8), and transferred to 2.0 ml tubes. The samples were centrifuged (13,000 *g* and 4 ºC for 10 min), and supernatants (protein extracts) were collected and stored (-80 ºC).

The soluble protein concentrations were determined in a 300 µl reaction mixture consisting of protein extract (6 µl) and Bradford reagent (Bradford, 1976). The mixture was analyzed in a spectrophotometer at 595 nm, and protein concentrations were calculated using a standard curve.

The glutathione reductase (GR, EC 1.6.4.2) and glutathione peroxidase (GPX, EC 1.11.1.12) activities were measured according to Khan *et al.* (2015). The GR activity was determined in a 180 µl reaction mixture consisting of protein extract (45 µl), phosphate buffer (50 mM $KH_2PO_4$, pH 7.8), GSSG (1 mM), and NADPH (75 µM). The GPX activity was determined in a 180 µl reaction mixture consisted of protein extract (45 µl), potassium phosphate buffer (50 mM, pH 7), EDTA (1 mM), $NaN_3$ (1 mM), GR (1 unit $ml^{-1}$), GSH (1 mM), $H_2O_2$ (0.25 mM) and NADPH (0.2 mM). The mixtures were analyzed in a spectrophotometer at 340 nm for 3 minutes (15-sec intervals), and GR and GPX activities were calculated using the coefficient extinction of 6.22 $mM^{-1}$ $cm^{-1}$.

*2.5.5. Hydrogen peroxide and malondialdehyde concentrations*

The hydrogen peroxide ($H_2O_2$) and malondialdehyde (MDA) concentrations were measured according to Velikova et al. (2000). Fresh samples (200 mg) were ground in liquid nitrogen with PVPP (30 mg), homogenized in 1.5 ml trichloroacetic acid solution (1 g $L^{-1}$), and transferred to 2 ml tubes. The samples were centrifuged (12,000 *g* and 4º C for 15 min), and supernatants were collected and stored (-80 ºC). The $H_2O_2$ concentrations were measured in a 180 µl reaction mixture consisting of supernatant (45 µl), potassium phosphate buffer (2.5 mM, pH 7), and potassium iodide (0.5 M). The mixture was analyzed in a spectrophotometer at 390 nm, and $H_2O_2$ concentrations were calculated using a standard curve. The MDA concentrations were measured in a 375 µl reaction mixture consisting of supernatant (125 µl), trichloroacetic acid (0.4 M), and thiobarbituric acid (23 mM). The reaction mixture was heated in a water bath (95 ºC for 30 min), cooled in an ice bath, and analyzed in a spectrophotometer at 535 and 600 nm. The MDA concentrations were calculated using the coefficient extinction of 156 $mM^{-1}$ $cm^{-1}$.

2.6. Statistical analyses

The obtained data were submitted to normality and variance analyses using SAS University Edition® software (Statistical Analysis System®), and the treatments were compared by the Scott-Knott test ($p < 0.05$) using the SISVAR® software (Ferreira, 2019).

## 3. Results

### 3.1. *Arabidopsis* seedlings in MS medium

The selenate doses promoted specific effects on root length according to the *Arabidopsis* genotype and medium composition (Figures 1a and 1b). The addition of 5 µM selenate did not affect the WT + GHS plants while causing severe toxicity to *pad2-1* and WT + BSO plants, which presented 70 and 51% lower root length, respectively, compared to the control treatment (WT + 0 µM Se). However, this selenate dose presented a less severe inhibition of root growth on *pad2-1* + GSH plants (-36%), which exhibited a root length of 2-folds higher than *pad2-1* plants grown under 5 µM selenate dose without GSH. The addition of 15 µM selenate presented a similar root inhibition for all plants, except for WT + GSH plants. Compared to the control treatment, the 15 µM dose decreased the root length of WT + GSH plants by 26% while decreasing it by around 75% on the other plants.

The selenate influence on sulfate transporters' gene expressions also varied according to the *Arabidopsis* genotype and medium composition (Figures 1c and 1d). Compared to the control treatment, the 5 µM selenate dose promoted an *AtSULTR1;1* expression 14-folds higher, except for WT + GSH plants, which were not affected. However, we observed a stronger influence at 15 µM selenate treatment. Compared to the control treatment, the 15 µM selenate dose increased the *AtSULTR1;1* expression by 208 and 148-folds on *pad2;1* and *pad2-1* + GSH plants, respectively. Similarly, compared to the control treatment, this dose increased the *AtSULTR1;1* expression by 54 and 21 times on WT and WT + GSH plants, respectively. Thus, the GSH supply inhibited the 15 µM selenate induction in the *AtSULTR1;1* expression by 30% on *pad2-1* plants and 60% on WT plants. Conversely, the BSO supply enhanced the 15 µM selenate induction in the *AtSULTR1;1* expression on WT plants, promoting a gene expression 2-folds higher than WT plants under the same selenate dose. Regarding *AtSULTR1;2*, we observed that 15 µM selenate promoted gene expressions 3.5 and 2.6-folds higher on *pad2-1* and *pad2-1* + GSH plants, respectively, compared to the control treatment.

The GSH and GSSG concentrations on plant shoots differed significantly according to *Arabidopsis* genotype and medium composition (Figures 2a and 2b). Regarding the GSH concentrations, we observed strong reductions on *pad2-1* (-95%), *pad2-1* + GSH (-81%), and WT + BSO plants (-36%), compared to control treatment. We observed similar reductions on GSSG concentrations on *pad2-1* (-97%), *pad2-1* + GSH (-80%), and WT + BSO plants (-13%), compared to control treatment. Interestingly, the GSH supply did not affect the GSH and GSSG concentrations on WT plants, while the *pad2-1* + GSH plants exhibited GSH and

GSSG concentrations 3.6 and 7.5-folds higher, respectively, compared to *pad2-1* plants cultivated without GSH supply. Despite this difference, both 5 and 15 µM selenate promoted similar reductions in glutathione concentrations on shoots of all plants, except *pad2-1* plants, which were not affected. The 15 µM selenate dose decreased the GSH and GSSG concentrations on shoots of WT plants (-31% GSH and -35% GSSG), WT + GSH plants (-29% GSH and -29% GSSG), WT + BSO plants (-34% GSH and -49% GSSG) and *pad2-1* + GSH plants (-48% GSH and -60% GSSG), compared to the same *Arabidopsis* types and medium compositions without selenate treatment.

Regarding the glutathione concentrations on roots, the GSH supply increased the GSH and GSSG concentrations on WT plants, while the BSO treatment decreased it severely (Figure 2c and 2d). The WT plants cultivated with GSH supply presented increases of 24 and 43% in GSH and GSSG concentrations on roots, respectively, compared to the control treatment. Conversely, the WT plants grown under BSO treatment presented 66 and 72% reductions in GSH and GSSG concentrations on roots, respectively, compared to the control treatment plants. Both GSH and GSSG concentrations on roots of *pad2-1* and *pad2-1* + GSH plants were too low to be detected by the measurement method used. Unlike the effect on shoots, we observed that just the 15 µM selenate dose affected the GSH and GSSG concentrations on roots of WT and WT + GSH plants, while the 5 µM selenate affected just the concentrations on WT under BSO treatment. The 15 µM selenate dose reduced the glutathione concentrations on roots of WT plants (-25% GSH and -29% GSSG), WT + GSH plants (-63% GSH and -67% GSSG), and WT + BSO plants (-33% GSH and -41% GSSG), compared to the same *Arabidopsis* genotype and medium compositions without selenate treatment.

### 3.2. *Arabidopsis* plants in nutrient solution

The selenate treatment strongly affected the *pad2-1* plant growth, mainly on the root production, while the WT plant growth was not affected by the selenate doses in the nutrient solution (Figures 3a, 3b, and 3c). The 15 µM selenate dose decreased the shoots and root production of *pad2-1* plants by 54 and 80%, respectively, compared to WT plants grown without selenate exposure (control treatment). Furthermore, this selenate dose reduced the shoots and root production by 35 and 72%, respectively, compared to WT plants cultivated with the same selenate dose on the nutrient solution.

Despite the specific effects on plant growth, the selenate doses promoted similar selenium concentrations in tissues of WT and *pad2-1* plants (Figures 4a and 4b). The selenate

doses increased the selenium concentrations on shoots and roots of WT and *pad2-1* plants. The 15 μM selenate dose promoted selenium concentrations around 0.8 g $kg^{-1}$ Se on shoots of WT and *pad2-1* plants, a value 4-folds higher than plants grown with 5 μM selenate. Similarly, the 15 μM selenate dose provided selenium concentrations around 0.5 g $kg^{-1}$ Se on the roots of WT and *pad2-1* plants, a value 2.5-folds higher than plants cultivated under the 5 μM selenate exposure.

The selenate doses also promoted similar sulfur concentrations on tissues of WT and *pad2-1* plants. The selenate doses enhanced the sulfur concentrations on shoots of WT and *pad2-1* plants while decreasing it on roots (Figures 4c and 4d). The 15 μM selenate dose promoted sulfur concentrations around 24 g $kg^{-1}$ S on shoots of WT and *pad2-1* plants, a concentration 2.6-folds higher than plants grown without selenate. However, the 15 μM selenate dose promoted sulfur concentrations of around 7.6 g $kg^{-1}$ S on roots of WT and *pad2-1* plants, a sulfur concentration 46% lower compared to control treatment plants.

### 3.3. Broccoli plants in nutrient solution

The low sulfur supply (0.5 mM S) in the nutrient solution did not affect the broccoli growth compared to the control treatment plants (2.0 mM S) (Figures 5a, 5b, and 5c). However, the plants cultivated with low sulfur supply exhibited severe growth inhibition under selenate treatment, while the selenite toxicity was less marked. Compared to the control treatment, the plants grown with low sulfur supply under selenate doses exhibited reductions of around 80% in shoots and roots productions, while the plants grown with 2.0 mM under selenate doses presented decreases of 13 and 40% on shoots and roots productions, respectively (Figures 5b and 5c). Thus, the plants cultivated with 2.0 mM S under selenate treatment presented shoots and root production by 5 and 3-folds higher, respectively, compared to low sulfur supply under selenate treatment.

The selenate treatment promoted markedly higher selenium concentrations on shoots of broccoli plants, regardless of the sulfur supply (Figure 5d). The selenate doses promoted selenium concentrations on shoots around 1.0 g $kg^{-1}$, a value 18 times higher than plants cultivated under selenite exposure. Conversely, the influence of selenium ionic forms on selenium concentrations on roots was dependent on the sulfur supply. The high sulfur supply increased the selenium concentrations on roots of plants cultivated with selenite while decreasing it on plants grown with selenate. At 80 μM selenium dose, the 2.0 mM S dose increased by 40% the selenium concentration on roots of broccoli cultivated with selenite while decreasing it by 46% on plants grown under selenate treatment (Figure 5e).

We observed a strong influence of sulfur and selenium in the sulfur contents on shoots of broccoli plants. The selenate treatment enhanced the sulfur concentration on shoots of plants grown with the high sulfur supply. The selenate doses increased by around 90% the sulfur concentrations on broccoli shoots grown with 2.0 mM S compared to the control treatment plants (Figure 5f), while the selenite did not affect these concentrations. The high sulfur supply promoted higher sulfur concentrations on the roots of broccoli plants regardless of the selenium addition. However, selenate increased the sulfur concentrations on roots compared to selenite, mainly under the low sulfur supply. The selenate doses promoted increases of 25% in sulfur concentrations on roots cultivated with 0.5 mM sulfur compared to plants under selenite at the same sulfur dose (Figure 5g).

The selenate treatment affected the *BoSULTR1;1* expression on broccoli roots under low sulfur supply, while selenite did not affect it regardless of the sulfur dose. The 80 μM selenate exposure in plants grown with 0.5 mM sulfur promoted a *BoSULTR1;1* expression 13-folds higher than in control treatment plants (Figure 6a). The treatments promoted a less marked influence on *BoSULTR1;2* expression broccoli roots. Compared to the control treatment, the plants cultivated with 0.5 mM sulfur presented a *BoSULTR1;2* expression 2.8-folds higher, while the 50 μM Se in both selenate and selenite forms promoted an expression around 4-folds higher in plants grown with 2.0 mM sulfur (Figure 6b). A similar induction was observed at 80 μM selenate dose on plants under low sulfur supply. We observed that selenate also induced the *BoCAT1* expression, mainly under low sulfur supply (Figures 6c and 6d). Compared to the control treatment, the 80 μM selenate dose induced a *BoCAT1* expression 4-folds higher in roots grown with 0.5 mM sulfur, while the same selenate dose promoted *BoCAT1* expressions 3-folds higher on shoots, regardless of the sulfur supply.

The glutathione concentrations on broccoli tissues were sharply affected by the treatments. The sulfur supply influenced shoots and roots' GSH and GSSG concentrations (Figure 7). Compared to the control treatment, the plants grown with 0.5 mM sulfur presented lower GSH concentrations on shoots (-32%) and roots (-49%), and lower GSSG concentrations on shoots (-35%) and roots (-51%). Furthermore, the selenate treatment decreased the glutathione concentrations on shoots, mainly in plants cultivated under low sulfur supply, while the selenite effect was less marked. The treatment with 80 μM selenate and 0.5 mM sulfur decreased the GSH and GSSG concentrations in shoots by 55 and 80%, respectively, compared to plants grown with 0.5 mM sulfur without selenium and plants under 80 μM selenite and the same sulfur dose. Regarding GSH in roots, the selenium treatment decreased by around 50%, regardless of the sulfur supply, except for the 80 μM

selenite dose at 0.5 mM S (Figure 7b). Regarding GSSG in roots, we observed an increase of 90% in plants grown under 80 μM selenite and 0.5 mM S compared to the control treatment (Figure 7d).

**4. Discussion**

Selenate treatment decreased the glutathione contents in *Arabidopsis*, inducing higher *AtSULTR1,1* expression in plants with lower GSH and GSSG concentrations (*pad2-1* and WT + BSO) (Figures 1 and 2), while *SULTR1;2* was less affected. Similarly, selenate decreased the glutathione contents in broccoli shoots cultivated with the low sulfur supply, inducing the *BoSULTR1;1* at the higher selenium dose (Figures 6 and 7). In contrast, the external GSH supply partially inhibited the induction of *AtSULTR1;1* expression in both WT and *pad2-1* under selenate exposure (Figure 1). Similarly, the selenate did not influence the *BoSULTR1,1* expression in broccoli grown with the higher sulfur supply, which presented higher glutathione concentrations. The sulfate transporters upregulation by selenate in plants has been reported (El Mehdawi et al., 2018; Tian et al., 2017). The slight *AtSULTR1,2* upregulation by selenate (Figure 1) is probably related to inhibitive competition with sulfate on *Arabidopsis* roots (Figure 3). Thus, selenate decreased the sulfur concentration on roots, inducing the *AtSULTR1,2* expression since this effect is a sulfur deficiency response (Zheng et al., 2014).

However, the mechanisms involved in *SULTR1;1* upregulation are still unclear, which is stronger under low sulfur supply and appears to mimic sulfur starvation (Barberon et al., 2008; Boldrin et al., 2016). Our results suggest that the *SULTR1;1* upregulation by selenate is related to glutathione depletion, which is a sulfur deficiency symptom (Lunde et al., 2008) and has been reported as a selenate effect in plants (Grant et al., 2011; Santiago et al., 2020; Schiavon et al., 2016). This hypothesis is reinforced by *pad2-1* mutation location and by BSO's effect, which impairs glutamate-cysteine ligase (Dubreuil-Maurizi et al., 2011; Wang et al., 2022), the first enzyme of GSH synthesis, while the cysteine, another candidate to a regulator of sulfate transporters (Koprivova and Kopriva, 2014), is not affected. GSH plays an essential role in the sulfur and selenium metabolism in plants, acting in the reducing process of sulfate and selenate to sulfide ($S^{2-}$) and selenide ($Se^{2-}$), forms inserted in the amino acids (Schiavon and Pilon-Smits, 2017; Terry et al., 2000). However, GSH also acts as an inhibitor of sulfate transporters, playing a role in cell signaling of sulfur status (Lappartient et al., 1999; Vauclare et al., 2002).

Interestingly, the GHS content can downregulate the sulfur deficiency responsive expression promoted by sulfur-responsive element (SURE), observed in the promoter region of SULTR1;1 (Maruyama-Nakashita et al., 2005), which is not present in SULTR1;2 (Takahashi et al., 2011). Thus, the GSH decrease can upregulate the SULTR1;1 activity specifically. This effect can explain the stronger influence of selenate treatment on *SULTR1;1* expression compared to *SULTR1;2* on *Arabidopsis* and broccoli plants (Figures 1 and 6). Similarly, many studies have demonstrated that selenate induction is more pronounced on *SULTR1;1* expression compared to *SULTR1;2* (Boldrin et al., 2016; Tian et al., 2017), which can be related to GSH disruption influence on the former. Furthermore, the GSH regulatory role on *SULTR1;1* expression and the specific GSH depletion by selenate can explain this gene expression upregulation by selenate, while selenite did not affect *SULTR1;1* and sulfur content on broccoli plants (Figures 6 and 7). Similarly, Tian *et al.* (2017) observed that selenate induced *SULTR1;1* expression, while selenite did not affect it in broccoli roots.

Conversely, the BSO treatment did not induce the *SULTR1;1* expression, even promoting GSH reductions similar on shoots (Figure 2a) and stronger on roots (Figure 2c) compared to 15 µM $SeO_4$ in WT plants. These results indicate that probably another factor contributes to *SULTR1;1* overexpression by selenate treatment, in addition to GSH depletion. We consider that the reduction of sulfate content in roots by selenate treatment (Figure 3c) is the best candidate for *SULTR1;1* post-transcriptional regulator, in addition to GSH depletion, since the *SULTR1;1* overexpression is a well-known response to sulfate deficiency in plants (Yoshimoto et al., 2002). However, future studies can also focus on the possible involvement of *O*-acetylserine in this pathway since this molecule production can be enhanced by selenate treatment (Ríos et al., 2008), and it can induce sulfate transporters gene expression on roots (Koprivova and Kopriva, 2014; Smith et al., 1997; White, 2018).

Since the sulfate metabolic pathway assimilates selenate, it is expected that adenosine phosphoselenate (APSe) can be reduced by adenosine phosphosulfate reductase (APR), using GSH as a reducing molecule, which is responsible by adenosine phosphosulfate (APS) reduction (Fu et al., 2018). This step produces sulfite ($SO_3^{2-}$) and GSSG, which is recycled to GSH by glutathione reductase activity (GR) (Cohen et al., 2020; Kopriva, 2006). Thus, this step would produce selenite ($SeO_3^{2-}$) and GSSG. However, a non-enzymatic reaction between APSe and GSH has been proposed, producing the GSH-conjugated selenite (GS-selenite) (Terry et al., 2000). Although we observed slight increases in *APR2* expression and GR activity by selenate treatment (Figures S1b, S2a, and S4b), the decreases in GSH and GSSG by selenate on *Arabidopsis* and broccoli indicate the GSH consumed by selenate is not

recycled, suggesting it is primarily used to produce the GS-selenite by the non-enzymatic pathway. Grant *et al.* (2011) demonstrated that glutathione directly precipitates the selenate *in vitro*. Thus, glutathione may precipitate the selenate, which explains the glutathione consumption by selenate treatment. We also observed that glutathione depletion in broccoli shoots was higher under selenate treatment than selenite, suggesting that glutathione consumption is mainly required for selenate assimilation.

The selenate toxicity was severe in plants with lower glutathione contents. The 5 µM $SeO_4$ dose inhibited the root growth of *pad2-1* and WT + BSO plants (Figure 1), while it did not affect control treatment plants. Furthermore, the selenate caused severe toxicity in *pad2-1* plants cultivated in nutrient solution and peat moss compost (Figures 3 and S3), especially for root growth (Figure 3c). Selenate also caused severe growth inhibition in broccoli with lower glutathione concentrations (0.5 mM S) (Figures 5 and 7), which seems to be strictly related to selenate toxicity since these plants did not exhibit sulfur deficiency symptoms. Grant *et al.* (2011) reported severe selenate toxicity in *Arabidopsis* plants with lower glutathione contents, correlating the tolerance with GSH form. Glutathione performs several roles in plant tolerance to abiotic stress, acting as an antioxidant molecule, cell redox buffer, reduced sulfur source, phytochelatin (PC) precursor, signal peptide, and gene regulator (Cohen et al., 2020; Hacham et al., 2014; Hendrix et al., 2020). In addition, glutathione participates in reactive oxygen species (ROS) scavenging as a cofactor of antioxidant enzyme activities, like glutathione peroxidase (GPX) and glutathione-S-transferase (GST), and it is necessary to ascorbate-glutathione cycle and ascorbate peroxidase (APX) activity (Hasanuzzaman et al., 2017).

In the present study, the selenate toxicity in plants with lower glutathione contents is probably related to the proposed glutathione's role in selenate assimilation. Thus, plants with lower glutathione contents present low selenate assimilation capacity, impairing the selenate storage in less harmful organic forms in vacuoles (Zhou et al., 2018), considering the high selenate transport to shoots (Figures 4 and 5). In addition, the glutathione depletion by selenate decreased the antioxidant capacity of plants, aggravating the selenate toxicity and ROS generation, considering the glutathione antioxidant functions (Van Hoewyk, 2013). This hypothesis is supported by the similar selenium concentrations on shoots of *Arabidopsis* and broccoli plants (Figures 4a and 5d), while the selenate toxicity was markedly higher in plants with lower glutathione contents. Conversely, the higher glutathione contents were associated with selenate tolerance, including the external GSH supply to *pad2-1* plants, increasing the glutathione contents on shoots, indicating that the selenate tolerance is specifically related to glutathione and not just to total sulfur or other sulfur compounds, like cysteine and

methionine. This hypothesis is supported by the severe selenate toxicity on *pad2-1* plants, although these plants presented enhancement in sulfur contents in shoots (Figures 3, 4, and S3).

The selenium toxicity was stronger in broccoli plants cultivated with low sulfur supply under selenate treatment than selenite. The selenate treatment severely inhibited the shoots and roots productions in broccoli grown with 0.5 mM S, while the sulfur availability did not affect the selenite toxicity (Figures 5a, 5b, and 5c). In addition to growth results, the *BoCAT1* expression and oxidative stress indicators ($H_2O_2$ and MDA) confirm the higher plant stress in broccoli under selenate treatment (Chiang et al., 2014; Li et al., 2015; Tian et al., 2017), particularly under sulfur deficiency (Figures 6c, 6d, S4e, and S4f). This difference is probably related to higher selenium transport from roots to shoots in broccoli treated with selenate, promoting selenium concentrations around 18-fold higher in shoots than in selenite treatment (Figure 5d). Furthermore, the lower concentrations of GSH and GSSG in broccoli shoots cultivated under lower sulfur availability (Figures 7a and 7c), combined with its higher selenium concentration, probably induced the higher selenate toxicity as previously discussed. Previous studies have demonstrated that selenate toxicity is related to a non-specific replacement of sulfur amino acids by seleno amino acids into the proteins (Tian et al., 2017; Van Hoewyk, 2013; White, 2016), which can also explain the selenate toxicity in broccoli, especially under low sulfur supply.

Many studies have described selenite as the most toxic selenium form for plants (Garousi et al., 2016; Hawrylak-Nowak, 2013; Van Hoewyk, 2013), including *Arabidopsis* plants (Grant et al., 2011). The higher selenite toxicity in plants can be linked to its quick assimilation, being converted into organic compounds still in roots (White, 2016), probably by sulfite reductase enzyme activity (SIR) (Huang et al., 2021), while selenate can be transported and stored on the shoots (Gupta and Gupta, 2017; Schiavon and Pilon-Smits, 2017). The quick selenite assimilation hypothesis is corroborated by the higher selenium concentration on roots of broccoli treated with selenite, considering the plants grown with 2.0 mM S (Figure 5e). However, the higher selenate transport to shoots seems more toxic for broccoli plants than selenite assimilation in roots, especially under a low sulfur supply (Tian et al., 2017). Conversely, the higher sulfate supply partially alleviated the selenate toxicity by increasing sulfur and glutathione content in broccoli shoots (Figures 5f, 7a, and 7c). This effect is probably promoted by the overexpression of sulfate transporters under selenate treatment, although we did not observe increases in the relative expression of *BoSULTR1;1* and *BoSULTR1;2* in these plants at harvest, considering the sulfate transporters

overexpression seem to be paused after the internal sulfate concentration be restored (El Mehdawi et al., 2018; Ferrari et al., 2022).

## 5. Conclusions

The selenate's induction on gene expression of sulfate transporters is related to glutathione depletion and sulfate content reduction on roots. The *SULTR1;1* and *SULTR1;2* sulfate transporters overexpression on roots is a protective mechanism against selenate toxicity, aiming to increase the sulfate uptake and accumulation. However, this mechanism is ineffective if sulfate can not be converted to glutathione. Thus, glutathione is crucial for selenate tolerance in plants, probably due to its role in selenate non-enzymatic assimilation. The severe toxicity of selenate in broccoli grown under sulfur deprivation is also related to glutathione depletion and higher selenium content on shoots compared to selenite. Thus, the present study provides important insights into selenium metabolism, toxicity, and alleviation mechanisms in plants, which can be used in future research about selenium phytoremediation in contaminated areas and biofortification on crops.

## REFERENCES

Alfthan, G., Eurola, M., Ekholm, P., Venäläinen, E.R., Root, T., Korkalainen, K., Hartikainen, H., Salminen, P., Hietaniemi, V., Aspila, P., Aro, A., 2015. Effects of nationwide addition of selenium to fertilizers on foods, and animal and human health in Finland: From deficiency to optimal selenium status of the population. J. Trace Elem. Med. Biol. 31, 142–147. https://doi.org/10.1016/j.jtemb.2014.04.009

Barberon, M., Berthomieu, P., Clairotte, M., Shibagaki, N., Davidian, J.-C.C.J., Gosti, F., 2008. Unequal functional redundancy between the two *Arabidopsis thaliana* high-affinity sulphate transporters SULTR1;1 and SULTR1;2. New Phytol. 180, 608–619. https://doi.org/10.1111/j.1469-8137.2008.02604.x

Boldrin, P.F., de Figueiredo, M.A., Yang, Y., Luo, H., Giri, S., Hart, J.J., Faquin, V., Guilherme, L.R.G., Thannhauser, T.W., Li, L., 2016. Selenium promotes sulfur accumulation and plant growth in wheat (*Triticum aestivum*). Physiol. Plant. 158, 80–91. https://doi.org/10.1111/ppl.12465

Bradford, M.M., 1976. A rapid and sensitive method for the quantitation of microgram quantities of protein utilizing the principle of protein-dye binding. Anal. Biochem. 72, 248–254. https://doi.org/10.1016/0003-2697(76)90527-3

Capaldi, F.R., Gratão, P.L., Reis, A.R., Lima, L.W., Azevedo, R.A., 2015. Sulfur metabolism and stress defense responses in plants. Trop. Plant Biol. 8, 60–73. https://doi.org/10.1007/s12042-015-9152-1

Chiang, C.M., Chen, S.P., Chen, L.F.O., Chiang, M.C., Chien, H.L., Lin, K.H., 2014. Expression of the broccoli catalase gene (*BoCAT*) enhances heat tolerance in transgenic *Arabidopsis*. J. Plant Biochem. Biotechnol. 23, 266–277. https://doi.org/10.1007/s13562-013-0210-1

Cohen, A., Hacham, Y., Welfe, Y., Khatib, S., Avice, J.C., Amir, R., 2020. Evidence of a significant role of glutathione reductase in the sulfur assimilation pathway. Plant J. 102, 246–261. https://doi.org/10.1111/tpj.14621

Dubreuil-Maurizi, C., Vitecek, J., Marty, L., Branciard, L., Frettinger, P., Wendehenne, D., Meyer, A.J., Mauch, F., Poinssot, B., 2011. Glutathione deficiency of the Arabidopsis mutant *pad2-1* affects oxidative stress-related events, defense gene expression, and the hypersensitive response. Plant Physiol. 157, 2000–2012. https://doi.org/10.1104/pp.111.182667

El Mehdawi, A.F., Jiang, Y., Guignardi, Z.S., Esmat, A., Pilon, M., Pilon-Smits, E.A.H., Schiavon, M., 2018. Influence of sulfate supply on selenium uptake dynamics and expression of sulfate/selenate transporters in selenium hyperaccumulator and nonhyperaccumulator Brassicaceae. New Phytol. 217, 194–205. https://doi.org/10.1111/nph.14838

Ferrari, M., Cozza, R., Marieschi, M., Torelli, A., 2022. Role of Sulfate Transporters in Chromium Tolerance in *Scenedesmus acutus* M. (Sphaeropleales). Plants 11, 1–27. https://doi.org/10.3390/plants11020223

Ferreira, D.F., 2019. Sisvar: a computer analysis system to fixed effects split plot type designs. Rev. Bras. Biometria 37, 529. https://doi.org/10.28951/rbb.v37i4.450

Fu, Y., Tang, J., Yao, G.F., Huang, Z.Q., Li, Y.H., Han, Z., Chen, X.Y., Hu, L.Y., Hu, K. Di, Zhang, H., 2018. Central role of adenosine 5′-phosphosulfate reductase in the control of plant hydrogen sulfide metabolism. Front. Plant Sci. 9, 1–6. https://doi.org/10.3389/fpls.2018.01404

Garousi, F., Veres, S., Kovács, B., 2016. Comparison of Selenium Toxicity in Sunflower and Maize Seedlings Grown in Hydroponic Cultures. Bull. Environ. Contam. Toxicol. 97, 709–713. https://doi.org/10.1007/s00128-016-1912-6

Grant, K., Carey, N.M., Mendoza, M., Schulze, J., Pilon, M., Pilon-Smits, E.A.H., Van Hoewyk, D., 2011. Adenosine 5′-phosphosulfate reductase (APR2) mutation in *Arabidopsis* implicates glutathione deficiency in selenate toxicity. Biochem. J. 438, 325–335. https://doi.org/10.1042/BJ20110025

Günal, S., Hardman, R., Kopriva, S., Mueller, J.W., 2019. Sulfation pathways from red to green. J. Biol. Chem. 294, 12293–12312. https://doi.org/10.1074/jbc.REV119.007422

Gupta, M., Gupta, S., 2017. An overview of selenium uptake, metabolism, and toxicity in plants. Front. Plant Sci. 7, 1–14. https://doi.org/10.3389/fpls.2016.02074

Hacham, Y., Koussevitzky, S., Kirma, M., Amir, R., 2014. Glutathione application affects the transcript profile of genes in Arabidopsis seedling. J. Plant Physiol. 171, 1444–1451. https://doi.org/10.1016/j.jplph.2014.06.016

Hasanuzzaman, M., Nahar, K., Anee, T.I., Fujita, M., 2017. Glutathione in plants: biosynthesis and physiological role in environmental stress tolerance. Physiol. Mol. Biol. Plants 23, 249–268. https://doi.org/10.1007/s12298-017-0422-2

Hawrylak-Nowak, B., 2013. Comparative effects of selenite and selenate on growth and selenium accumulation in lettuce plants under hydroponic conditions. Plant Growth Regul. 70, 149–157. https://doi.org/10.1007/s10725-013-9788-5

Hendrix, S., Jozefczak, M., Wójcik, M., Deckers, J., Vangronsveld, J., Cuypers, A., 2020. Glutathione: A key player in metal chelation, nutrient homeostasis, cell cycle regulation and the DNA damage response in cadmium-exposed Arabidopsis thaliana. Plant Physiol. Biochem. 154, 498–507. https://doi.org/10.1016/j.plaphy.2020.06.006

Huang, S.W., Wang, Y., Tang, C., Jia, H.L., Wu, L., 2021. Speeding up selenite bioremediation using the highly selenite-tolerant strain Providencia rettgeri HF16-A novel mechanism of selenite reduction based on proteomic analysis. J. Hazard. Mater. 406, 124690. https://doi.org/10.1016/j.jhazmat.2020.124690

Kaur, B., Kaur, G., Asthir, B., 2017. Biochemical aspects of nitrogen use efficiency: An overview. J. Plant Nutr. 40, 506–523. https://doi.org/10.1080/01904167.2016.1240196

Khan, M.I.R., Nazir, F., Asgher, M., Per, T.S., Khan, N.A., 2015. Selenium and sulfur influence ethylene formation and alleviate cadmium-induced oxidative stress by improving proline and glutathione production in wheat. J. Plant Physiol. 173, 9–18. https://doi.org/10.1016/j.jplph.2014.09.011

Kopriva, S., 2006. Regulation of sulfate assimilation in Arabidopsis and beyond. Ann. Bot. 97, 479–495. https://doi.org/10.1093/aob/mcl006

Koprivova, A., Kopriva, S., 2014. Molecular mechanisms of regulation of sulfate assimilation: first steps on a long road. Front. Plant Sci. 5, 1–11. https://doi.org/10.3389/fpls.2014.00589

Lappartient, A.G., Vidmar, J.J., Leustek, T., Glass, A.D.M., Touraine, B., 1999. Inter-organ signaling in plants: Regulation of ATP sulfurylase and sulfate transporter genes expression in roots mediated by phloem-translocated compound. Plant J. 18, 89–95. https://doi.org/10.1046/j.1365-313X.1999.00416.x

Li, Z.-R., Hu, K.-D., Zhang, F.-Q., Li, S.-P., Hu, L.-Y., Li, Y.-H., Wang, S.-H., Zhang, H., 2015. Hydrogen Sulfide Alleviates Dark-promoted Senescence in Postharvest Broccoli. HortScience 50, 416–420. https://doi.org/10.21273/HORTSCI.50.3.416

Lunde, C., Zygadlo, A., Simonsen, H.T., Nielsen, P.L., Blennow, A., Haldrup, A., 2008. Sulfur starvation in rice: the effect on photosynthesis, carbohydrate metabolism, and oxidative stress protective pathways. Physiol. Plant. 134, 508–521. https://doi.org/10.1111/j.1399-3054.2008.01159.x

Maruyama-Nakashita, A., Nakamura, Y., Watanabe-Takahashi, A., Inoue, E., Yamaya, T., Takahashi, H., 2005. Identification of a novel cis-acting element conferring sulfur deficiency response in Arabidopsis roots. Plant J. 42, 305–314. https://doi.org/10.1111/j.1365-313X.2005.02363.x

Maruyama-Nakashita, A., Nakamura, Y., Yamaya, T., Takahashi, H., 2004. Regulation of high-affinity sulphate transporters in plants: Towards systematic analysis of sulphur signalling and reguation. J. Exp. Bot. 55, 1843–1849. https://doi.org/10.1093/jxb/erh175

Rahman, I., Kode, A., Biswas, S.K., 2007. Assay for quantitative determination of glutathione and glutathione disulfide levels using enzymatic recycling method. Nat. Protoc. 1, 3159–3165. https://doi.org/10.1038/nprot.2006.378

Ramos, S.J., Rutzke, M.A., Hayes, R.J., Faquin, V., Guilherme, L.R.G., Li, L., 2011. Selenium accumulation in lettuce germplasm. Planta 233, 649–660. https://doi.org/10.1007/s00425-010-1323-6

Ríos, J.J., Blasco, B., Cervilla, L.M., Rubio-Wilhelmi, M.M., Ruiz, J.M., Romero, L., 2008. Regulation of sulphur assimilation in lettuce plants in the presence of selenium. Plant Growth Regul. 56, 43–51. https://doi.org/10.1007/s10725-008-9282-7

Santiago, F.E.M., Silva, M.L.S., Cardoso, A.A.S., Duan, Y., Guilherme, L.R.G., Liu, J., Li, L., 2020. Biochemical basis of differential selenium tolerance in arugula (*Eruca sativa* Mill.) and lettuce (*Lactuca sativa* L.). Plant Physiol. Biochem. 157, 328–338. https://doi.org/10.1016/j.plaphy.2020.11.001

Schiavon, M., Berto, C., Malagoli, M., Trentin, A., Sambo, P., Dall'Acqua, S., Pilon-Smits, E.A.H., 2016. Selenium biofortification in radish enhances nutritional quality via accumulation of methyl-selenocysteine and promotion of transcripts and metabolites related to glucosinolates, phenolics amino acids. Front. Plant Sci. 7. https://doi.org/10.3389/fpls.2016.01371

Schiavon, M., Pilon-Smits, E.A.H., 2017. The fascinating facets of plant selenium accumulation – biochemistry, physiology, evolution and ecology. New Phytol. 213, 1582–

1596. https://doi.org/10.1111/nph.14378

Schiavon, M., Pittarello, M., Pilon-Smits, E.A.H., Wirtz, M., Hell, R., Malagoli, M., 2012. Selenate and molybdate alter sulfate transport and assimilation in *Brassica juncea* L. Czern.: Implications for phytoremediation. Environ. Exp. Bot. 75, 41–51. https://doi.org/10.1016/j.envexpbot.2011.08.016

Smith, F.W., Hawkesford, M.J., Ealing, P.M., Clarkson, D.T., Vanden Berg, P.J., Belcher, A.R., Warrilow, A.G.S., 1997. Regulation of expression of a cDNA from barley roots encoding a high affinity sulphate transporter. Plant J. 12, 875–884. https://doi.org/10.1046/j.1365-313X.1997.12040875.x

Takahashi, H., Kopriva, S., Giordano, M., Saito, K., Hell, R., 2011. Sulfur Assimilation in Photosynthetic Organisms: Molecular Functions and Regulations of Transporters and Assimilatory Enzymes. Annu. Rev. Plant Biol. 62, 157–184. https://doi.org/10.1146/annurev-arplant-042110-103921

Takahashi, H., Watanabe-Takahashi, A., Smith, F.W., Blake-Kalff, M., Hawkesford, M.J., Saito, K., 2000. The roles of three functional sulphate transporters involved in uptake and translocation of sulphate in *Arabidopsis thaliana*. Plant J. 23, 171–182. https://doi.org/10.1046/j.1365-313x.2000.00768.x

Terry, N., Zayed, A.M., Souza, M.P. de, Tarun, A.S., 2000. Selenium in higuer plants. Annu. Rev. Plant Physiol. Plant Mol. Biol. 51, 401–432.

Tian, M., Hui, M., Thannhauser, T.W., Pan, S., Li, L., 2017. Selenium-Induced Toxicity Is Counteracted by Sulfur in Broccoli (*Brassica oleracea* L. var. italica). Front. Plant Sci. 8, 1–13. https://doi.org/10.3389/fpls.2017.01425

Toler, H.D., Charron, C.S., Kopsell, D.A., Sams, C.E., Randle, W.M., 2007. Selenium and sulfur increase sulfur uptake and regulate glucosinolate metabolism in *Brassica oleracea*. Acta Hortic. 744, 311–316. https://doi.org/10.17660/ActaHortic.2007.744.32

Van Hoewyk, D., 2013. A tale of two toxicities: Malformed selenoproteins and oxidative stress both contribute to selenium stress in plants. Ann. Bot. 112, 965–972. https://doi.org/10.1093/aob/mct163

Van Hoewyk, D., Takahashi, H., Inoue, E., Hess, A., Tamaoki, M., Pilon-Smits, E.A.H., 2008. Transcriptome analyses give insights into selenium-stress responses and selenium tolerance mechanisms in *Arabidopsis*. Physiol. Plant. 132, 236–253. https://doi.org/10.1111/j.1399-3054.2007.01002.x

Vauclare, P., Kopriva, S., Fell, D., Suter, M., Sticher, L., Von Ballmoos, P., Krähenbühl, U., Op Den Camp, R., Brunold, C., 2002. Flux control of sulphate assimilation in *Arabidopsis thaliana*: Adenosine 5′-phosphosulphate reductase is more susceptible than ATP sulphurylase to negative control by thiols. Plant J. 31, 729–740. https://doi.org/10.1046/j.1365-313X.2002.01391.x

Velikova, V., Yordanov, I., Edreva, A., 2000. Oxidative stress and some antioxidant systems in acid rain-treated bean plants. Plant Sci. 151, 59–66. https://doi.org/10.1016/S0168-9452(99)00197-1

Wang, Y., Kang, Y., Yu, W., Lyi, S.M., Choi, H.W., Xiao, E., Li, L., Klessig, D.F., Liu, J., 2022. AtTIP2;2 facilitates resistance to zinc toxicity via promoting zinc immobilization in the root and limiting root-to-shoot zinc translocation in Arabidopsis thaliana. Ecotoxicol. Environ. Saf. 233. https://doi.org/10.1016/j.ecoenv.2022.113333

White, P.J., 2018. Selenium metabolism in plants. Biochim. Biophys. Acta - Gen. Subj. 1862, 2333–2342. https://doi.org/10.1016/j.bbagen.2018.05.006

White, P.J., 2016. Selenium accumulation by plants. Ann. Bot. 117, 217–235. https://doi.org/10.1093/aob/mcv180

White, P.J., Bowen, H.C., Parmaguru, P., Fritz, M., Spracklen, W.P., Spiby, R.E., Meacham, M.C., Mead, A., Harriman, M., Trueman, L.J., Smith, B.M., Thomas, B., Broadley, M.R., 2004. Interactions between selenium and sulphur nutrition in *Arabidopsis thaliana*. J. Exp. Bot. 55, 1927–1937. https://doi.org/10.1093/jxb/erh192

Wiesner-Reinhold, M., Schreiner, M., Baldermann, S., Schwarz, D., Hanschen, F.S., Kipp, A.P., Rowan, D.D., Bentley-Hewitt, K.L., McKenzie, M.J., 2017. Mechanisms of Selenium Enrichment and Measurement in Brassicaceous Vegetables, and Their Application to Human Health. Front. Plant Sci. 8. https://doi.org/10.3389/fpls.2017.01365

Yoshimoto, N., Takahashi, H., Smith, F.W., Yamaya, T., Saito, K., 2002. Two distinct high-affinity sulfate transporters with different inducibilities mediate uptake of sulfate in *Arabidopsis* roots. Plant J. 29, 465–473. https://doi.org/10.1046/j.0960-7412.2001.01231.x

Zhang, L., Hu, B., Li, W., Che, R., Deng, K., Li, H., Yu, F., Ling, H., Li, Y., Chu, C., 2014. OsPT2, a phosphate transporter, is involved in the active uptake of selenite in rice. New Phytol. 201, 1183–1191. https://doi.org/10.1111/nph.12596

Zhang, Y., Pan, G., Chen, J., Hu, Q., 2003. Uptake and transport of selenite and selenate by soybean seedlings of two genotypes. Plant Soil 253, 437–443. https://doi.org/10.1023/A:1024874529957

Zheng, Z.L., Zhang, B., Leustek, T., 2014. Transceptors at the boundary of nutrient transporters and receptors: A new role for *Arabidopsis* SULTR1;2 in sulfur sensing. Front. Plant Sci. 5, 1–5. https://doi.org/10.3389/fpls.2014.00710

Zhou, Y., Tang, Q., Wu, M., Mou, D., Liu, H., Wang, S., Zhang, C., Ding, L., Luo, J., 2018. Comparative transcriptomics provides novel insights into the mechanisms of selenium tolerance in the hyperaccumulator plant *Cardamine hupingshanensis*. Sci. Rep. 8, 1–17. https://doi.org/10.1038/s41598-018-21268-2

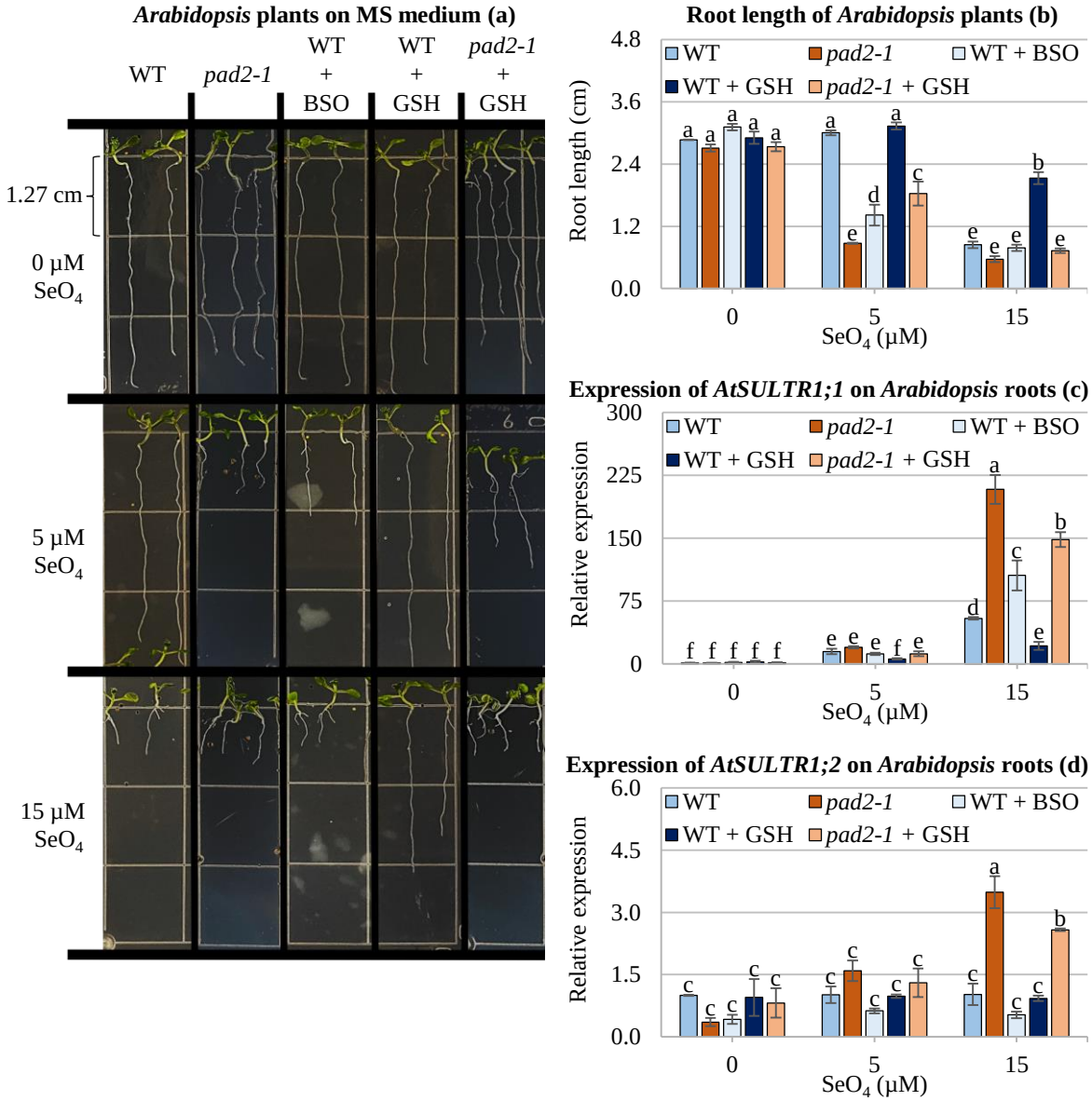


Figure 1. *Arabidopsis* plants grown in ½ MS medium under doses of selenate ($SeO_4$), reduced glutathione (50 µM GSH), and buthionine sulfoximine (50 µM BSO). Plants at harvest time (a). Root length (b). Relative expression of *AtSULTR1;1* (c) and *AtSULTR1;2* (d) genes on roots. Columns with different letters differ by the Scott-Knott test (n = 45, $p < 0.05$).

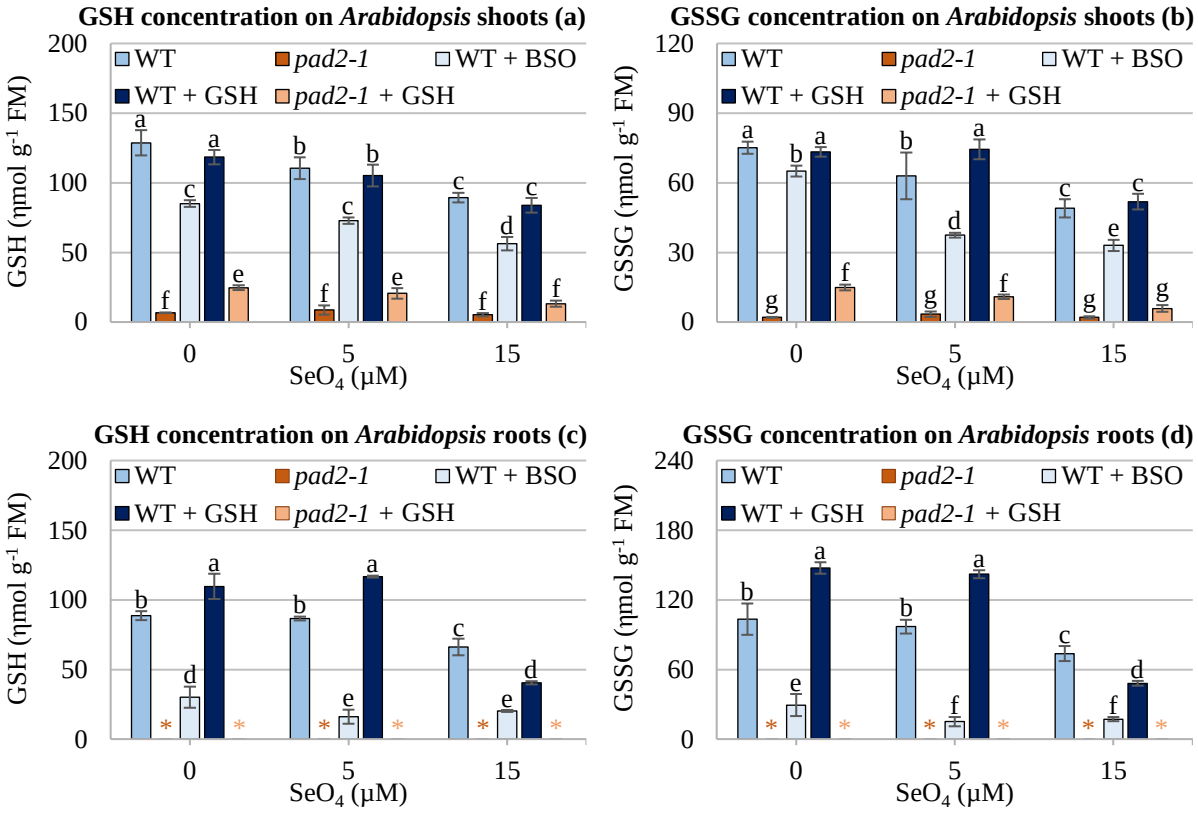


Figure 2. Glutathione concentrations on *Arabidopsis* plants grown in ½ MS medium under doses of selenate ($SeO_4$), reduced glutathione (50 µM GSH), and buthionine sulfoximine (50 µM BSO). Reduced glutathione (GSH) concentrations on shoots (a) and roots (b). Oxidized glutathione (GSSG) concentrations on shoots (c) and roots (d). Columns with different letters differ by the Scott-Knott test (n = 45, $p < 0.05$). * Below detection limit.

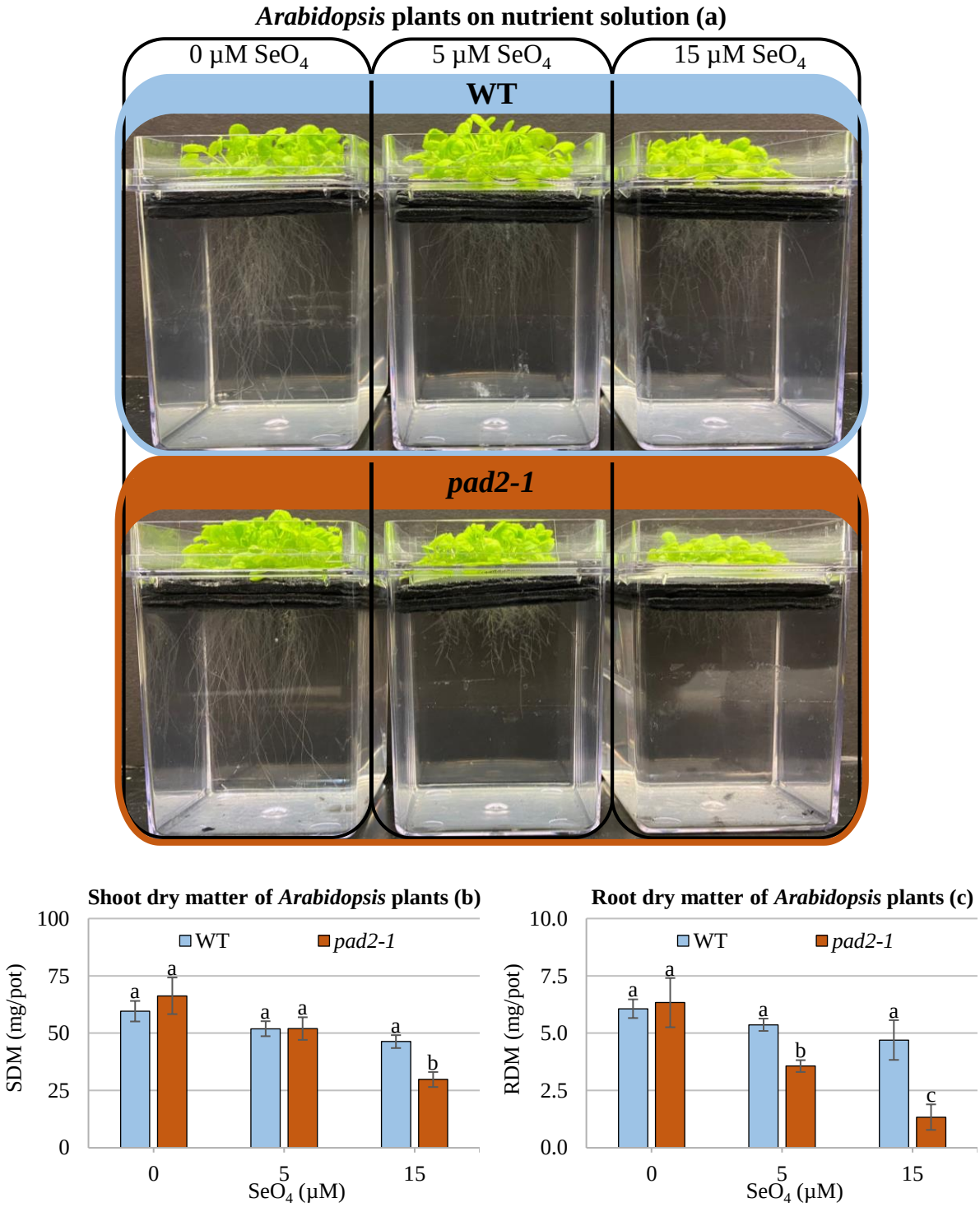


Figure 3. *Arabidopsis* plants grown in nutrient solutions under selenate doses ($SeO_4$). Plants at harvest time (a). Shoots (SDM, b) and roots (RDM, c) dry matter productions. Columns with different letters differ by the Scott-Knott test (n = 18, $p < 0.05$).

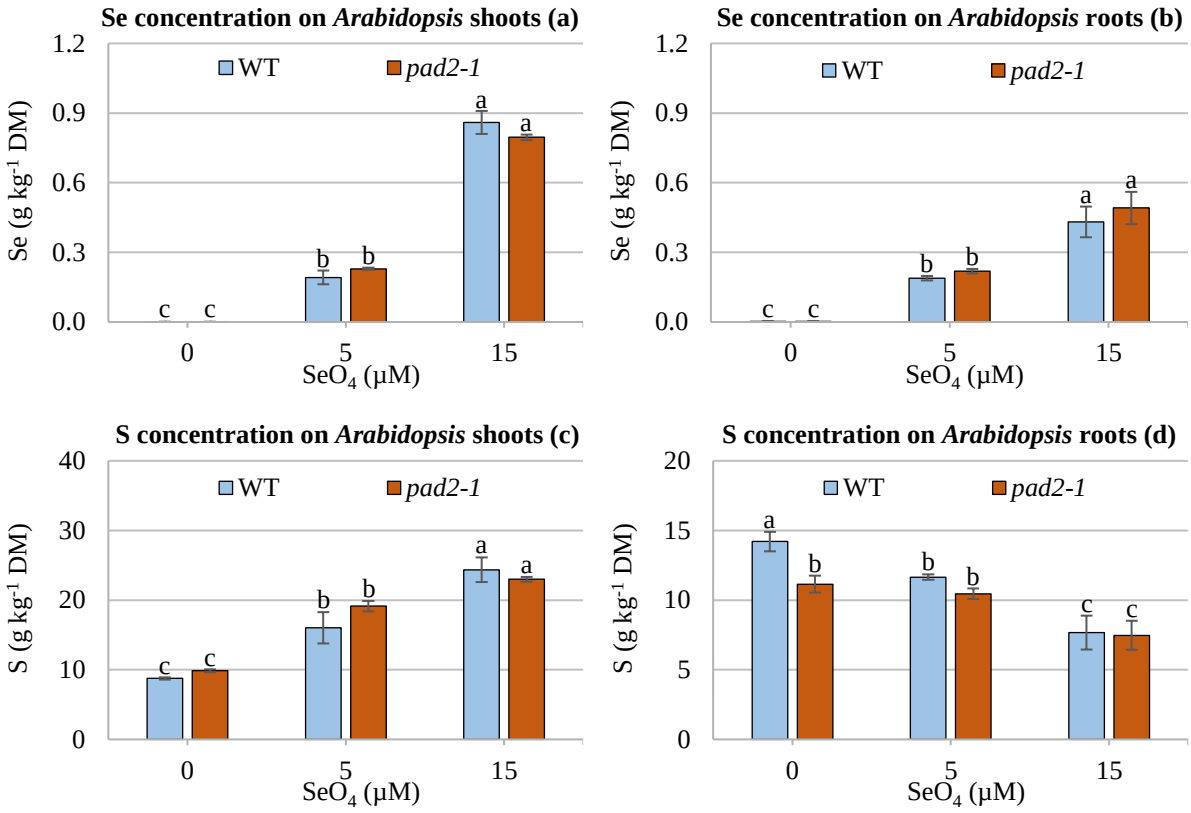


Figure 4. Selenium and sulfur concentrations of *Arabidopsis* plants grown in nutrient solutions under selenate doses ($SeO_4$). Selenium on shoots (a) and roots (b). Sulfur on shoots (c) and roots (d). Columns with different letters differ by the Scott-Knott test (n = 18, $p < 0.05$).

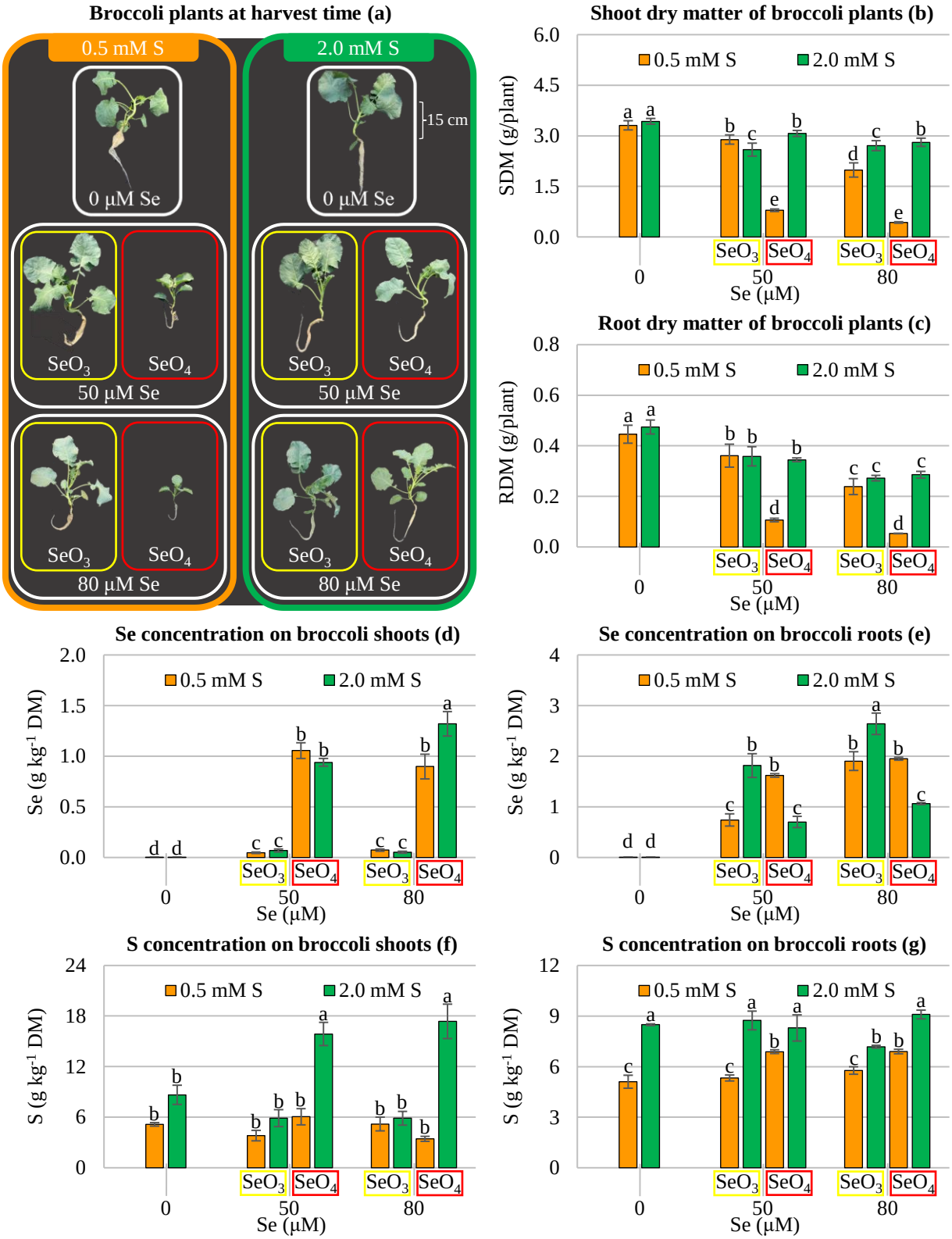


Figure 5. Broccoli plants grown in nutrient solutions under doses of sulfur, selenite ($SeO_3$), and selenate ($SeO_4$). Plants at harvest time (a). Shoots (SDM, b) and roots (RDM, c) dry matter productions. Selenium concentrations on shoots (d) and roots (e). Sulfur concentrations on shoots (f) and roots (g). Columns with different letters differ by the Scott-Knott test (n = 30, $p < 0.05$).

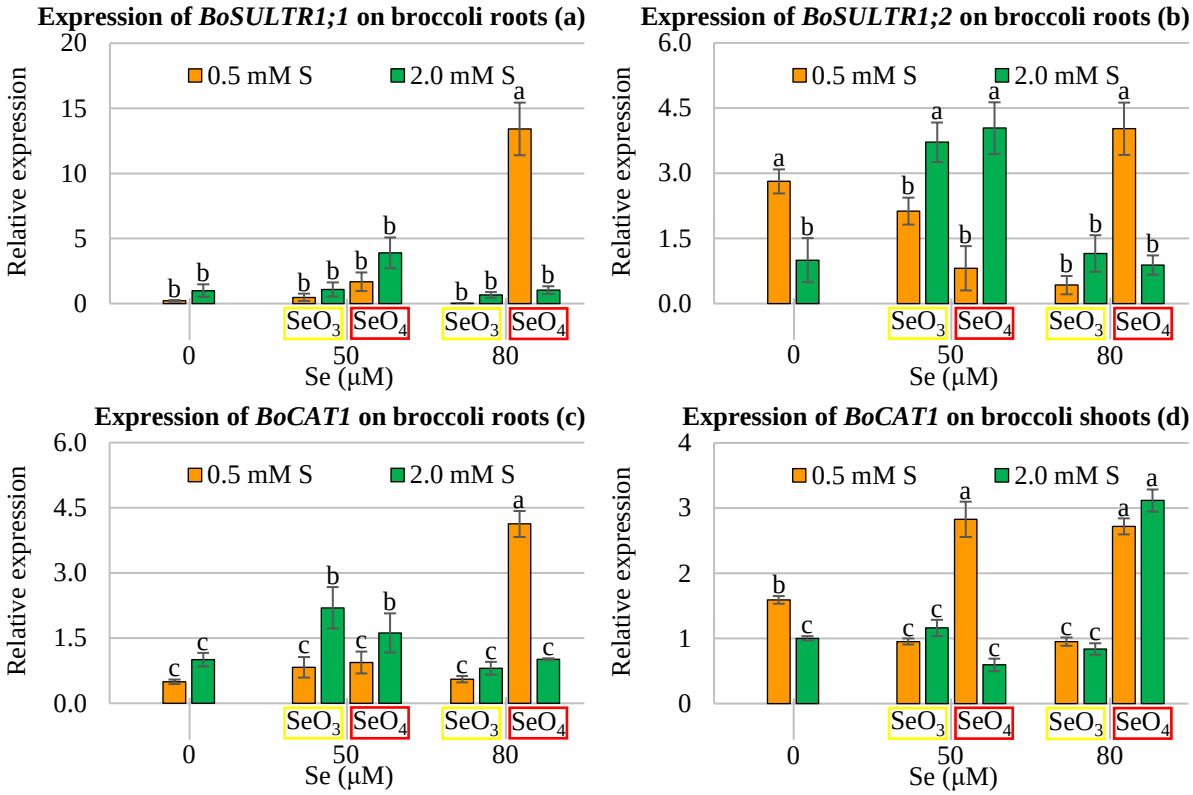


Figure 6. Relative expression of *BoSULTR1;1* (a) and *BoSULTR1;2* (b) on roots and *BoCAT1* on roots (c) and shoots (d) of broccoli plants grown in nutrient solutions under doses of sulfur, selenite ($SeO_3$), and selenate ($SeO_4$). Columns with different letters differ by the Scott-Knott test (n = 30, $p < 0.05$).

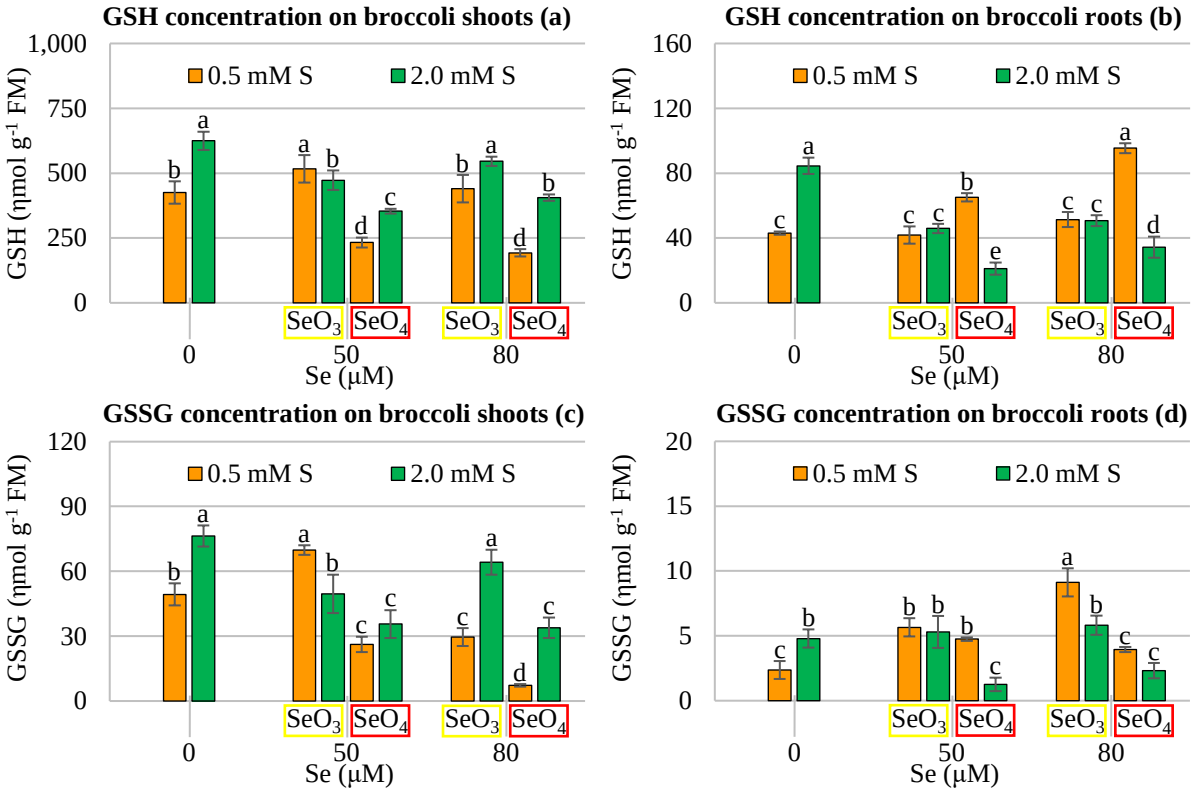


Figure 7. Glutathione concentrations on broccoli plants grown in nutrient solutions under doses of sulfur, selenite ($SeO_3$), and selenate ($SeO_4$). Reduced glutathione (GSH) concentrations on shoots (a) and roots (b). Oxidized glutathione (GSSG) concentrations on shoots (c) and roots (d). Columns with different letters differ by the Scott-Knott test (n = 30, $p < 0.05$).

**Supplemental**

Table S1. MS medium composition for *Arabidopsis* cultivation (ml $L^{-1}$).

| Medium composition | $Na_2SeO_4$ (10 mM) | BSO (10 mM) | GSH (10 mM) |
|---|---|---|---|
| 0 µM $SeO_4$ | - | - | - |
| 5 µM $SeO_4$ | 0.5 | - | - |
| 15 µM $SeO_4$ | 1.5 | - | - |
| 0 µM $SeO_4$ + 50 µM BSO | - | 5 | - |
| 5 µM $SeO_4$ + 50 µM BSO | 0.5 | 5 | - |
| 15 µM $SeO_4$ + 50 µM BSO | 1.5 | 5 | - |
| 0 µM $SeO_4$ + 50 µM GSH | - | - | 5 |
| 5 µM $SeO_4$ + 50 µM GSH | 0.5 | - | 5 |
| 15 µM $SeO_4$ + 50 µM GSH | 1.5 | - | 5 |

Basic ½ MS medium: 2.15 g $L^{-1}$ MS salt (RPI®, M10200), 10 g $L^{-1}$ sucrose, 8 g $L^{-1}$ agar, pH 5.8. BSO: buthionine sulfoximine. GSH: reduced glutathione.

Table S2. Nutrient solution composition for *Arabidopsis* cultivation (ml $L^{-1}$).

| Se dose | $Na_2SeO_4$ (10 mM) | $MgSO_4$ (1 M) | $KNO_3$ (1 M) | $Ca(NO_3)_2$ (1 M) | $KH_2PO_4$ (1 M) | Micronutrient solution | Fe-EDTA |
|---|---|---|---|---|---|---|---|
| 0 µM $SeO_4$ | - | 2 | 5 | 5 | 1 | 1 | 1 |
| 5 µM $SeO_4$ | 0.5 | 2 | 5 | 5 | 1 | 1 | 1 |
| 15 µM $SeO_4$ | 1.5 | 2 | 5 | 5 | 1 | 1 | 1 |

Micronutrient solution: $H_3BO_3$ (46 mM), $CuCl_2$ (0.3 mM), $MnCl_2 \cdot 4H_2O$ (9.1 mM), $H_2MoO_4$ (0.1 mM), and $ZnCl_2$ (0.7 mM). Fe-EDTA: $FeCl_2 \cdot 6H_2O$ (100 mM) + EDTA (89 mM) dissolved in NaOH (89 mM).

Table S3. Nutrient solution composition for broccoli cultivation (ml $L^{-1}$).

| Treatment | $Na_2SeO_3$ (10 mM) | $Na_2SeO_4$ (10 mM) | $MgSO_4$ (1 M) | $MgCl_2$ (1 M) | $KNO_3$ (1 M) | $Ca(NO_3)_2$ (1 M) | $KH_2PO_4$ (1 M) | Micronutrient solution | Fe-EDTA |
|---|---|---|---|---|---|---|---|---|---|
| 0.5 mM S | - | - | 0.5 | 1.5 | 5 | 5 | 1 | 1 | 1 |
| 2.0 mM S | - | - | 2.0 | - | 5 | 5 | 1 | 1 | 1 |
| 0.5 mM S + 50 µM $SeO_3$ | 5 | - | 0.5 | 1.5 | 5 | 5 | 1 | 1 | 1 |
| 2.0 mM S + 50 µM $SeO_3$ | 5 | - | 2.0 | - | 5 | 5 | 1 | 1 | 1 |
| 0.5 mM S + 50 µM $SeO_4$ | - | 5 | 0.5 | 1.5 | 5 | 5 | 1 | 1 | 1 |
| 2.0 mM S + 50 µM $SeO_4$ | - | 5 | 2.0 | - | 5 | 5 | 1 | 1 | 1 |
| 0.5 mM S + 80 µM $SeO_3$ | 8 | - | 0.5 | 1.5 | 5 | 5 | 1 | 1 | 1 |
| 2.0 mM S + 80 µM $SeO_3$ | 8 | - | 2.0 | - | 5 | 5 | 1 | 1 | 1 |
| 0.5 mM S + 80 µM $SeO_4$ | - | 8 | 0.5 | 1.5 | 5 | 5 | 1 | 1 | 1 |
| 2.0 mM S + 80 µM $SeO_4$ | - | 8 | 2.0 | - | 5 | 5 | 1 | 1 | 1 |

Micronutrient solution: $H_3BO_3$ (46 mM), $CuCl_2$ (0.3 mM), $MnCl_2 \cdot 4H_2O$ (9.1 mM), $H_2MoO_4$ (0.1 mM), and $ZnCl_2$ (0.7 mM). Fe-EDTA: $FeCl_2 \cdot 6H_2O$ (100 mM) + EDTA (89 mM) dissolved in NaOH (89 mM).

Table S4. Primers sequences used in the study.

| Symbol | Description | Sequence | GenBank accession |
|---|---|---|---|
| *AtSULTR1;1* | *A. thaliana* sulfate transporter 1;1 | F: TCCGGCAATTGCGCCTCTTATTT<br>R: GAACCGACGACGTTCATAGTCCCTA | NM_116931 |
| *AtSULTR1;2* | *A. thaliana* sulfate transporter 1;2 | F: CTGGCATGGTCGCTTTAACAG<br>R: AGAATGCTCCAATACAGGCGATGA | NM_106449 |
| *AtAPS1* | *A. thaliana* ATP sulfurylase 1 | F: CAAGACGCAAGGCAAGATGG<br>R: ACTGGTATATTACCTTAGTGCCG | NM_113189 |
| *AtAPR2* | *A. thaliana* 5'-adenylylsulfate reductase 2 | F: TTAGACCTTTGCGTCGTGCT<br>R: TCTCGTACCCGGAGATTGGT | NM_104899 |
| *AtGR2* | *A. thaliana* glutathione reductase 2 | F: AAGCTGGAGATGGCTCGTTC<br>R: CTTGCGACCAGTTGCAAACA | NM_115323 |
| *AtGPX1* | *A. thaliana* glutathione peroxidase 1 | F: GTGAATGGACCAAGCACAGC<br>R: GGGAGGGTACCTCTCAACGA | NM_128065 |
| *AtGSH1* | *A. thaliana* glutamate-cysteine ligase 1 | F: GGGAAATCGTTTGGGAGGGT<br>R: CGTCGCCTTTGCCTTGAAAT | NM_118439 |
| *AtPCS1* | *A. thaliana* phytochelatin synthase 1 | F: TGATGACTCTGAAGGCACGG<br>R: TTGCGTCGATGGCACTAACA | NM_123774 |
| *AtACT8* | *A. thaliana* actin 8 (act8) | F: ATGAAGATTAAGGTCGTGGC<br>R: TCCGAGTTTGAAGAGGCTAC | NM_103814 |
| *BoSULTR1;1* | *B. oleracea* sulfate transporter 1;1 | F: GATTCTGCTGCAAGTGACGA<br>R: ACGCGAATGATCAAGATTCC | XM_013763767 |
| *BoSULTR1;2* | *B. oleracea* sulfate transporter 1;2 | F: GATTCTGCTGCAAGTGACGA<br>R: ACGCGAATGATCAAGATTCC | AJ416460 |
| *BoCAT1* | *B. oleracea* catalase 1 | F: GCTTGCCTTCTGTCCTGCTA<br>R: AGGTCCAAGACGGTGTCTCT | GQ500124 |
| *BoAPS1* | *B. oleracea* ATP sulfurylase 1 | F: AGACGACGAGCAAAAGGCTA<br>R: GGTTGTACCCCATGTTCTGG | XM_013774858 |
| *BoAPR2* | *B. oleracea* 5'-adenylylsulfate reductase 2 | F: TCTTTGGTTACCCGTGCTTC<br>R: GGAGAAGCCTCTTCCAGCTT | XM_013781409 |
| *BoACT1* | *B. oleracea* actin (act1) | F: CCGAGAGAGGTTACATGTTCACCA<br>R: GCTGTGATCTCTTTGCTCATACGGT | AF044573 |

F: forward primer. R: reverse primer.

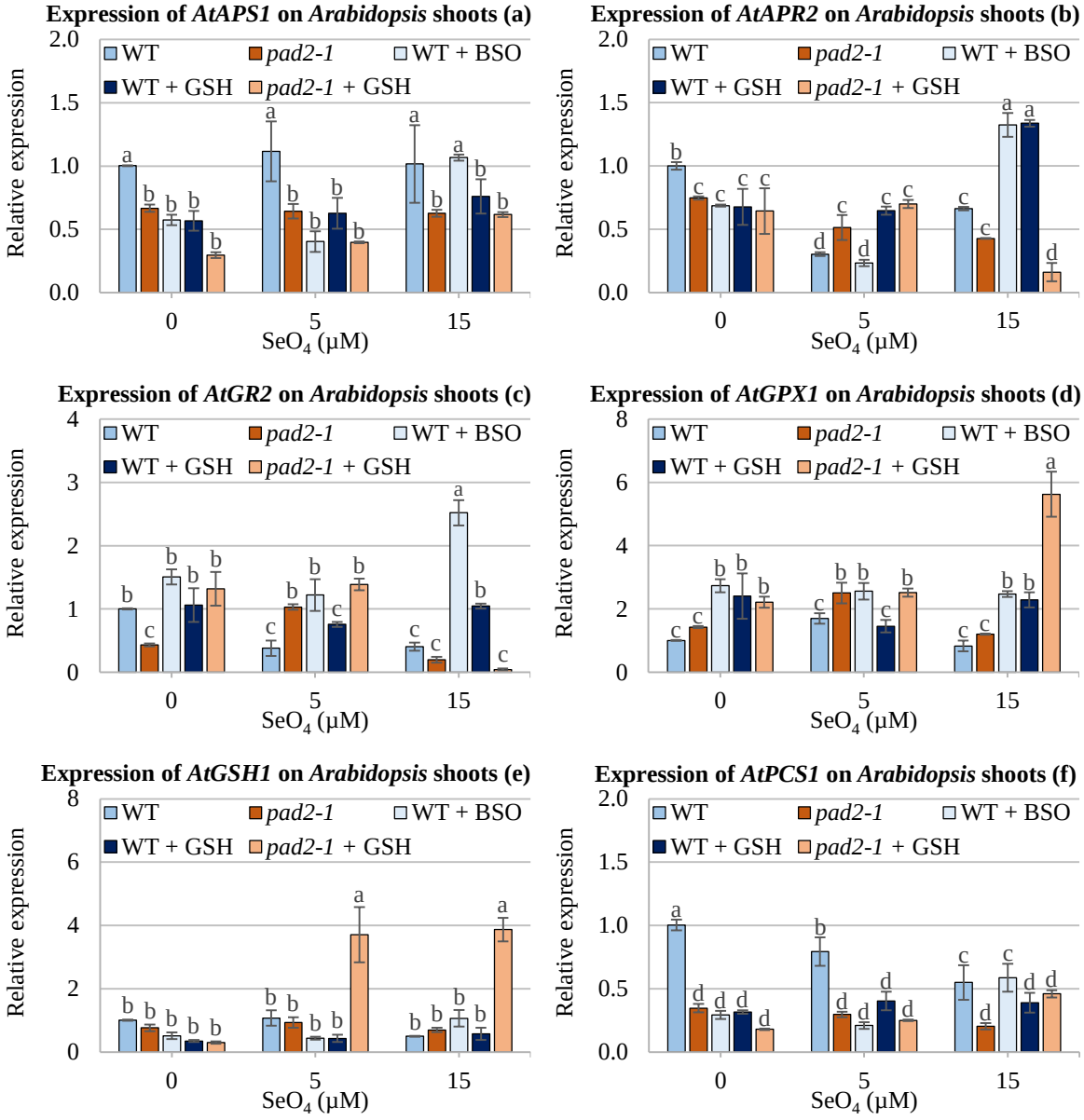


Figure S1. Relative expression of *AtAPS1* (a), *AtAPR2* (b), *AtAGR2* (c), *AtGPX1* (d), *AtGSH1* (e) and *AtPCS1* (f) genes on shoots of *Arabidopsis* plants grown in ½ MS medium under doses of selenate ($SeO_4$), reduced glutathione (50 µM GSH) and buthionine sulfoximine (50 µM BSO). Columns with different letters differ by the Scott-Knott test (n = 45, $p < 0.05$).

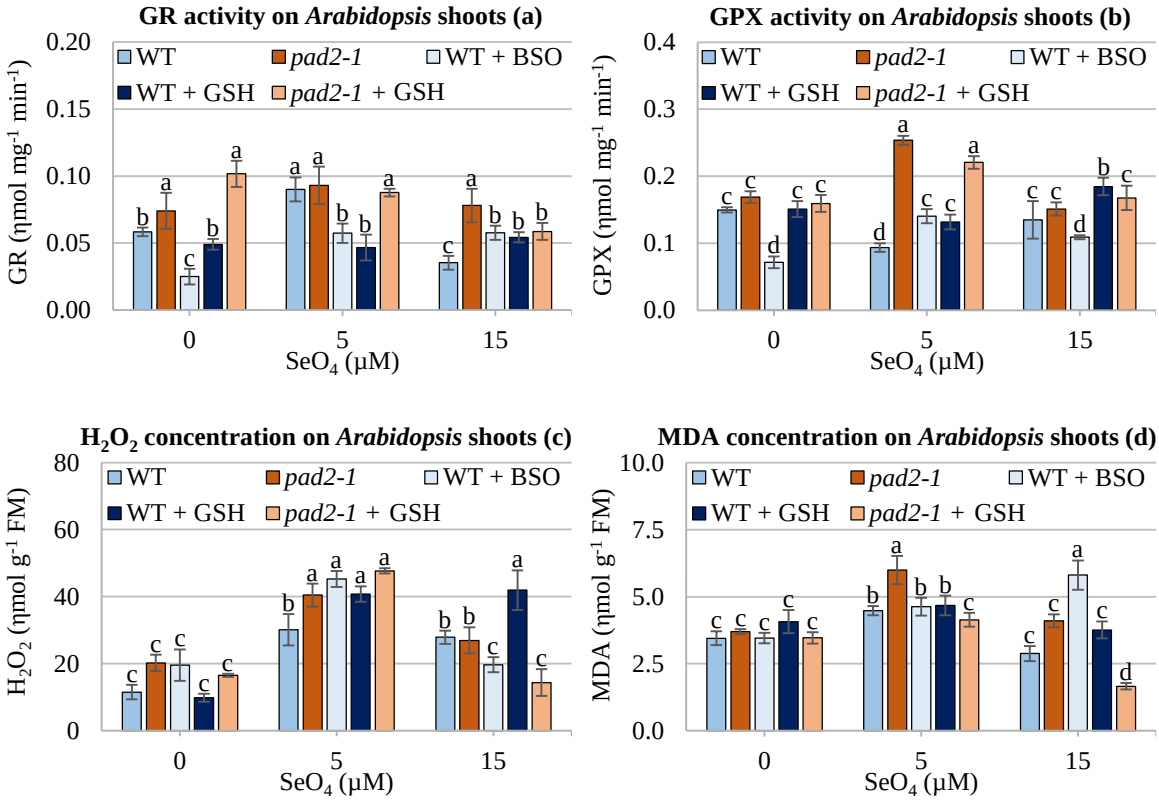


Figure S2. Enzyme activity and oxidative stress indicators on shoots of *Arabidopsis* plants grown in ½ MS medium under doses of selenate ($SeO_4$), reduced glutathione (50 µM GSH), and buthionine sulfoximine (50 µM BSO). Glutathione reductase (GR, a) and glutathione peroxidase (GPX, b) activities. Hydrogen peroxide ($H_2O_2$, c) and malondialdehyde (MDA, d) concentrations. Columns with different letters differ by the (n = 45, $p < 0.05$).

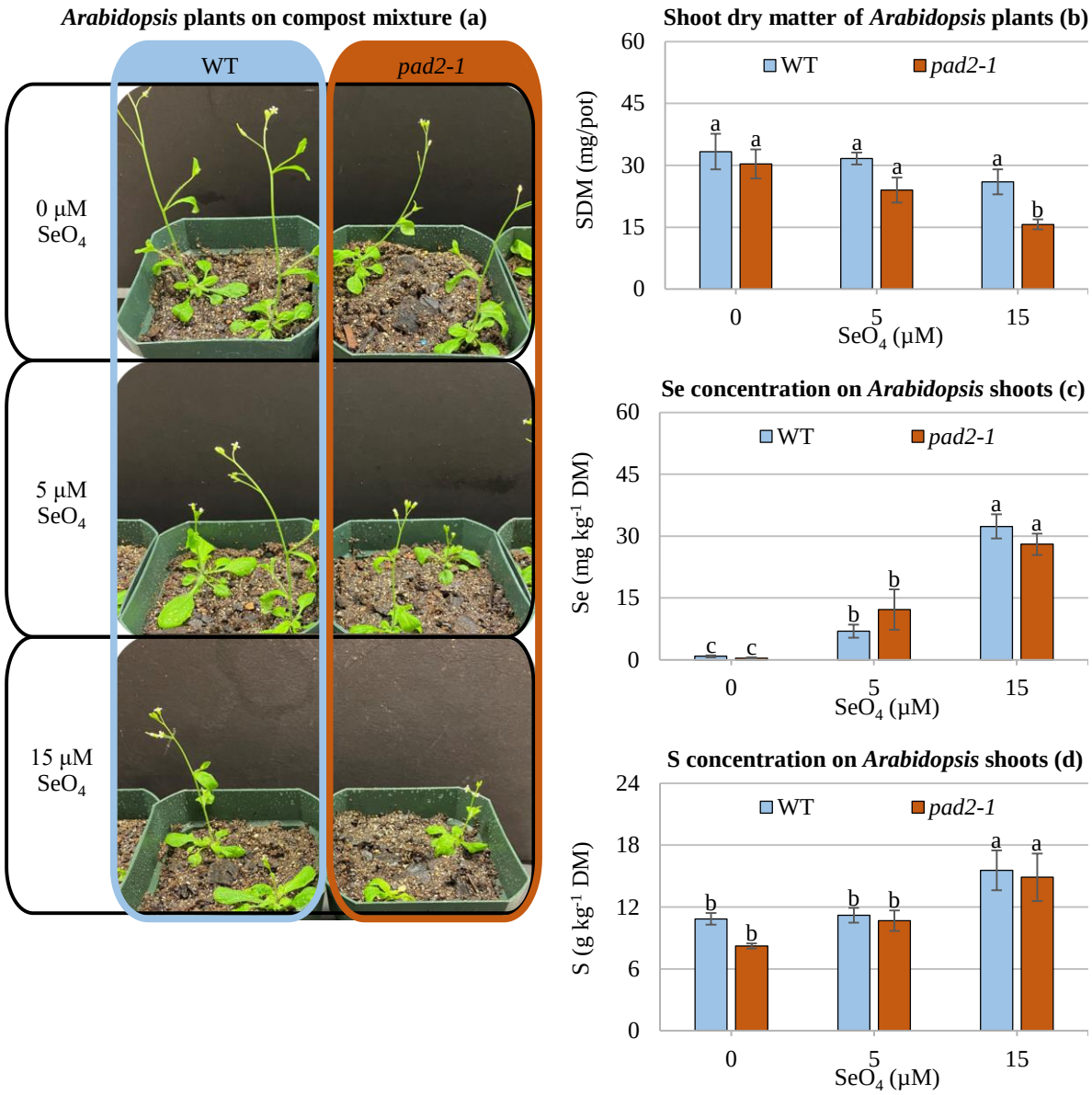


Figure S3. *Arabidopsis* plants in peat moss compost under selenate doses ($SeO_4$). Plants at harvest time (a). Shoots dry matter production (SDM, b). Selenium (b) and sulfur (c) concentrations on shoots. Columns with different letters differ by the Scott-Knott test (n = 18, $p < 0.05$).

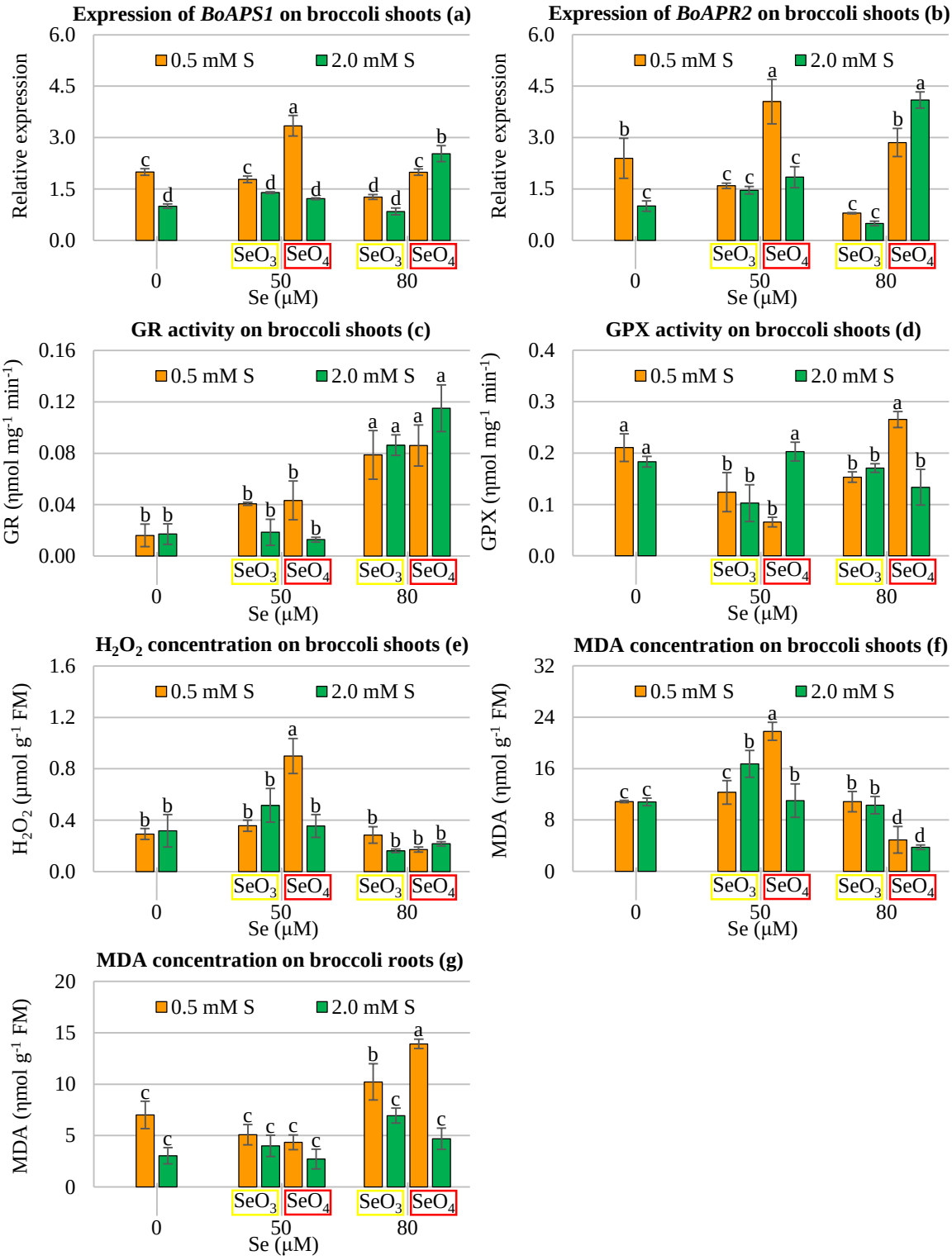


Figure S4. Gene expression, enzyme activity, and oxidative stress indicators on broccoli plants grown in nutrient solutions under doses of sulfur, selenite ($SeO_3$), and selenate ($SeO_4$). Relative expression of *BoAPS1* (a) and *BoAPR2* (b) on shoots. Glutathione reductase (GR, c) and glutathione peroxidase (GPX, d) activities on shoots. Hydrogen peroxide ($H_2O_2$, e) concentration on shoots. Malondialdehyde (MDA) concentrations on shoots (f) and roots (g). Columns with different letters differ by the Scott-Knott test (n = 30, $p < 0.05$). $H_2O_2$ concentrations in roots were below the detection limit.